

European Journal of Agronomy
Quantifying critical N dilution curves across G × E × M effects for potato using a partially-pooled Bayesian hierarchical method
--Manuscript Draft--

Manuscript Number:	EURAGR11860R2
Article Type:	Research paper
Section/Category:	Crop Management
Keywords:	critical N concentration; Critical nitrogen dilution curve; nitrogen nutrition index; Nitrogen use efficiency; potato; Bayesian; genotype-by-environment-by-management interactions
Corresponding Author:	Brian Joseph Bohman, Ph.D. University of Minnesota Twin Cities: University of Minnesota Twin Cities UNITED STATES
First Author:	Brian Joseph Bohman, Ph.D.
Order of Authors:	Brian Joseph Bohman, Ph.D. Michael J. Culshaw-Maurer Feriel Ben Abdallah Claudia Giletto Gilles Bélanger Fabián G. Fernández Yuxin Miao David J. Mulla Carl J. Rosen
Abstract:	Multiple critical N dilution curves [CNDCs] have been previously developed for potato; however, attempts to directly compare differences in CNDCs across genotype [G], environment [E], and management [M] interactions have been confounded by non-uniform statistical methods, biased experimental data, and lack of proper quantification of uncertainty in the critical N concentration [%N _c]. This study implements a partially-pooled Bayesian hierarchical method to develop CNDCs for previously published and newly reported experimental data, systematically evaluates the difference in %N _c [$\Delta\%$ N _c] across G × E × M effects, and directly compare CNDCs from the Bayesian framework to CNDCs from conventional statistical methods. The partially-pooled Bayesian hierarchical method implemented in this study has the advantage of being less susceptible to inferential bias at the level of individual G × E × M interactions compared to alternative statistical methods that result from insufficient quantity and quality of experimental datasets (e.g., unbalanced distribution of N limiting and non-N limiting observations). This method also allows for a direct statistical comparison of differences in %N _c across levels of the G × E × M interactions. Where found to be significant, $\Delta\%$ N _c was hypothesized to be related to variation in the timing of tuber initiation (e.g., maturity class) and the relative rate of tuber bulking (e.g., planting density) across G × E × M interactions. In addition to using the median value for %N _c (i.e., CNDC), the lower and upper boundary values for the credible region (i.e., CNDC _{lo} and CNDC _{up}) derived using the Bayesian framework should be used in calculation of N nutrition index (and other calculations) to account for uncertainty in %N _c . Overall, this study provides additional evidence that %N _c is dependent upon G × E × M interactions; therefore, evaluation of crop N status or N use efficiency must account for variation in %N _c across G × E × M interactions.
Suggested Reviewers:	Ignacio Ciampitti ciampitti@ksu.edu Dr. Ciampitti has authored a number of studies on similar topics to this manuscript and would be an excellent reviewer/editor.

	<p>Gilles Lemaire gilles.lemaire.inra@gmail.com Dr. Lemaire has authored a number of studies on similar topics to this manuscript and would be an excellent reviewer.</p>
	<p>David Makowski makowski@grignon.inra.fr Dr. Makowski has authored a number of studies on similar topics to this manuscript and would be an excellent reviewer.</p>
	<p>Javier Fernández jafernandez@ksu.edu Dr. Fernández has authored a number of studies on similar topics to this manuscript and would be an excellent reviewer.</p>
	<p>Victor Sadras victor.sadras@sa.gov.au Dr. Sadras has authored a number of studies on similar topics to this manuscript and would be an excellent reviewer.</p>

4 January 2023

To the Reviewers:

We would like to thank the two reviewers of this manuscript for their careful consideration of our work and helpful suggestions for improvement. In the revised manuscript we are resubmitting, we have addressed every reviewer comment in the manner specified below.

Reviewers' comments:

Reviewer #1:

Authors have made a great effort for improving their manuscripts. I observe that they have more particularly improved the statistical analysis. They have also tried to take into account of my own suggestion for formulating the hypothesis that a part of the "uncertainty" in the mono-phasic N dilution curve could be due to the fact that the true model would be bi-phasic? Authors have mentioned clearly this hypothesis... BUT they did not try to go further...! I think that without any more modification in their manuscript, authors should try to provide in "supplemental material" a log-log graph showing if yes or not the log%N-logBiomass is mono-phasic or bi-phasic? This information is important for discussing the "Genotype-Environment".... Perhaps the difference in the slopes (b_1 vs b_2) is low or undetectable and then the mono-phasic model is a good approximation.... or perhaps this difference is high enough and then it could lead to high uncertainty?

My own opinion is that the paper could be accepted in its present form, but that it would be a pity to not include this more fundamental aspect in the discussion of such a paper.

- *We thank the Reviewer for their insightful comments on this important research question that is worthy of follow-up investigation. However, we have chosen not to change the manuscript in response to this comment for the following reasons. First, data for this manuscript were aggregated on a whole plant basis (i.e., vines and tubers combined) (Table S2). Data segregated between vine and tuber for biomass and nitrogen concentration are not presently available for all studies included in this manuscript. Second, we find that the suggestion that the Reviewer is making is fundamentally outside of the primary scope of the present manuscript. Our contribution is focused on the novel application of statistical methods to detect differences in N dilution across G x E x M effects. While this question posed by the reviewer is necessarily related to the investigation of the source of variation in dilution across G x E x M effects, it is adjacent to our primary focus. In essence, we concur with the suggestion of Reviewer 2 from their comments on the original manuscript draft that "the paper [is] excessively (and unnecessary) long in several sections, so my first main suggestion is to reduce the length of the manuscript*

reorganizing paragraphs and ideas ... Similarly, I would suggest reducing the number of figures considering the complexity of the methodology and number of panels. I believe the paper will have more impact if ideas (including figures) are more succinct." *We hope to answer this important, although adjacent, research question suggested by Reviewer 1 in a subsequent manuscript while maintaining focus on the core research questions addressed in the current manuscript.*

Specific Comments:

- 4. Could the manuscript benefit from additional tables or figures, or from improving or removing (some of the) existing ones? – YES, I think that it should be important to test if the N dilution curve for potatoes is monophasic or bi-phasic....according to "only vegetative" and "vegetative+tuber" development as I suggested in my previous reviewing. This test should be realized in the discussion paragraph in order to know if part of uncertainty of the "mono-phasic" dilution model could be explained by variations in the phenology of cultivars?
 - Addressed in comments above.
- 7. Have the authors clearly stated the limitations of their study/theory/methods/argument? – See above remarks
 - Addressed in comments above.

Reviewer #2:

Authors addressed all suggested changes in the manuscript; I appreciate that the authors considered my comments. From my perspective the manuscript did improve considerably, and I recommend it to be accepted for publication.

- Thank you once again for the previous suggestions and comments. We agree that the manuscript has improved considerably as a result of suggestions from both Reviewers.

- Critical N dilution curves [CNDCs] for potato are subject to G x E x M effects
- Bayesian methods can quantify uncertainty in critical N concentration [%N_c]
- Partial pooling Bayesian method enables direct comparison of G x E x M effects
- Variation in %N_c for potato due to tuber initiation timing and tuber bulking rate
- N use efficiency and N nutrition index depend on %N_c variability and uncertainty

Notes detailing specific revisions can be found in the Covering Letter submitted with this Revised Manuscript.

[Click here to access/download](#)

Supplementary material for on-line publication only
bayesian-cndc-potato_eja-submission_supplement-
v1.docx

[Click here to access/download](#)

Supplementary material for on-line publication only
bayesian-cndc-potato_eja-submission_supplement-
v1.xlsx

Brian J. Bohman: Writing - Original Draft, Formal Analysis, Data Curation, Visualization, Investigation, Conceptualization, Methodology, Software

Michael J. Culshaw-Maurer: Writing - Original Draft, Methodology, Software, Formal Analysis, Visualization

Feriel Ben Abdallah: Writing - Review & Editing, Investigation, Data Curation

Claudia Giletto: Writing - Review & Editing, Investigation, Data Curation

Gilles Bélanger: Writing - Review & Editing, Investigation, Data Curation

Fabián G. Fernández: Writing - Review & Editing, Supervision

Yuxin Miao: Writing - Review & Editing, Supervision

David J. Mulla: Writing - Review & Editing, Supervision

Carl J. Rosen: Writing - Review & Editing, Project Administration, Funding Acquisition, Supervision, Investigation, Methodology, Data Curation, Resources

Declaration of interests

The authors declare that they have no known competing financial interests or personal relationships that could have appeared to influence the work reported in this paper.

The authors declare the following financial interests/personal relationships which may be considered as potential competing interests:

Carl J. Rosen reports financial support was provided by Minnesota Area II Potato Growers Research and Promotion Council.

1 1 **Quantifying critical N dilution curves across G × E × M effects for potato using a partially-**
2 2 **pooled Bayesian hierarchical method**

3 Brian J. Bohman^{1*}, Michael J. Culshaw-Maurer², Feriel Ben Abdallah³, Claudia Giletto⁴, Gilles
4 Bélanger⁵, Fabián G. Fernández¹, Yuxin Miao¹, David J. Mulla¹, and Carl J. Rosen¹

5 1. Department of Soil, Water, and Climate, University of Minnesota. 1991 Upper Buford
6 Circle, St. Paul MN 55108

7 2. CyVerse, University of Arizona, Tuscon, AZ

8 3. Productions in Agriculture Department, Crop Production Unit, Walloon Agricultural
9 Research Centre (CRA-W), Gembloux, Belgium

10 4. Unidad Integrada Balcarce, Facultad de Ciencias Agrarias (UNMdP)-INTA Balcarce. Ruta
11 226 km 73,5 (7620) Balcarce, Buenos Aires, Argentina

12 5. Science and Technology Branch, Agriculture and Agri-Food Canada, Québec City, Canada

13 * Corresponding Author: bohm0072@umn.edu

1
2
3
4 **Abstract:** Multiple critical N dilution curves [CNDCs] have been previously developed for potato;
5
6 however, attempts to directly compare differences in CNDCs across genotype [G], environment
7 [E], and management [M] interactions have been confounded by non-uniform statistical methods,
8
9 biased experimental data, and lack of proper quantification of uncertainty in the critical N
10
11 concentration [%N_c]. This study implements a partially-pooled Bayesian hierarchical method to
12
13 develop CNDCs for previously published and newly reported experimental data, systematically
14
15 evaluates the difference in %N_c [$\Delta\%N_c$] across G × E × M effects, and directly compare CNDCs
16
17 from the Bayesian framework to CNDCs from conventional statistical methods. The partially-
18
19 pooled Bayesian hierarchical method implemented in this study has the advantage of being less
20
21 susceptible to inferential bias at the level of individual G × E × M interactions compared to
22
23 alternative statistical methods that result from insufficient quantity and quality of experimental
24
25 datasets (e.g., unbalanced distribution of N limiting and non-N limiting observations). This method
26
27 also allows for a direct statistical comparison of differences in %N_c across levels of the G × E ×
28
29 M interactions. Where found to be significant, $\Delta\%N_c$ was hypothesized to be related to variation
30
31 in the timing of tuber initiation (e.g., maturity class) and the relative rate of tuber bulking (e.g.,
32
33 planting density) across G × E × M interactions. In addition to using the median value for %N_c
34
35 (i.e., CNDC), the lower and upper boundary values for the credible region (i.e., CNDC_{lo} and
36
37 CNDC_{up}) derived using the Bayesian framework should be used in calculation of N nutrition index
38
39 (and other calculations) to account for uncertainty in %N_c. Overall, this study provides additional
40
41 evidence that %N_c is dependent upon G × E × M interactions; therefore, evaluation of crop N status
42
43 or N use efficiency must account for variation in %N_c across G × E × M interactions.

1
2
3
4 36 **Keywords:** critical N concentration; critical nitrogen dilution curve; nitrogen nutrition index;
5
6 37 nitrogen use efficiency; potato; Bayesian; genotype-by-environment-by-management interactions
7
8
9
10 38

11
12
13
14 39 **Abbreviations:** NUE, nitrogen use efficiency; NUpE, nitrogen uptake efficiency; NUtE, nitrogen
15 utilization efficiency; NNI, nitrogen nutrition index; CNDC, critical nitrogen dilution curve;
16
17 41 CNUC, critical nitrogen uptake curve; CNUtEC, critical nitrogen utilization efficiency curve; W,
18
19 42 total dry weight plant biomass; N_{Plant} , plant nitrogen content, $\%N_{Plant}$, plant nitrogen concentration;
20
21 43 $\%N_c$, critical plant nitrogen concentration; NUtE_c, critical nitrogen utilization efficiency; $\Delta\%N_c$,
22
23
24 44 difference in critical nitrogen concentration; $\%N_{c,up}$, upper bounds of credible interval for critical
25
26 45 nitrogen concentration; $\%N_{c,lo}$, lower bounds of credible interval for critical nitrogen
27
28 46 concentration; NNI_{up}, upper bound of credible interval for nitrogen nutrition index value; NNI_{lo},
29
30
31 47 lower bound of credible interval for nitrogen nutrition index value; CNDC_{lo}, lower boundary of
32
33 48 credible region for critical nitrogen dilution curve; CNDC_{up}, upper boundary of credible region for
34
35 49 critical nitrogen dilution curve; G, genotype; E, environment; M, management; EONR,
36
37
38 50 economically optimum nitrogen rate
39
40
41
42
43 51
44
45
46
47
48
49
50
51
52
53
54
55
56
57
58
59
60
61
62
63
64
65

1
2
3
4 52 **1. Introduction**
5
6
7
8 53 Identifying optimal crop nitrogen [N] status to maximize growth and yield production is an elusive
9
10 54 goal. Traditionally, either the yield-goal approach or rate-response curves have been used to
11
12 55 identify optimal N fertilizer application rate (Morris et al., 2018). The N nutrition index [NNI] is
13
14 56 an alternative approach to the current paradigm and comprises a well-developed framework to
15
16 57 determine optimal crop N status (Lemaire et al., 2019). Typically, NNI is used to determine crop
17
18 58 N status using whole plant analysis and to direct adaptive N management within a growing season
19
20 59 (Houlès et al., 2007; Morier et al., 2015). The NNI framework has conventionally been considered
21
22 60 generalizable across E × M effects (e.g., year-to-year, geographic, or cultural practices variability)
23
24 61 and can be defined for any particular G effect (e.g., crop species or cultivar). In this manner, NNI
25
26 62 reflects intrinsic physiological properties and reflects absolute crop N status across variation in
27
28 63 environmental conditions (e.g., net soil N supply) or management practices (e.g., rate, source,
29
30 64 timing, and placement of N fertilizer) (Sadras & Lemaire, 2014).

36
37
38 65 The NNI approach is defined based on the allometric relationship of declining plant N
39
40 66 concentration [%N_{Plant}] with increasing plant biomass, referred to as the critical N dilution curve
41
42 67 [CNDC], which defines the critical N concentration [%N_c] below which relative growth rate is
43
44 68 reduced (Gastal et al., 2015):

45
46 69 %N_c = a W^{-b} [1]
47
48
49
50
51

52 70 where W represents dry weight plant biomass, and a and b are empirically fitted parameters.
53
54 71 Parameter a is numerically equivalent to %N_c expressed in units of g N 100 g⁻¹ when W is equal
55
56 72 to 1 Mg ha⁻¹, and parameter b represents the ratio of the relative rate of decline in %N_c to the
57
58
59
60
61
62
63
64
65

1
2
3
4 73 relative rate of increase in W. Using the CNDC, NNI values are then calculated as ratio of %N_{Plant}
5
6 74 and %N_c:

7
8
9
10 75 $NNI = \%N_{Plant} / \%N_c$ [2]
11
12
13
14
15
16
17
18
19
20
21
22
23
24
25
26
27
28
29
30
31
32
33
34
35
36
37
38
39
40
41
42
43
44
45
46
47
48
49
50
51
52
53
54
55
56
57
58
59
60
61
62
63
64
65

When NNI is greater than 1.0, crop N status is said to be in excess, and crop growth is not limited by N, while when NNI is less than 1.0, crop N status is deficient, and crop growth is limited by N. At NNI equal to 1.0, crop N status is optimal (Lemaire & Gastal, 1997).

A robust theoretical framework has been developed to explain decline in N concentration as biomass increases, but the application of this theory is most commonly restricted to the vegetative period where only metabolic and structural tissues are present (Greenwood et al., 1990; Justes et al., 1994; Sadras & Lemaire, 2014). Dilution of N in vegetative tissue occurs in relationship to an increasing proportion of structural biomass, with low N concentration, relative to metabolic (i.e., photosynthetic) biomass, with high N concentration (Lemaire & Gastal, 1997; Gastal et al., 2015).

Multiple previous studies have extended and empirically validated the CNDC relationships beyond its typical applications to describe declining N concentration over the entire crop growth cycle, including periods of reproductive growth, by including consideration of storage tissues in addition to structural and metabolic tissues (Greenwood et al., 1986; Duchenne et al., 1997; Plénet & Lemaire, 2000; Herrmann & Taube, 2004). Acceleration of N dilution beyond the vegetative period primarily occurs as low N biomass (i.e., starch) accumulates in storage tissues such as grain or tubers where the rate of decline is determined by the relative N concentration in storage biomass compared to vegetative biomass (Duchenne et al., 1997; Plénet & Lemaire, 2000). Duchenne et al. (1997) observed that as an increasing proportion of biomass accumulates in tubers, the rate of decline in N concentration increases with increasing biomass. Certain crops, such as potato,

1
2
3
4 95 exclusively use a CNDC based on whole plant biomass due to the complex relationship between
5
6 96 vine growth and tuber production (Duchenne et al., 1997; Bélanger et al., 2001a; Giletto &
7
8 97 Echeverría, 2015; Ben Abdallah et al., 2016). Despite the validity of this approach, interpreting
9
10 98 variation in CNDC observed between cultivars and geographies has been challenging.
11
12

13
14
15 99 However, recent work by Giletto et al. (2020) identified a mechanistic relationship underpinning
16
17 100 the observed empirical relationships in N dilution for potato. The CNDC based on whole plant
18
19 101 biomass reflects dilution in both the tuber and vine biomass, individually, and the increasing
20
21 102 proportion of biomass allocated to low concentrations of N in biomass (i.e., tubers) as whole plant
22
23 103 biomass increases. Giletto et al. (2020) also observed that varieties and locations with a greater
24
25 104 proportion of biomass allocated to tubers have a greater value for parameter b of the CNDC, where
26
27 105 parameter b of the CNDC represents the relative rate of decline in %N_c as biomass increases.
28
29
30

31
32
33 106 Based on this framework developed by Giletto et al. (2020), it is reasonable to expect that variation
34
35 107 in CNDC for potato would occur due to variation in total biomass and harvest index (i.e., timing
36
37 108 of tuber initiation, relative rate of tuber bulking) across G × E × M gradients. Understanding the
38
39 109 effects of G × E × M interactions on crop N requirements and status is critical to improving
40
41 110 agronomic outcomes and N use efficiency [NUE] within cropping systems (Lemaire & Ciampitti,
42
43 111 2020).

44
45
46
47
48
49 112 Previous CNDCs for potato have been developed with different statistical methods and limited
50
51 113 quantification of their uncertainty (Duchenne et al., 1997; Bélanger et al., 2001a; Giletto &
52
53 114 Echeverría, 2015; Ben Abdallah et al., 2016). This makes it difficult to ascertain whether observed
54
55 115 differences in CNDCs result from underlying G × E × M effects, are confounded by the limitations
56
57
58
59
60
61
62
63
64
65

1
2
3
4 116 of the statistical approach, or biased due to insufficient quantity or quality of experimental data
5
6 117 (e.g., unbalanced distribution of N limiting and non-N limiting observations).
7
8
9
10 118 The conventional approach to fit a CNDC consists of a two-step process: first, the critical points
11
12 119 from the relationship of %N_{Plant} as a function of biomass are selected using statistical criteria;
13
14 120 second, a negative exponential curve is fit to the subset of critical points using non-linear
15 regression. There are two commonly used statistical approaches to identify critical points: (1)
16
17 121 linear-plateau curve fit and (2) ANOVA and protected multiple comparison. Using a linear-plateau
18
19 curve to derive critical points was originally suggested by Justes et al. (1994). This approach is
20
21 rigorous and requires sufficient empirical data such that a linear-plateau curve can be identified
22
23 (i.e., at least one N limiting and at least two non-N limiting data points) for each observation date.
24
25
26 125 Therefore, this approach can be difficult or impossible to implement due to potential limitations
27
28 of the experimental data used such as insufficient levels of N treatments (i.e., fewer than three
29
30 treatment levels) or interactions between management practices and environmental conditions (i.e.,
31
32 all observations are either N limiting or non-N limiting). In contrast, many studies use methods
33
34 similar to Ben Abdallah et al. (2016) where critical points are determined using a simplified
35
36 statistical method. In this approach, ANOVA is first used to identify experimental dates where
37
38 variation in biomass is statistically significant. Subsequently, a protected multiple comparisons
39
40 analysis is used to identify which experimental treatments had the highest level of biomass – the
41
42 treatment level with the significantly greatest level of biomass is then defined as the critical point.
43
44
45 134 While this statistical method is more flexible to implement, it cannot resolve deficiencies in the
46
47 underlying empirical data (e.g., insufficient level of N treatments, interactions with environmental
48
49 conditions). Therefore, the critical points selected using the simplified method may be biased due
50
51 to inherent deficiencies of the underlying experimental data used.
52
53
54
55
56
57
58
59
60
61
62
63
64
65

1
2
3
4 139 Novel statistical methods developed first by Makowski et al. (2020) provide a framework which
5
6 140 allows for standardization in statistical approach and quantification of uncertainty for deriving in
7
8 141 CNDCs which enables comparison of %N_c across G × E × M interactions. In short, this framework
9
10 142 implements a hierarchical Bayesian model which simultaneously identifies critical points using
11
12 143 the linear-plateau method (e.g., Justes et al. (1994)) while fitting the negative exponential curve
13
14 144 which defines %N_c. The advantage of this method is that it fits the CNDC from the entire set of
15
16 145 experimental data for a given G × E × M interaction level and removes the arbitrary intermediate
17
18 146 step of separately identifying critical points. This approach has already been successfully used by
19
20 147 Ciampitti et al. (2021), Yao et al. (2021), and Fernández et al. (2021) to evaluate differences in
21
22 148 CNDCs across G × E × M interactions for maize, wheat, and tall fescue cropping systems,
23
24 149 respectively. Through this single-step process, the Bayesian hierarchical method both eliminates
25
26 150 the need to separately identify critical points and implements the theoretically preferred method
27
28 151 (e.g., linear-plateau curve fit) to select critical points.
29
30
31
32
33
34
35
36
37 152 The Bayesian hierarchical method, however, remains subject to inferential bias due to both limited
38
39 153 quantity and quality of experimental data (Fernández et al., 2021; Fernandez et al., 2022). With
40
41 154 respect to quantity, having an insufficient number of observations from a limited number of
42
43 155 experimental trials to derive an individual CNDC will result in increased bias in %N_c. With respect
44
45 156 to quality, using experimental data that does not reflect a full range of biomass values or does not
46
47 157 sufficiently represent both limiting and non-limiting N conditions will result in increased bias in
48
49 158 %N_c. Datasets used to derive the CNDC using the Bayesian hierarchical method should contain at
50
51 159 least eight experimental trials containing at least three N treatments and at least three sampling
52
53 160 dates (Fernández et al., 2022).

58
59
60
61
62
63
64
65

1
2
3
4 161 However, there are multiple approaches to pooling across $G \times E \times M$ interactions within the
5
6 162 Bayesian hierarchical method to address this bias due to experimental data limitations: no pooling,
7
8 163 full pooling, and partial pooling. The no pooling approach treats each experimental data level
9 independently where experimental data from one level is not used in inference for any other level
10
11 164 (McElreath, 2020). The no pooling approach was used by Makowski et al. (2020), Ciampitti et al.
12
13 165 (2021), Yao et al. (2021), and Fernández et al. (2021) to develop independent models for each G
14
15 166 $\times E \times M$ interaction. For the Bayesian hierarchical method, the no pooling approach is directly
16
17 167 limited by the quantity and quality of experimental data for each $G \times E \times M$ interaction level. The
18
19 168 full pooling approach, in contrast, treats each experimental data level in an equivalent manner
20
21 169 where the experimental data from all levels are used simultaneously for inference (McElreath,
22
23 170 2020). The full pooling approach was used by Fernández et al. (2021) to develop a single model
24
25 171 across $G \times E \times M$ interaction levels. While this approach was found by Fernández et al. (2021) to
26
27 172 potentially reduce inferential bias from the Bayesian hierarchical method (i.e., by increasing the
28
29 173 combined quantity and quality of data used to fit a given CNDC), the fully pooled approach has
30
31 174 the explicit tradeoff that inference at individual levels of $G \times E \times M$ interactions is not possible.
32
33 175 The partial pooling approach balances the tradeoffs between fitting a single population-level model
34
35 176 (i.e., full pooling) and fitting multiple independent group-level models (i.e., no pooling) by using
36
37 177 the entire set of experimental data to fit a single model with where the data from all other levels of
38
39 178 an effect influence the inference for a particular level and reduce inferential bias (McElreath,
40
41 179 2020). In this manner, individual effect levels are said to be “borrowing strength” through the
42
43 180 process of “shrinkage”, where more extreme values are pulled toward the average (Lindstrom &
44
45 181 Bates, 1990; Bates, 2010). Therefore, using a partially-pooled Bayesian hierarchical method
46
47 182 should reduce the inferential bias for a given $G \times E \times M$ interaction level where the quantity and
48
49 183 should reduce the inferential bias for a given $G \times E \times M$ interaction level where the quantity and
50
51 184 should reduce the inferential bias for a given $G \times E \times M$ interaction level where the quantity and
52
53 185 should reduce the inferential bias for a given $G \times E \times M$ interaction level where the quantity and
54
55 186 should reduce the inferential bias for a given $G \times E \times M$ interaction level where the quantity and
56
57 187 should reduce the inferential bias for a given $G \times E \times M$ interaction level where the quantity and
58
59 188 should reduce the inferential bias for a given $G \times E \times M$ interaction level where the quantity and
60
61 189 should reduce the inferential bias for a given $G \times E \times M$ interaction level where the quantity and
62
63 190 should reduce the inferential bias for a given $G \times E \times M$ interaction level where the quantity and
64
65 191 should reduce the inferential bias for a given $G \times E \times M$ interaction level where the quantity and

1
2
3
4 184 quality of experimental data are not otherwise sufficient and enable inference for each individual
5
6 185 $G \times E \times M$ interaction level. However, the partial pooling approach has not yet been implemented
7
8 186 within in the Bayesian hierarchical method to derive CNDCs.
9
10
11
12

13 187 Building upon previous work, the objectives of this study are to 1) develop CNDCs using the
14
15 188 hierarchical Bayesian framework for potato varieties in Minnesota (from both previously
16
17 189 published and unpublished experimental data) and for potato varieties in Argentina (Giletto &
18
19 190 Echeverría, 2015), Canada (Bélanger et al., 2001a), and Belgium (Ben Abdallah et al., 2016) (from
20
21 191 previously published experimental data), 2) extend the implementation of the hierarchical
22
23 192 Bayesian framework using a partial pooling approach to compare CNDCs across $G \times E \times M$
24
25 193 interactions based on the uncertainty in $\%N_c$ and curve parameters a and b , 3) identify the optimal
26
27 194 methods to determine uncertainty in $\%N_c$ for use in calculating NNI and other derivative metrics,
28
29 195 and 4) compare CNDCs developed with the hierarchical Bayesian framework methods to
30
31 196 previously published CNDCs for the same data with different statistical methods.
32
33
34
35
36
37
38
39 197 **2. Materials and Methods**
40
41
42 198 *2.1. Experimental Data*
43
44
45
46 199 This study combines experimental data from both newly reported and previously published sources
47
48 200 (Ben Abdallah et al., 2016; Giletto et al., 2020). The data used for analysis in this study are
49
50 201 summarized in Table 1 and the relevant methods related to the experimental trials are reported
51
52 202 below. All individual experimental observations used in this study are presented in the
53
54 203 Supplemental Materials (Table S1).
55
56
57
58
59
60
61
62
63
64
65

1
2
3
4
5 **Table 1.** Summary of experimental data used in this study.

Study	Location	Variety	Site-Years	Sampling Dates	Samples
Present Study	Minnesota	Clearwater	2	10	30
		Dakota Russet	2	14	70
		Easton	2	14	70
		Russet Burbank	9	52	328
		Umatilla Russet	2	10	30
Giletto et al. (2020)	Argentina	Bannock Russet	3	13	52
		Gem Russet	4	18	72
		Innovator	4	18	72
		Markies Russet	2	9	36
		Umatilla Russet	3	14	56
Ben Abdallah et al. (2016)	Canada	Russet Burbank	4	30	104
		Shepody	4	30	105
Belgium		Bintje	17	49	238
		Charlotte	7	24	114

204
205 2.1.1. Newly Reported Data – Minnesota

206 Six individual plot-scale field experiments were conducted over a total of eight years (MN-1:
207 1991–1992; MN-2: 2014-2015, MN-3: 2016, MN-4: 2018-2019, MN-5: 2019, MN-6: 2020) at the
208 Sand Plain Research Farm [SPRF] in Becker, MN ($45^{\circ} 23' N$, $93^{\circ} 53' W$). A summary of the
209 treatments and sampling design for each experiment is presented in Table 2, and a summary of key
210 experimental factors across G, E, and M effects are presented in Table 3.

211 A randomized complete block design with three or four replicates was used in each field
212 experiment. All experiments evaluated at least three N rates ($0 - 400 \text{ kg N ha}^{-1}$) for Russet Burbank
213 potato [*Solanum tuberosum* (L.)], with some studies evaluating additional potato varieties (Table
214 2). Nitrogen fertilizer was applied using various source and timing regimes including polymer
215 coated urea applied at planting and/or emergence, split-applied urea and urea-ammonium nitrate
216 at emergence and/or post-emergence, ammonium nitrate at planting, emergence, and/or post-
217 emergence. Experiments that evaluated multiple varieties had either a factorial design, or split-plot
218 design with variety treatment as the whole-plot and N treatment as the split-plot. Plots in these

1
 2
 3
 4 219 studies were between 5.4 – 6.4 m wide (6 or 7 × 0.9 m rows) and 6.1 – 9.1 m long. Experiments
 5
 6 220 were planted each year in late-April to early-May and were mechanically harvested in mid-
 7
 8 221 September with vines terminated one to two weeks prior to harvest. Apart from experimental N
 9
 10 222 and variety treatments, all management and cultural practices were managed by the staff at the
 11
 12 223 SPRF in accordance with common practices for the region (Egel, 2017). Nutrients were applied
 13
 14 224 based on soil samples and University recommendations (Franzen et al., 2018; Rosen, 2018), and
 15
 16 225 supplemental irrigation was applied based on the University recommended checkbook method
 17
 18 226 (Wright, 2002; Steele et al., 2010). Additional details on experimental procedures for these studies
 19
 20 227 have been previously reported (Table 2).
 21
 22
 23
 24
 25
 26
 27

Table 2. Summary of newly reported experimental small-plot trials in Minnesota, USA

Experiment	Year	N trts. [†]	N rates [kg ha ⁻¹]	Varieties	Sampling Dates	Reference
MN-1	1991	10	0, 135,	Russet Burbank	12 June, 24 June, 2 July,	Rosen et al. (1992); Rosen et al. (1993); Errebbi et al. (1998)
			180, 225,		16 July, 30 July, 13 Aug.,	
			270		10 Sept.	
	1992	10	0, 135, 180, 225, 270	Russet Burbank	10 June, 25 June, 17 July, 5 Aug., 26 Aug., 15 Sept.	
MN-2	2014	5	135, 200, 270, 335,	Russet Burbank, Dakota Russet,	30 June, 15 July, 24 July,	Sun (2017); Sun et al. (2019); Sun et al. (2020)
			400	Easton	11 Aug., 26 Aug., 8 Sept., 15 Sept.	
			135, 200, 270, 335,	Russet Burbank, Dakota Russet,	23 June, 7 July, 21 July, 4 Aug., 17 Aug., 1 Sept., 16 Sept.	
	2015	5	400	Easton		
MN-3	2016	4	45, 180, 245, 335	Russet Burbank	28 June, 13 July, 26 July, 3 Aug., 10 Aug., 13 Sept.	Crants et al. (2017)
MN-4	2018	3	135, 270, 400	Russet Burbank, Clearwater, Umatilla Russet	26 June, 10 July, 18 July, 1 Aug., 13 Sept.	Gupta and Rosen (2019); Gupta et al. (2020); Li et al. (2021)
			135, 270, 400	Russet Burbank, Clearwater, Umatilla Russet	26 June, 11 July, 24 July, 7 Aug., 16 Sept.	
MN-5	2019	8	45, 155, 245, 290, 335	Russet Burbank	25 June, 9 July, 23 July, 6 Aug., 21 Aug., 16 Sept	Bohman et al. (2020)
MN-6	2020	8	55, 155, 245, 270, 290, 335	Russet Burbank	24 June, 7 July, 22 July, 4 Aug., 16 Sept.	Rosen et al. (2021)

[†] Including N source, timing, and placement combinations occurring at an equivalent N rate

1
2
3
4 228 Samples of vine biomass were harvested immediately prior to mechanical termination for
5
6 229 determination of fresh weight vine yield. Harvested tubers were mechanically sorted into weight
7
8 230 classes and graded (USDA, 1997), and fresh weight tuber yield was determined as the sum of all
9
10 231 weight classes and tuber grades. Harvested biomass was oven dried at 60°C to determine dry matter
11
12 232 content of vines and tubers. Dry weight tuber and vine biomass was calculated as the product of
13
14 233 fresh weight and dry matter content for each tissue respectively. Total N concentration of vines
15
16 234 and tubers was determined from subsamples of plant tissues with either combustion analysis
17
18 235 (Elementar Vario EL III, Elementar Americas Inc., Mt. Laurel, NJ) using standard methods
19
20 236 (Horneck & Miller, 1998), or with the salicylic Kjeldahl method (Horwitz et al., 1970). Total N
21
22 237 content of vines and tubers was calculated as the product of N concentration and dry weight
23
24 238 biomass for each tissue respectively. Total plant N content [N_{Plant}] (kg N ha^{-1}) was calculated from
25
26 239 the sum of tuber and vine N content. Total plant dry weight biomass [W] ($\text{Mg dry wt. ha}^{-1}$) was
27
28 240 calculated from the sum of vine and tuber dry weight biomass. Plant N concentration [% N_{Plant}] (g
29
30 241 N 100 g^{-1} dry wt.) was calculated as the ratio of N_{Plant} to W.
31
32
33
34
35
36
37
38
39 242 Whole-plant samples were also regularly collected during the period of late-May to early-
40
41 243 September (Table 2). Two to three plants were harvested from each plot on four to six dates each
42
43 244 year with vines, roots, and tubers each measured separately. Dry weight biomass, N concentration,
44
45 245 and N content for vines and tubers were determined for these in-season plant tissue samples using
46
47 246 the methods described above. Calculations for W, N_{Plant} , and % N_{Plant} were the same as methods
48
49 247 previously described above.
50
51
52
53
54

55 248 2.1.2. Previously Published Data – Belgium, Argentina, and Canada
56
57
58
59
60
61
62
63
64
65

1
2
3
4 249 Data reported in two previous studies, Giletto et al. (2020) and Ben Abdallah et al. (2016), were
5
6 250 included in the analysis conducted for the present study. The data from Giletto et al. (2020)
7
8 251 comprises two separate experimental data sets from small-plot experiments conducted in Balcarce
9
10 252 in the province of Buenos Aires, Argentina ($37^{\circ} 45' S$; $58^{\circ} 18' W$) (Giletto & Echeverría, 2015)
11
12 253 and in the upper St. John River Valley of New Brunswick, Canada ($47^{\circ} 03' N$; $67^{\circ} 45' W$)
13
14 254 (Bélanger et al., 2000, 2001a, 2001b). All data from the Giletto et al. (2020) study used in the
15
16 255 present analysis was included in this previous publication.
17
18
19
20
21

22 256 The data from Ben Abdallah et al. (2016) represents multiple experimental data set from small-
23
24 257 plot experiments were conducted in Gembloux, Belgium ($50^{\circ} 33' N$; $4^{\circ} 43' E$). Only a portion of
25
26 258 the data from the Ben Abdallah et al. (2016) study used in the present analysis was included in this
27
28 259 previous publication – while the dry weight biomass data were previously reported, the N
29
30 260 concentration data from the Ben Abdallah et al. (2016) experiment is reported for the first time in
31
32 261 this work.
33
34
35
36
37

38 262 A summary of experimental data from each trial used in the present study is presented in Table 1,
39
40 263 and a summary of key experimental factors across G, E, and M effects is presented in Table 3.
41
42
43

44 264
45
46
47
48
49
50
51
52
53
54
55
56
57
58
59
60
61
62
63
64
65

14
15
16
17
18
1920 265
21

Table 3. Comparison of key experimental factors including for Genotype [G]: variety maturity class [Maturity Class]; Environment [E]: soil texture classification [Soil Texture], dates of typical growing season [Growing Season], soil organic matter content [OM], growing season mean daily temperature [T_{Mean}], growing season cumulative precipitation [Precip.], growing season mean diurnal temperature difference [$\Delta T_{Diurnal}$] calculated as the average of daily diurnal temperature difference (i.e., difference between daily max temperature and daily minimum temperature), growing season cumulative growing degree days [GDD] calculated with base temperature of 7 °C and maximum temperature of 30 °C, growing season mean daily incident solar radiation [Sol. Rad.]; and Management [M]: planting density [Density], N fertilizer application source and timing [N Source & Timing], and use of supplemental irrigation [Irr.].

Location	Variety	G		E						M			
		Maturity Class [†]	Soil Texture [‡]	OM [%]	Growing Season [§]	T_{Mean} [°C]	Precip. [mm]	$\Delta T_{Diurnal}$ [°C]	GDD [°C d]	Sol. Rad. [MJ m ⁻²]	Density [plants ha ⁻¹]	N Source & Timing [¶]	Irr.
Argentina	Bannock Russet	L to VL	L	4.2 – 5.2	1 June – 10 Oct.	18.4	428	13.6	1739	25.5	59,000	Urea @ PL	Yes
	Gem Russet	M to L											
	Innovator	E to M											
	Markies Russet	L to VL											
	Umatilla Russet	ML to L											
Belgium	Bintje	L	SiCL, SiL, L, SL	1.3 – 2.6	10 Oct. – 10 Mar.	15.5	244	8.3	1313	20.0	38,000	AN @ PL	No
	Charlotte	M											
Canada	Russet Burbank	L to VL	CL, L	2.6 – 3.0	20 Apr – 20 Sept.	15.7	371	10.0	1150	19.1	29,000 44,000	AN @ PL	Yes
	Shepody	E to ME											
Minnesota	Clearwater	ML	LS	1.3 – 2.5	1 May – 15 Sept.	18.9	383	11.6	1638	22.7	36,000*	AN, Urea, UAN, and/or PCU @ PL, EM, and/or P-EM	Yes
	Dakota Russet	ML											
	Easton	L											
	Russet Burbank	L to VL											
	Umatilla Russet	ML to L											

† Early [E], medium-early [ME], medium [M], medium-late [ML], late [L], very late [VL] as classified by Stark et al. (2020), OSU (2021), Giletto & Echeverría (2015), CFIA (2013), AHDB (2015), Thompson (2013), and Porter (2014)

‡ Silty clay loam [SiCL], clay loam [CL], silt loam [SiL], loam [L], sandy loam [SL], loamy sand [LS]

§ Summary weather data based on typical growing season dates and historical climate reconstruction for the period of 1980-2016 (Gelaro et al., 2017; Weather Spark, 2021)

¶ Ammonium nitrate [AN], urea-ammonium nitrate [UAN], polymer-coated urea [PCU], planting [PL], emergence [EM], post-emergence [P-EM]

* Russet Burbank in MN-1 was planted at a density of 48,000 plants ha⁻¹

266

267

268

269

270

271

272

273

274

275

1
2
3
4
5 269 2.2. Statistical Methods
6
7
8
9 270 Based on the general approach outlined by Makowski et al. (2020), this study implemented a
10
11 271 partially-pooled Bayesian hierarchical framework to infer CNDC parameters for each location and
12
13 272 variety within location, assess the uncertainty in model parameters and %N_c, and compare fitted
14
15 273 CNDCs across the effects of location and variety.
16
17
18
19
20 274 The Bayesian hierarchical framework outlined by Makowski et al. (2020) was extended to
21
22 275 explicitly include the G × E × M interaction levels within the fitted model using a partial pooling
23
24 276 approach. Experimental data were nested according to location and variety within location, where
25
26 277 the linear-plateau curve fitted for each experimental sampling date is nested within a given level
27
28 278 of variety within location (Figure 1). This model structure leverages the advantages of partial
29
30 279 pooling to addresses the limitations identified by Fernández et al. (2021) that a sufficient quantity
31
32 279 and quality of experimental data are required while still enabling direct inference on the individual
33
34 280 G × E × M interaction levels. Using *R* (R Core Team, 2021a), the *brms* package (Bürkner, 2017,
35
36 281 2018) was used to implement the statistical framework outlined by Makowski et al. (2020) with
37
38 282 the modifications as previously described (Figure 1). The *brms* package, an interface to *Stan*
39
40 283 (Carpenter et al., 2017), was chosen due to the ability to include group-level effects (i.e., random
41
42 284 effects) which allows for the fit of this particular partially-pooled Bayesian hierarchical model.
43
44 285 The *brms* package includes a user-friendly modeling language, robust documentation, and a
45
46 286 diverse set of tools to analyze and assess models.
47
48
49 287 288
50
51
52
53
54
55
56
57
58
59
60
61
62
63
64
65

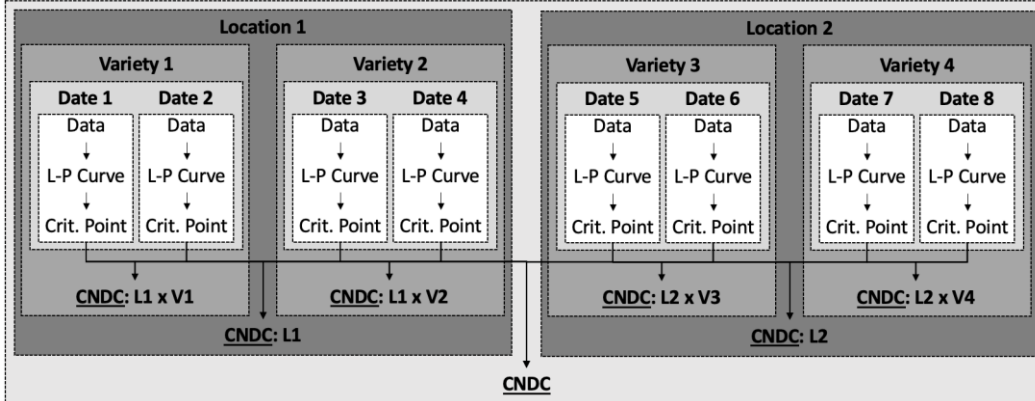


Figure 1. Flowchart showing nested structure used to fit critical N dilution curves [CNDC] using the hierarchical Bayesian method based on Makowski et al. (2020). Linear-plateau (L-P) curves and critical points (i.e., the fitted join point of each linear-plateau curve) are identified at the level of each experimental sampling date and pooled at various levels of location and variety within location to determine the CNDC for that level. This hierarchical model structure simultaneously fits all individual levels of location and variety within location, as well as for the global level of all experimental data, which allows for direct comparison across levels.

289
290 A non-linear *brms* model was defined by combining the two separate expressions used by
291 Makowski et al. (2020) to parameterize the Bayesian hierarchical model as previously
32 implemented with *rjags* (Plummer, 2019) and *JAGS* statistical software (Plummer, 2013).

36 293 The first expression from Makowski et al. (2020) represents the linear-plateau component:

38 294
$$W = \min(W_{Max,i} + S_i \cdot (\%N_{Plant} - \%N_c), W_{Max,i}) \quad [3]$$

42 295 where S_i and $W_{Max,i}$ are the slope of the linear-plateau curve and the maximum value of biomass
43 (i.e., plateau) for a given date [i], respectively, \min represents the minima function (i.e., the plateau
46 component), and W , $\%N_{Plant}$, and $\%N_c$ have the same meaning as previously defined in this present
47 study. This linear-plateau curve is defined with N concentration as the independent variable and
51 biomass as the dependent variable and is written in point-slope form where the reference point
53 used is the critical point.

57 301 The second expression from Makowski et al. (2020) represents the CNDC component:

1
2
3
4 302 $\%N_c = a W_{Max,i}^{-b}$ [4]
5
6
7

8 303 where a and b are the parameters that define the negative exponential curve and $\%N_c$ and $W_{Max,i}$
9
10 304 have the same meanings as defined above.
11
12

13
14 305 Using algebraic substitution (i.e., for $\%N_c$), these two expressions (Eq. [3] and Eq. [4]) were
15
16 306 combined to produce following non-linear *brms* model formula:
17
18

19
20 307 $W \sim min(W_{Max,i} + S_i (\%N_{Plant} - (a W_{Max,i}^{-b})), W_{Max,i})$ [5]
21
22

23 308 Two group-level (i.e., random) effects were specified for this *brms* model to parameterize the
24
25 309 nested structure (Figure 1). First, the parameters S and W_{Max} included group-level effects to fit a
26
27 310 linear-plateau curve to each experimental sampling date:
28
29
30

31 311 $W_{Max} + S \sim 1 + (1 | index)$ [6]
32
33
34

35 312 where *index* represents the unique level of each experimental sampling date, nested within a given
36
37 313 level of variety within location. Second, the parameters a and b included group-level effects to fit
38
39 314 the CNDC:
40
41
42

43 315 $a + b \sim 1 + (1 | location) + (1 | location:variety)$ [7]
44
45
46

47 316 where *location* and *location:variety* represents the unique effect level for location and variety
48
49 317 within location, respectively. Models were fit using treatment-level means (i.e., an effect of
50
51 318 *replicate* was not included in the model).
52
53
54

55 319 The *brms* model was fitted using 4 chains and 10000 iterations with 3000 warmups per chain.
56
57

58 320 Model convergence was verified by determining that all parameters had satisfactory R-hat values
59
60 321 of less than 1.01 with bulk-ESS and tail-ESS values of at least 100 samples per chain (Vehtari et
61
62
63
64

4 322 al., 2021). The priors for this model were chosen based on expert knowledge (i.e., previously
 5 reported values), empirical observations (i.e., summary values from the data set), and inspection
 6 of the joint prior predictive distribution. Evaluating the joint prior predictive distribution is
 7 particularly important for hyperparameters dealing with the standard deviation between groups in
 8 a hierarchical model due to the propagation of variance throughout model levels. If a set of
 9 relatively uninformative priors led to biologically or physically impossible predictions which
 10 prevented model convergence, the prior ranges were narrowed (Schad et al., 2021). In particular,
 11 325 a positive value for S is required to represent the positive physiological relationship between W
 12 and $\%N_{Plant}$ (i.e., linear-plateau curve where W increases as $\%N_{Plant}$ up to W_{max} at $\%N_c$). Similarly,
 13 having non-positive value for W_{max} is physically impossible. A summary of the prior values used
 14 326 in this model is given below (Table 4).

Table 4. Priors used in fitting the hierarchical Bayesian model with *brms*.

Parameter	Distribution	Bounds	
		Lower	Upper
a	Normal (5.3, 0.1)	0	∞
$\sigma(a location)$	Normal (0.10, 0.02)	$-\infty$	∞
$\sigma(a location:variety)$	Normal (0.05, 0.01)	$-\infty$	∞
b	Normal (0.40, 0.01)	0	1
$\sigma(b location)$	Normal (0.05, 0.02)	$-\infty$	∞
$\sigma(b location:variety)$	Normal (0.02, 0.01)	$-\infty$	∞
W_{max}	Normal (8.0, 0.1)	1	∞
$\sigma(W_{max,index})$	Normal (7.0, 1.0)	$-\infty$	∞
S	Normal (6.0, 0.1)	0	∞
$\sigma(S_{index})$	Normal (1.0, 0.1)	$-\infty$	∞
σ	Student's t (3, 1.0, 0.1)	$-\infty$	∞

47 333 The entire statistical and data workflow used to generate this analysis is reproducible and available
 48
 49 334 via GitHub repository (<https://github.com/bohm0072/bayesian-cndc-potato>). The *renv* package
 50
 51 335 (Ushey, 2021) was used to document the computing environment utilized while conducting this
 52
 53 336 analysis to ensure code portability and reproducibility.

60 338 2.3. Evaluating Uncertainty

1
2
3
4 339 2.3.1. Critical N Dilution Curve Parameter Uncertainty
5
6
7

8 340 After the statistical model was successfully fit to the data (n=28,000 draws), values for parameters
9
10 341 a and b of the CNDC were reported at the 0.05, 0.50 (i.e., median) and 0.95 quantiles for the effect
11
12 342 levels of *location* and *location:variety* to determine the 90% credible interval for each parameter.
13
14
15 343 The correlation between values for parameters a and b was determined for each effect level of
16
17 344 *location:variety* using the fitted parameter values at the level of the individual draws.
18
19
20

21 345 2.3.2. Critical N Concentration Uncertainty
22
23

24 346 Uncertainty in %N_c was characterized using three methods: (1) directly modeled 0.05 and 0.95
25
26 347 quantile value of posterior distribution of %N_c; (2) parameterized approximation of 0.05 and 0.95
27
28 348 quantile value of posterior distribution of %N_c; (3) indirect calculation of %N_c using 0.05 and 0.95
29
30 349 quantile values for a and b .
31
32
33

34
35 350 For the directly modeled method, %N_c for a set of discrete values of W between 1 Mg dry wt. ha⁻¹
36
37 351 ¹ and the maximum observed value of W in the experimental data set was calculated for each
38
39 352 individual posterior draw based on the fitted values of parameters a and b for that draw. From the
40
41 353 distribution of %N_c values, the 0.05, 0.50 (i.e., median) and 0.95 quantile values were identified
42
43 354 for each effect level of *location:variety* to determine the 90% credible region for %N_c. This
44
45 355 approach makes maximal use of the jointly estimated parameters contained in the posterior
46
47 356 distribution.
48
49

50
51
52
53 357 For the parameterized approximation method, two negative exponential curve of the same form as
54
55 358 the CNDC (i.e., $y = a x^{-b}$) were fit using *nls* (R Core Team, 2021b) to the 0.05 and 0.95 quantile
56
57 359 values of the posterior distribution of %N_c computed using the directly modeled method described
58
59

above. This approach to derive parameterized approximation of the 90% credible region attempts to simplify the complexity of communicating and propagating uncertainty in $\%N_c$. These parameterized curves approximating the upper and lower boundaries of the credible region for the CNDC are respectively referred to as $CNDC_{up}$ and $CNDC_{lo}$, where parameters a_{up} and b_{up} correspond to $CNDC_{up}$ and parameters a_{lo} and b_{lo} correspond to $CNDC_{lo}$:

$$365 \quad \%N_{c,lo} = a_{lo} W^{-b_{-lo}} \quad [8]$$

$$366 \quad \%N_{c,up} = a_{up} W^{-b_{-up}} \quad [9]$$

For the indirect calculation method, an estimate of the 90% credible region for $\%N_c$ was calculated by using the boundary values of the 90% credible interval of parameters a and b . The estimate for the upper boundary of the credible region for $\%N_c$ was determined from the 0.95 quantile value for parameter a and 0.05 quantile value for parameter b ; the estimate for the lower boundary of the credible region of $\%N_c$ was determined from the 0.05 quantile value for parameter a and 0.95 quantile value for parameter b . This approach does not account for the joint estimation of parameters offered by the Bayesian approach; therefore, the paired combination for parameters a and b (i.e., 0.05 and 0.95 quantiles, respectively) might not actually occur in the posterior distribution.

Difference in critical N concentration [$\Delta\%N_c$] were calculated as the difference between a reference value [$\%N_{c,ref}$] and a comparison value [$\%N_{c,i}$]:

$$378 \quad \Delta\%N_c = \%N_{c,ref} - \%N_{c,i} \quad [10]$$

To compare differences between the various methods used to quantify uncertainty in $\%N_c$, $\Delta\%N_c$ was calculated (Eq. [10]) where $\%N_{c,ref}$ was set as the median value (i.e., 0.50 quantile) of $\%N_c$

1
2
3
4 381 from the directly modeled method, while $\%N_{c,i}$ was varied and set as the upper and lower values
5
6 382 of $\%N_c$ from the directly modeled, parameterized approximation, and indirect calculation methods
7
8 383 as described above.
9
10
11
12

13 384 2.3.3. Comparing Critical N Concentration across $G \times E \times M$ Effects
14
15

16 385 Using the directly modeled method described above, $\%N_c$ for each posterior draw was calculated.
17
18 386 At the effect level of *location:variety*, $\Delta\%N_c$ was calculated (Eq. [10]) where $\%N_{c,ref}$ is the median
19
20 387 $\%N_c$ from the posterior distribution for the reference level and $\%N_{c,i}$ was the median $\%N_c$ from
21
22 388 the posterior distribution for each pairwise comparison of all other levels. From this computed set
23
24 389 of $\Delta\%N_c$, the 0.05, 0.50 (i.e., median) and 0.95 quantile values were identified for each pairwise
25
26 390 comparison of *location:variety* levels to determine the 90% credible region for $\Delta\%N_c$. The
27
28 391 comparison curve was considered to be not significantly different from the reference curve when
29
30 392 the 90% credible region for $\Delta\%N_c$ contained zero. This approach allows for the direct evaluation
31
32 393 of differences in $\%N_c$ across $G \times E \times M$ effects (i.e., *location:variety* levels).
33
34
35
36
37
38

39 394 2.3.4. Comparing Critical N Concentration across Statistical Methods
40
41

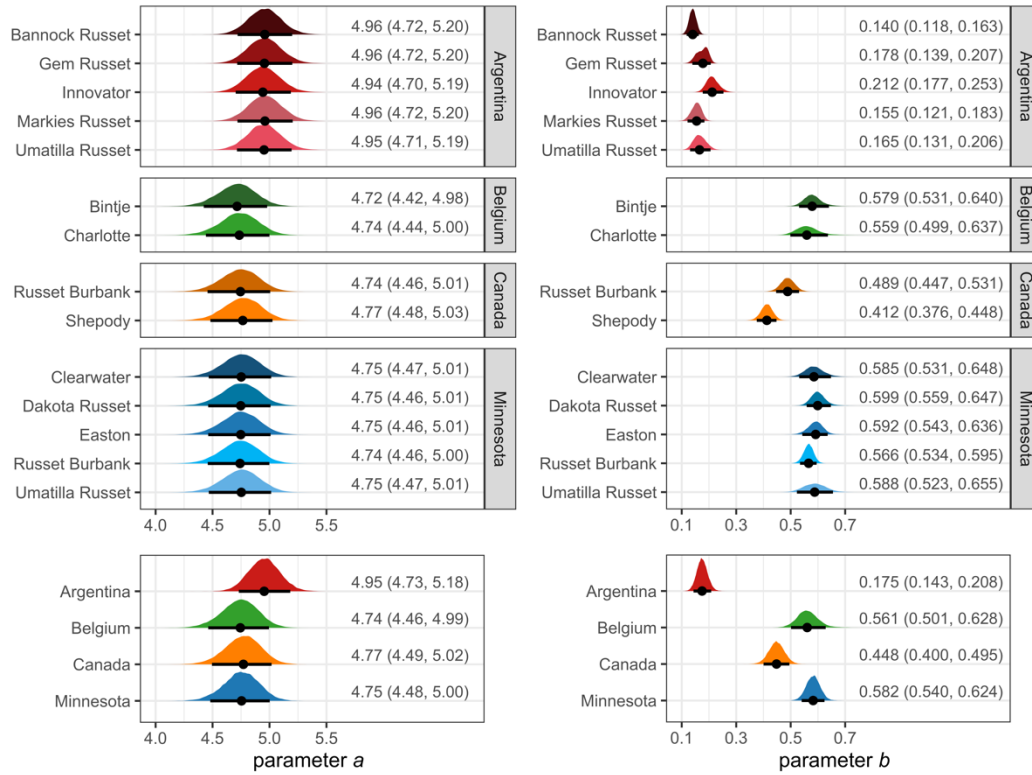
42 395 An analogous method was also used to compare the CNDCs fitted in the present study to the
43
44 396 CNDCs published in previous studies (i.e., Ben Abdallah et al. (2016); Giletto et al. (2020)).
45
46 397 Specifically, $\Delta\%N_c$ for each level of *location:variety* with previously published CNDC was
47
48 398 calculated (Eq. [10]) using where $\%N_{c,ref}$ was set as the median value (i.e., 0.50 quantile) of $\%N_c$
49
50 399 from the directly modeled method, and $\%N_{c,i}$ was set as the previously published values of $\%N_c$.
51
52 400 If $\Delta\%N_c$ falls outside of the 90% credible region for $\%N_c$ determined from the directly modeled
53
54 401 method, then the two curves are determined to be significantly different over the range for which
55
56 402 the previous value falls outside of the credible region. This approach allows for direct evaluation
57
58
59
60 403
61
62
63
64
65

1
2
3
4 403 of differences in %N_c for CNDCs developed from the same set of data across various statistical
5
6
7 404 methods.
8
9
10

11 405 **3. Results**
12
13
14

15 406 *3.1. Fitted Critical N Dilution Curve*
16
17

18 407 The posterior distribution of fitted values for CNDC parameters a and b are presented in Figure 2
19
20 408 showing the median value and 90% credible interval (i.e., 0.05 and 0.95 quantile values). For
21
22 409 parameter a , there was no significant difference for the effect of location at 90% credible interval
23
24 410 threshold (Figure 2a). Although Argentina has a numerically greater value of parameter a (4.95)
25
26 411 than the other three locations (4.74 – 4.77), these differences are not significant. Additionally, the
27
28 412 variation in parameter a for the variety within location effect is negligible and not statistically
29
30 413 significant (Figure 2a).
31
32
33 414
34
35
36
37
38
39
40
41
42
43
44
45
46
47
48
49
50
51
52
53
54
55
56
57
58
59
60
61
62
63
64
65



(a)

(b)

Figure 2. Posterior distribution of variety and variety within location effects for (a) parameter *a*; and (b) parameter *b*. Points represent median value and line represents 0.05 and 0.95 quantile range. Values displayed with the figures are the median value with the 90% credible interval boundaries (i.e., 0.05 and 0.95 quantiles) displayed within the parentheses.

For parameter *b*, there were significant differences for both the effect of location and variety within location at a 90% credible interval threshold (Figure 2b). For location, Argentina had the lowest value for parameter *b* (0.175), while Canada had a greater value for parameter *b* (0.448) than Argentina but lower than either Belgium (0.561) or Minnesota (0.582). The difference between parameter *b* for Belgium and Minnesota was not significant. For the variety within location effect, parameter *b* significantly varied for varieties in Argentina and Canada, while there were no significant differences in parameter *b* within either Belgium or Minnesota. For Argentina, Innovator had the greatest value for parameter *b* (0.212), followed by Gem Russet, Umatilla Russet, Markies Russet, and Bannock Russet (0.178, 0.165, 0.155, and 0.140, respectively). The

difference between Innovator and Umatilla Russet, Markies Russet, and Bannock Russet was significant, while all other differences between varieties were not significant. For Canada, Russet Burbank had a significantly higher value for parameter b (0.489) than Shepody (0.412).

There was a positive correlation found between parameters a and b (Figure 3) which indicates that quantifying differences in these parameter values independently (Figure 2) is not appropriate to describe the uncertainty in $\%N_c$ determined by the correlated parameters. Stated alternatively, significant differences for either parameter a or b do not necessarily imply that differences in $\%N_c$ are also significant.

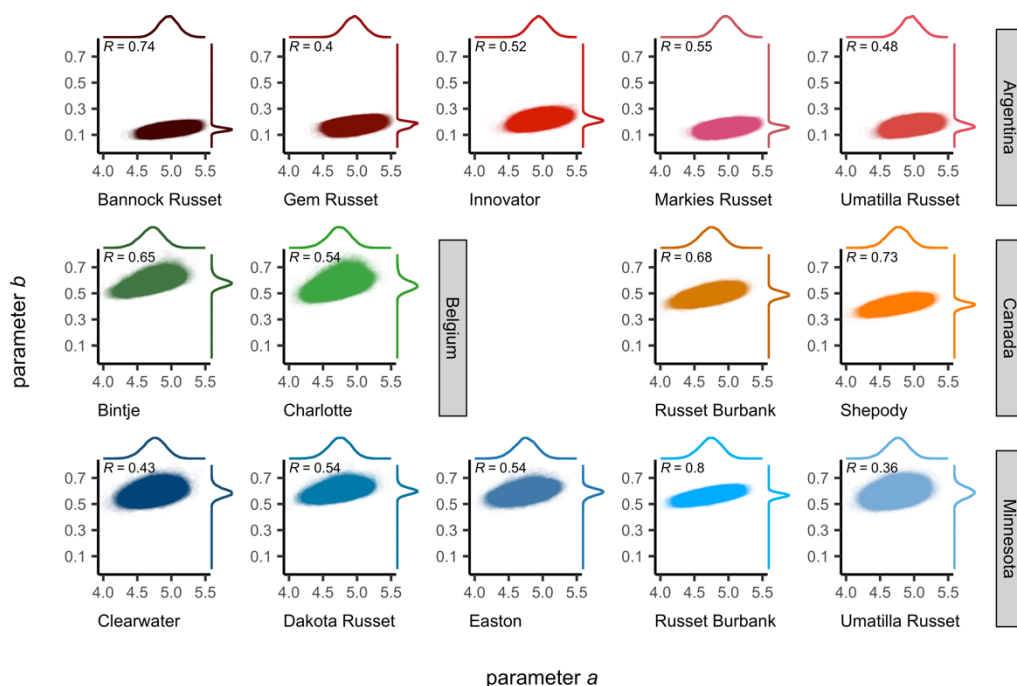
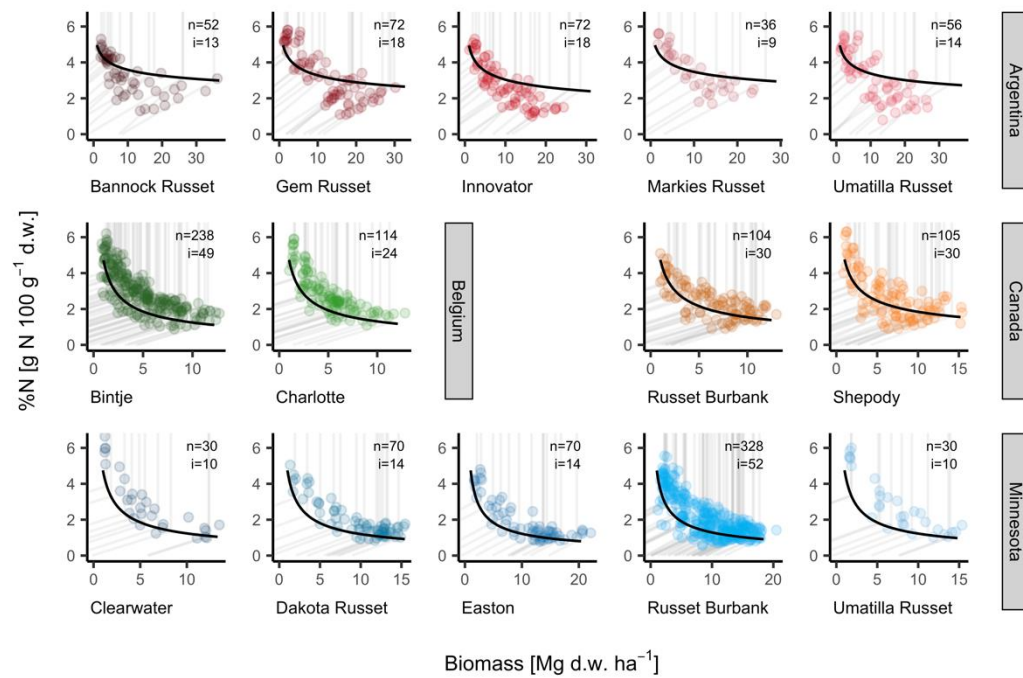


Figure 3. Distribution of posterior values for parameters a and b for each location within variety shown as a scatterplot with marginal density distribution given for each parameter. Pearson correlation coefficient [R] is displayed for the relationship between parameters a and b . Data are shown at the level of individual draws ($n=28,000$).

Critical N dilution curves for each variety within location and the experimental data, median linear-plateau curve for each experimental sampling date, and median value of $\%N_c$ are presented (Figure

4 437 4). The individual linear-plateau curves fitted for each experimental sampling date nested within
 5 each level of the variety within location effect are presented in the Supplemental Materials (Figure
 6 438 S1).



36 **Figure 4.** Critical N dilution curves (i.e., median value of critical N concentration [%N_c]) fitted from the
 37 hierarchical Bayesian model are shown as a solid black lines for each variety within location. Biomass
 38 and N concentration [%N] data are displayed as points with the median linear-plateau curve for each
 39 sampling date shown as grey line. The number of samples [n] and the number of sampling dates [i] are
 40 displayed on each individual panel.

42 441
 43
 44 442 For the Argentina varieties, more than 60% of the observed data fall below the CNDC (i.e.,
 45 represent N limiting conditions) with over 40% of sampling dates having exclusively N limiting
 46 conditions observed. For both the Belgium and Minnesota varieties, more than 80% of the
 47 observed data fall above the CNDC (i.e., represent non-N limiting conditions) with almost 30% of
 48 sampling dates having exclusively non-N limiting conditions observed. For the Canada varieties,
 49 over 60% of observed data represented non-N limiting conditions but less than 10% of sampling
 50 dates had exclusively non-N limiting conditions observed (Figure S1).

1
2
3
4 449 *3.2. Critical N Concentration Uncertainty*
5
6
7

8 450 The credible region for %N_c varies across variety within location and across levels of biomass
9
10 451 (Figure 5). The symmetry of the credible region distribution varies by variety within location.
11
12 452 Some levels of variety within location, such as Argentina × Gem Russet, have a skewed
13
14 453 distribution, while other levels, such as Canada × Shepody, have a symmetrical distribution (Figure
15
16 454 5a). There are also differences in the range of the credible region, where some varieties within
17
18 455 location, such as Argentina × Umatilla Russet, have greater uncertainty in %N_c than others, such
19
20 456 as Minnesota × Russet Burbank. The uncertainty in %N_c also varies across the level of biomass
21
22 457 for a given CNDC. For example, as the level of biomass increases, Argentina × Umatilla Russet
23
24 458 has an increasing credible region range, Minnesota × Russet Burbank has a decreasing credible
25
26 459 region range, and Argentina × Bannock Russet has a nearly constant credible region range.
27
28
29
30 460
31
32
33
34
35
36
37
38
39
40
41
42
43
44
45
46
47
48
49
50
51
52
53
54
55
56
57
58
59
60
61
62
63
64
65

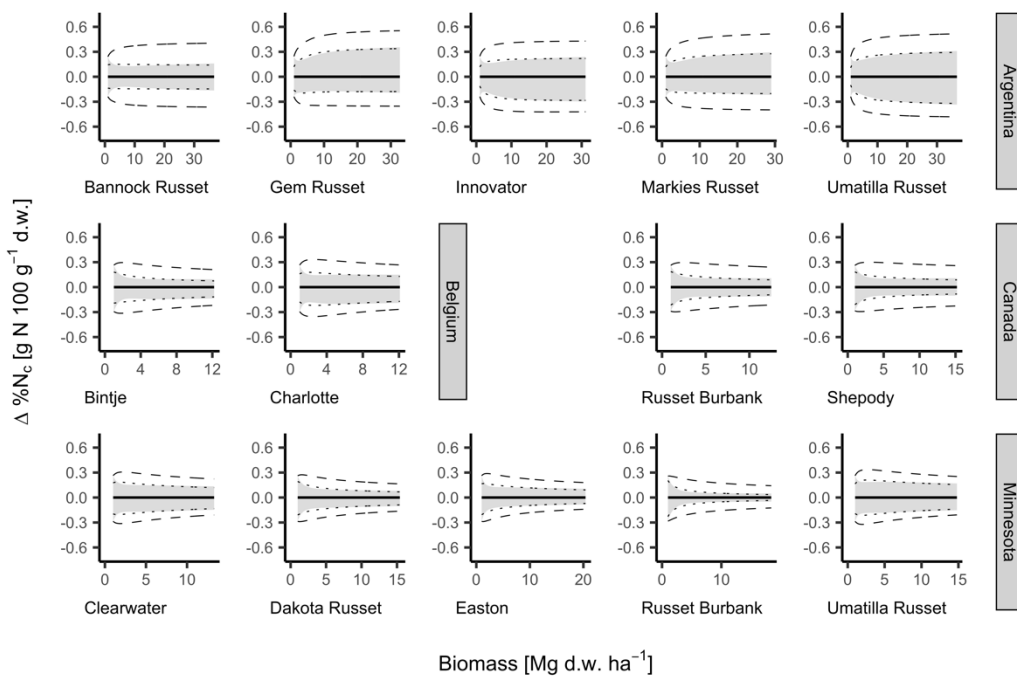


Figure 5. Comparison of the difference in critical N concentration values [$\Delta\%N_c$]. The reference critical N concentration [% $N_{c,\text{ref}}$] is represented as a solid black line at constant $\Delta\%N_c$ value of zero. The grey shaded region represents the 90% credible region of $\%N_c$ from the directly modeled approach (i.e., $\%N_c$ computed from parameter estimates of each posterior draw). The dotted lines represent the estimated upper and lower bounds of $\%N_c$ from the parameterized estimate approach (i.e., $CNDC_{lo}$ and $CNDC_{up}$). The dashed lines represent the approximated lower and upper bounds of $\%N_c$ from the indirect calculation approach (i.e., $\%N_c$ computed based on posterior distribution of parameters a and b). Data are presented for all levels of variety within location.

461

462 Estimation of the upper and lower boundaries of the 90% credible region using the parameterized
 463 estimate approach (i.e., CNDC_{lo} and CNDC_{up}) (Table 5) appears to be reasonable based on
 464 graphical evaluation (Figure 5). However, these fitted CNDC_{lo} and CNDC_{up} curves do not
 465 themselves represent a draw directly from the posterior distribution and do not necessarily
 466 represent the most extreme possible curves. While credible regions with boundaries that are non-
 467 monotonic (e.g., Argentina \times Innovator) have portions of the curve fit approximation that are
 468 poorer performing, the credible regions with monotonic boundaries (e.g., Minnesota \times Dakota
 469 Russet) seem to be satisfactory across the entire range of the curve.
 470

Table 5. Critical N dilution curve parameters for each variety within location, with the median value of the posterior distribution for parameters a and b (CNDC), and the estimates for the credible region lower (CNDC_{lo}) and upper (CNDC_{up}) boundaries using the parameterized estimate approach.

Location	Variety	<u>CNDC_{lo}</u>		<u>CNDC</u>		<u>CNDC_{up}</u>	
		a_{lo}	b_{lo}	a	b	a_{up}	b_{up}
Argentina	Bannock Russet	4.82	0.146	4.96	0.140	5.10	0.135
	Gem Russet	4.80	0.190	4.96	0.178	5.07	0.152
	Innovator	4.83	0.241	4.94	0.212	5.06	0.193
	Markies Russet	4.82	0.167	4.96	0.155	5.08	0.135
	Umatilla Russet	4.85	0.195	4.95	0.165	5.06	0.143
Belgium	Bintje	4.52	0.606	4.72	0.579	4.90	0.567
	Charlotte	4.56	0.607	4.74	0.559	4.89	0.531
Canada	Russet Burbank	4.53	0.498	4.74	0.489	4.93	0.480
	Shepody	4.55	0.416	4.77	0.412	4.95	0.406
Minnesota	Clearwater	4.56	0.622	4.75	0.585	4.93	0.558
	Dakota Russet	4.54	0.619	4.75	0.599	4.94	0.588
	Easton	4.54	0.608	4.75	0.592	4.91	0.567
	Russet Burbank	4.51	0.562	4.74	0.566	4.95	0.567
	Umatilla Russet	4.56	0.631	4.75	0.588	4.92	0.546

471
 472 However, the approximation of uncertainty in $\%N_c$ based on the indirect calculation method were
 473 found to contain the entire credible region for all varieties within location evaluated (Figure 5).
 474 Therefore, the indirect calculation approach based on uncertainty in CNDC parameters is less
 475 informative than either the directly modeled or parameterized estimate approaches. In the absence
 476 of the credible region defined directly from the fitted hierarchical Bayesian model (i.e., directly

1
2
3
4 477 modeled approach), using the CNDC_{lo} and CNDC_{up} (Table 5) (i.e., parameterized estimate
5
6 478 approach) is a suitable first-order representation of the credible region for %N_c.
7
8
9

10 479 *3.3. Evaluating Differences between Critical N Concentration*
11
12

13 480 3.3.1. Differences Related to G × E × M Effects
14
15

16
17 481 While an evaluation of the pairwise differences between all varieties within location was
18
19 482 conducted and is presented in the Supplemental Materials (Figure S2), a subset of the results
20
21 483 comparing Minnesota × Russet Burbank to all other varieties within location, Argentina ×
22
23 484 Innovator to all other varieties within Argentina, Canada × Russet Burbank to all other varieties
24
25 485 within Canada, and Belgium × Bintje to all other varieties within Belgium are presented in detail
26
27 486 here (Figure 6).
28
29
30 487
31
32
33
34
35
36
37
38
39
40
41
42
43
44
45
46
47
48
49
50
51
52
53
54
55
56
57
58
59
60
61
62
63
64
65

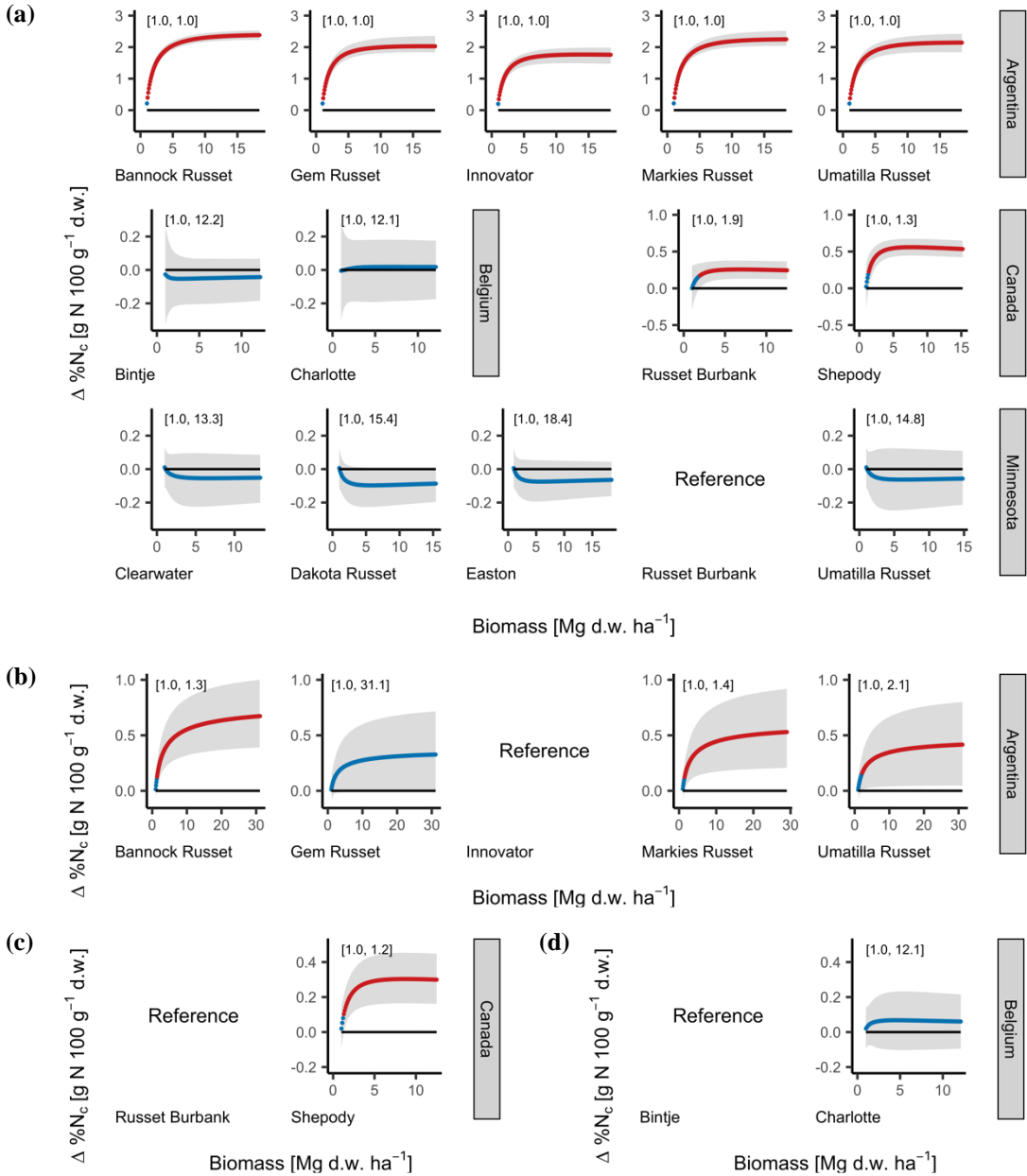


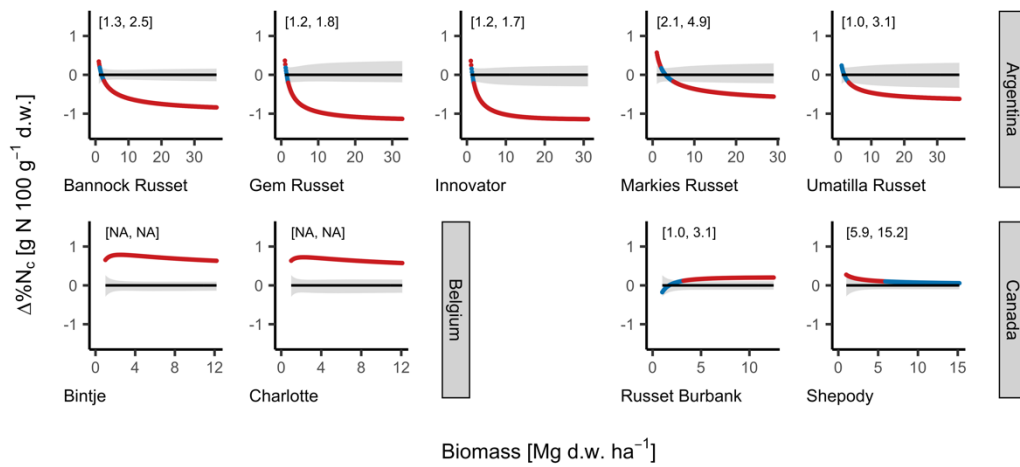
Figure 6. Comparison of the difference in critical N concentration values [$\Delta\%N_c$] between (a) Minnesota \times Russet Burbank and all other varieties within location, (b) Argentina \times Innovator and all other varieties within Argentina, (c) Canada \times Russet Burbank and all other varieties within Canada, and (d) Belgium \times Bintje and all other varieties within Belgium. The grey shaded region represents the 90% credible region for $\Delta\%N_c$. The colored points represent the median value for $\Delta\%N_c$ at a given biomass level where blue or red color respectively indicates that the 90% credible region for $\Delta\%N_c$ does or does not contain zero. The solid black line at constant $\Delta\%N_c$ value of zero represents $\%N_c$ for the reference curve [$\%N_{c,\text{ref}}$] (i.e., Minnesota \times Russet Burbank, Argentina \times Innovator, Canada \times Russet Burbank, and Belgium \times Bintje). The range of biomass values for which $\Delta\%N_c$ is not significantly different (i.e., 90% credible region contains zero) is given in brackets.

1
2
3
4 489 For Minnesota × Russet Burbank, there were no significant differences in %N_c for any level of W
5
6 490 evaluated with any of the other varieties in Minnesota (i.e., Clearwater, Dakota Russet, Easton,
7
8 491 and Umatilla Russet) or with the Belgium varieties (i.e., Bintje, and Charlotte) (Figure 6a). The
9
10 492 %N_c values for both of the Canadian varieties (i.e., Russet Burbank, and Shepody) were
11
12 493 significantly greater than that for Minnesota × Russet Burbank when biomass values were greater
13
14 494 than 2 Mg ha⁻¹ dry wt. The %N_c for Canada × Russet Burbank and Canada × Shepody were up to
15
16 495 0.3 and 0.6 g N 100 g⁻¹ dry wt. greater than that for Minnesota × Russet Burbank, respectively.
17
18 496 The %N_c for the Argentina varieties (i.e., Bannock Russet, Gem Russet, Innovator, Markies
19
20 497 Russet, and Umatilla Russet) were significantly greater than for Minnesota × Russet Burbank,
21
22 498 except at a biomass value of 1.0 Mg dry wt. ha⁻¹, with a difference in value depending on variety
23
24 499 of up to 2.4 g N 100 g⁻¹ dry wt.

30
31
32 500 For Argentina × Innovator, %N_c was significantly lower than for Argentina × Bannock Russet,
33
34 501 Argentina × Markies Russet, and Argentina × Umatilla Russet but was not significantly different
35
36 502 from Argentina × Gem Russet (Figure 6b). The %N_c values for Argentina × Bannock Russet,
37
38 503 Argentina × Markies Russet, and Argentina × Umatilla Russet were up to 0.5 g N 100 g⁻¹ dry wt.
39
40 504 greater than that for Argentina × Innovator. For Canada × Russet Burbank, %N_c was significantly
41
42 505 lower than for Canada × Shepody (Figure 6c), with a difference in %N_c of up to 0.3 g N 100 g⁻¹
43
44 506 dry wt. For Belgium × Bintje, %N_c was not significantly different from Belgium × Charlotte
45
46 507 (Figure 6d).

50
51
52
53 508 There are two notable findings to point out. First, there were no significant differences between
54
55 509 Minnesota × Russet Burbank and any other varieties evaluated in Minnesota or between Belgium
56
57 510 × Bintje and Belgium × Charlotte. This finding did not hold true for all varieties within location
58
59 511 evaluated, however; Significant differences between varieties were found for both Argentina and

1
 2
 3
 4 512 Canada. Second, the comparison between the Minnesota \times Russet Burbank and Canada \times Russet
 5
 6 513 Burbank curves as well as the comparison between the Minnesota \times Umatilla Russet and Argentina
 7
 8 514 \times Umatilla (Figure S2) were both significantly different.
 9
 10
 11
 12 515 3.3.2. Differences Related to Statistical Methods
 13
 14
 15
 16 516 When comparing the curves fit in the present study with the Bayesian hierarchical method to the
 17
 18 517 curves fit in the previous studies using conventional statistical methods, there were significant
 19
 20
 21 518 differences between statistical curve fit methods for all varieties within location evaluated (Figure
 22
 23 519 7). None of the previous CNDCs fall entirely within the credible region for the respective CNDCs
 24
 25
 26 520 developed in the present study.
 27
 28 521



46
 47 **Figure 7.** Comparison of the difference in critical N concentration values [$\Delta\%N_c$] between the
 48 conventional statistical methods used in previous studies (i.e., Argentina – Giletto and Echeverría (2015);
 49 Belgium – Ben Abdallah et al. (2016); Canada – Bélanger et al. (2001a)) and the hierarchical Bayesian
 50 method used in the present study. The grey shaded region represents the 90% credible region for critical
 51 N concentration [%N_c] using the directly modeled method. The solid black line at a constant $\Delta\%N_c$ value
 52 of zero represents the median value for %N_c using the directly modeled method. Red or blue points
 53 respectively indicate that $\Delta\%N_c$ falls outside of (i.e., is significant) or falls within (i.e., is not significant)
 54 the 90% credible region for %N_c determined by the directly modeled method. The range of biomass values
 55 for which $\Delta\%N_c$ is not significant is given in brackets.
 56 522
 57
 58
 59
 60
 61
 62
 63
 64

1
2
3
4 523 The %N_c values from the previously developed CNDCs for the Argentina varieties (Giletto &
5
6 Echeverría, 2015) were significantly less than that from the present CNDCs across all varieties for
7
8 biomass levels of greater 5 Mg dry wt. ha⁻¹ (Figure 7). The magnitude of this difference was
9
10 relatively large, with the Δ%N_c between the previous and present method ranging up to -0.6 to -
11
12 1.1 g N 100 g⁻¹ dry wt., depending on variety. Therefore, relative to the statistical method used in
13
14 this study it appears that the statistical methods used by Giletto and Echeverría (2015) selected
15
16 biased critical points due to an overrepresentation of N limiting observations in the experimental
17
18 dataset (Figure 4, Figure S1) leading to a systematic underestimation of %N_c.
19
20
21
22
23
24
25 531 The %N_c from the previously developed CNDCs for Belgium (Ben Abdallah et al., 2016) were
26
27 significantly greater than that from the CNDCs developed in the present study (Figure 7). For all
28
29 levels of biomass, Δ%N_c between the previous and present methods was significantly different
30
31 with a value of 0.7 g N 100 g⁻¹ dry wt. Therefore, relative to the statistical method used in this
32
33 study, it appears that the statistical methods used by Ben Abdallah et al. (2016) selected biased
34
35 critical points due to overrepresentation of non-N limiting observations in the experimental dataset
36
37 leading to a systematic overestimation of the %N_c.
38
39
40
41
42
43 538 The %N_c from the previously developed CNDCs for Canada (Bélanger et al., 2001a) was
44
45 significantly greater for both Canada × Russet Burbank and Canada × Shepody than the present
46
47 CNDCs for biomass levels of less than 3 Mg dry wt ha⁻¹ and greater than 6 Mg dry wt ha⁻¹,
48
49 respectively (Figure 7). Relative to the other locations, however, the CNDCs for Canada were the
50
51 most similar between statistical methods, with a small value for Δ%N_c of only 0.2 g N 100 g⁻¹ dry
52
53 wt. Therefore, relative to the statistical method used in this study, it appears that the statistical
54
55 method used by Bélanger et al. (2001a) did not select biased critical points likely due to the lesser
56
57 bias observed in this experimental dataset.
58
59
60 545
61
62
63
64
65

1
2
3
4 546 Because a CNDC using the conventional statistical methods has not been previously published for
5 potato in Minnesota, no comparison across statistical methods is made for this experimental
6
7 547 dataset. However, the bias observed in the Minnesota experimental dataset is similar to the bias
8 found in the Belgium experimental dataset; therefore, using the conventional statistical methods
9
10 549 to derive a CNDC for Minnesota would likely overestimate %N_c relative to the hierarchical
11
12 550 Bayesian method.
13
14
15
16
17
18
19
20

21 552 **4. Discussion**
22
23

24 553 *4.1. Mechanisms of Dilution*
25
26
27

28 554 While the present study presents direct evidence of significant differences between CNDCs for
29 potato across G × E × M effects, previous studies help describe the potential physiological
30
31 555 mechanisms for this source of variation. Reviewing previous work on this topic, Lemaire et al.
32
33 556 (2019) described a framework with which to consider the variation in relative partitioning of dry
34
35 557 matter. First, relative partitioning varies as biomass varies over the growing season indicating that
36
37 558 there is an ontogenetic relationship between harvest index and biomass. Second, the allometric
38
39 559 trajectory of relative allocation (e.g., harvest index at a given level of biomass) is subject to
40
41 560 variation in non-ontogenetic factors (i.e., G × E × M interactions).
42
43
44
45
46
47

48 562 The findings of Giletto et al. (2020) suggest that the variation in CNDCs for potato are due to non-
49
50 563 ontogenetic factors. In general, G × E × M interactions that result in greater and more rapid relative
51
52 564 partitioning of biomass from vines (i.e., high N metabolic and structural tissue) to tubers (i.e., low
53
54 565 N storage tissues) will result in greater N dilution (i.e., lower %N_c) at the same level of total plant
55
56 566 biomass (Lemaire et al., 2019). The two factors described by Giletto et al. (2020) affecting N
57
58
59
60
61
62
63
64
65

1
2
3
4 567 dilution due to non-ontogenetic factors are total plant biomass at tuber initiation (i.e., timing of
5 tuber initiation) and relative rate of tuber growth to plant growth (i.e., relative rate of tube bulking).
6
7 568 These two factors are affected by various physiological mechanisms and G × E × M interactions;
8
9 569 however, relatively limited work has been conducted to comprehensively evaluate the combined
10
11 570 effect of G × E × M interaction on these two physiological mechanisms for potato.
12
13
14 571
15
16

17 572 4.1.1. Timing of Tuber Initiation
18
19
20

21 573 The timing of tuber initiation is affected primarily by variety maturity class (i.e., G). Potato
22 varieties are classified on a spectrum of growth patterns where early maturing varieties are
23 considered to be determinate and later maturing varieties are considered to be indeterminate
24 (Thornton, 2020). Compared to indeterminate varieties, determinate varieties progress more
25 quickly to the tuber initiation growth stage (i.e., at lower total plant biomass) and have a more
26 rapid tuber bulking (i.e., biomass increase) with limited additional canopy and vine biomass
27 growth (i.e., increased harvest index for a given level of biomass) (Kleinkopf et al., 1981).
28
29 577
30 578
31 579
32
33 578
34
35 579
36
37 580 Therefore, it is expected that increasing earliness of maturity for a potato variety would result in
38
39 581 an increase in N dilution.
40
41
42
43

44 582 In the present study, differences in maturity class between varieties resulted in differences in %N_c.
45
46 583 For example, Argentina × Innovator, which has an early to medium maturity class, had
47 significantly lower %N_c than Argentina × Bannock Russet, Argentina × Markies Russet, and
48
49 584 Argentina × Umatilla Russet, which have either a medium-late to late or late to very late maturity
50 class; however, Argentina × Gem Russet, which has a medium to late maturity class did not have
51
52 585
53 586
54 587 a significantly different %N_c from Argentina × Innovator (Figure S2). This finding supports the
55
56
57
58
59
60
61
62
63
64

1
2
3
4 588 hypothesis that varieties with an earlier maturity class (i.e., earlier tuber initiation) will have lower
5
6 589 %N_c (i.e., greater N dilution).
7
8
9

10 590 Timing of tuber initiation is also subject to G × E × M interactions. Ideal conditions for tuber
11
12 591 initiation are moderate to low soil N availability, shorter day length, high light intensity, and cool
13
14 592 nighttime temperatures (Ewing & Struik, 1992; Thornton, 2020); when N fertilizer management
15
16 593 results in excessively high soil N availability (Kleinkopf et al., 1981), under conditions of reduced
17
18 594 solar irradiance (Menzel, 1985), or when nighttime soil temperatures are elevated (Slater, 1968;
19
20 595 Kim & Lee, 2019), tuber initiation can be delayed. Therefore, both M effects that result in
21
22 596 excessive early-season soil N availability (e.g., all N applied at planting in a soluble form) and E
23
24 597 effects that result in increased solar irradiance or reduced nighttime temperatures (i.e., increased
25
26 598 diurnal temperature difference) could result in an increase in N dilution.
27
28
29
30
31
32

33 599 However, due the limitation of the experimental studies (i.e., the effect of M was not systematically
34
35 600 varied across a given G × E interaction), it is not possible to directly assess the impact of diurnal
36
37 601 temperature difference, solar irradiance, or N fertilizer source and timing (Table 3) on the timing
38
39 602 of tuber initiation and N dilution distinct from the combined effect of G × E × M interactions.
40
41
42
43

44 603 4.1.2. Rate of Tuber Bulking 45 46

47 604 The rate of tuber bulking and allocation of biomass to tubers is subject to the effects of E.
48
49 605 Conventionally, potential biomass production has been considered as the product of total solar
50
51 606 radiation and radiation use efficiency (Monteith, 1977; Sinclair & Muchow, 1999) as has been
52
53 607 successfully applied to potato (Allen & Scott, 1980). Previous studies have suggested that
54
55 608 decreasing diurnal temperature difference results in a reduction in tuber bulking rate (i.e., radiation
56
57 609 use efficiency), most likely as a result of increasing utilization of photosynthesis assimilates for
58
59
60
61
62
63
64

1
2
3
4 610 maintenance (via increased respiration) as nighttime temperature increases (Benoit et al., 1986;
5
6 611 Bennett et al., 1991; Lizana et al., 2017); however, Kim & Lee (2019) did not observe any effect
7
8 612 of increasing diurnal temperature difference on tuber bulking rate.
9
10

11
12 613 Given the limitation of the experimental studies (i.e., the effect of E was not systematically varied
13
14 614 across a given G x M interaction), it is not possible to directly assess the impact of diurnal
15
16 615 temperature difference and solar radiation (Table 3) on the rate of tuber bulking across G x E x M
17
18 616 interactions.
19
20

21
22
23 617 Planting density is an important effect of M that may play a key role in determining the relative
24
25 618 partitioning of biomass for to tuber. Previous studies investigating this effect have found that as
26
27 619 planting density increases, leaf area index increases (Bremner & Taha, 1966; Ifenkwe & Allen,
28
29 620 1978; Allen & Scott, 1980), tuber dry weight biomass on a per area basis increases (Bremner &
30
31 621 Taha, 1966; Ifenkwe & Allen, 1978), while tuber dry weight biomass on a per plant basis decreases
32
33 622 (Bremner & Taha, 1966; Ifenkwe & Allen, 1978). The combination of the effect of increasing
34
35 623 planting density could plausibly result in the net effect of an increased relative proportion of
36
37 624 biomass allocated to vines (i.e., reduction in harvest index) (Vander Zaag et al., 1990), therefore
38
39 625 reducing N dilution and resulting in an increased %N_c.
40
41

42
43 626 In the present study, variations in %N_c due to variation in planting density were observed. For
44
45 627 example, Argentina has the highest planting density of any location (Table 3) which resulted in
46
47 628 greater %N_c than all other locations (Figure S2). The relative effect of planting density also appears
48
49 629 to be of greater magnitude than other sources of variation (e.g., maturity class). For example,
50
51 630 Canada × Russet Burbank, which has a late to very late maturity class and planting density of
52
53 631 29,000 plants ha⁻¹, had a lower %N_c than Canada × Shepody, which has an early to medium-early
54
55
56
57
58
59
60
61
62
63
64
65

1
2
3
4 632 maturity class and planting density of 44,000 plants ha⁻¹ (Table 3, Figure 6c). Therefore, this
5
6 633 finding suggests that the effect of planting density (i.e., rate of tuber bulking) may be relatively
7
8 634 more important at controlling %N_c than the effect of maturity class (i.e., timing of tuber initiation).
9
10
11
12

13 635 Because there was only a single level of M (e.g., planting density) within each level of G × E for
14
15 636 the experimental trials considered here, additional experimentation is required to fully consider the
16
17 637 independent effects of G, E, and M on critical N dilution. Therefore, future experimental studies
18
19 638 explicitly investigating the effect of M (e.g., planting density) on %N_c should be conducted to
20
21 639 properly consider the combined effects the G × E × M interaction.
22
23
24
25

26 640 4.1.3. Comparison to Other Crops 27 28

29 641 These findings contrast somewhat with the previous studies evaluating G × E × M effects on %N_c.
30
31 642 Yao et al. (2021) found a similar magnitude of effect on %N_c for both G and E effects for wheat
32
33 643 in China; however, Yao et al. (2021) also reported an E effect where %N_c for wheat in China was
34
35 644 significantly different from that reported by Makowski et al. (2020) for wheat in France. Ciampitti
36
37 645 et al. (2021) identified variation in %N_c for maize as a result of G × M interactions due to variation
38
39 646 in hybrid and planting density. Fernández et al. (2021) found that variation in %N_c for tall fescue
40
41 647 across G × E × M effects was negligible. In any case, the magnitude of the difference in %N_c
42
43 648 across G × E × M interactions reported by the previous studies for wheat, maize, and tall fescue
44
45 649 (Makowski et al., 2020; Ciampitti et al., 2021; Fernández et al., 2021; Yao et al., 2021) is less than
46
47 650 that was observed in the present study for potato.
48
49
50
51
52

53
54 651 Therefore, the impact of G × E × M on %N_c is not only significant for potato, but is also of
55
56 652 potentially of much greater relative importance compared to other crops (e.g., wheat, maize, tall
57
58 653 fescue). This is because the magnitude of variability in %N_c due to G × E × M interactions found
59
60
61
62
63
64
65

1
2
3
4 654 in the present study is relatively greater for potato than other crops; however, further additional
5
6 655 experimental data are needed to confirm that this finding is not an artifact of the statistical methods
7
8 656 or limitations of experimental data used in the present study.
9
10
11
12

13 657 4.1.4. Limitations of Interpretation
14
15

16 658 Previous studies, including that of Giletto et al. (2020) on potatoes, have identified that N dilution
17
18 659 follows a two-step process where the rate of N dilution varies between the vegetative period (i.e.,
19
20 660 parameter b_1) and the period of storage tissue accumulation (i.e., parameter b_2) (Duchenne et al.,
21
22 661 1997; Plénet & Lemaire, 2000; Gastal et al., 2015). Our study, however, did not directly evaluate
23
24 662 if the rate of N dilution during the pre-tuber initiation (i.e., vegetative growth) and post-tuber
25
26 663 initiation (i.e., accumulation of storage tissue) periods varies due to $G \times E \times M$ interactions.
27
28 664 Variation in parameters b_1 and b_2 across $G \times E \times M$ effects is a plausible physiological mechanism
29
30 665 that could occur in addition to the non-ontogenetic allometric effects (i.e., timing of tuber
31
32 666 initiation, relative rate of tube bulking) identified in the present study and used to explain variation
33
34 667 in parameter b . This alternative hypothesis could be evaluated by modifying the Bayesian
35
36 668 hierarchical method of the present study to include another hierarchical level representing the pre-
37
38 669 and post-tuber initiation periods to determine if parameter b varies within these periods across to
39
40 670 $G \times E \times M$ interactions.
41
42
43
44
45
46
47
48

49 671 4.2. Implication of $G \times E$ Variation on N Use Efficiency
50
51

52 672 Understanding and properly interpreting the impact of $G \times E \times M$ effects on NUE is a critical goal
53
54 673 necessary to improve N fertilizer use; however, this must be done while controlling for the effect
55
56 674 of crop N status (Lemaire & Ciampitti, 2020). The previous findings of Bohman et al. (2021)
57
58 675 demonstrated that interpreting NUE and its constituent component of N utilization efficiency
59
60
61
62
63
64
65

1
2
3
4 676 [NUtE] is directly related to the parameters of the CNDC through the critical N utilization
5
6 677 efficiency curve [CNUtEC] which defines the critical value of NUtE [NUtE_c]:
7
8
9

10 678 $NUtE_c = 1000 (10 a W^{-b})^{-1}$ [11]
11
12
13

14 679 where parameters *a* and *b*, and W have the same meaning and units as previously defined in the
15
16 680 present study and NUtE_c has units of g dry wt. g⁻¹ N. When NUtE is greater than NUtE_c, crop N
17
18 681 status is deficient (i.e., NNI less than 1); conversely, when NUtE is less than NUtE_c, crop N status
19
20 682 is excessive (i.e., NNI greater than 1).
21
22
23

24 683 The finding in the present study that the CNDC can vary across G × E × M interactions and the
25
26 684 finding from Bohman et al. (2021) of the intrinsic relationship between NUE and the CNDC
27
28 685 together lead to the conclusion that the CNUtEC must also vary across the same G × E × M effects
29
30 686 as the CNDC. Therefore, the effect of G × E × M on variation of NUtE_c is one of the multiple set
31
32 687 of factors that ultimately control NUE. Understanding and accounting for the G × E × M effect on
33
34 688 the CNUtEC is therefore critically important to understand the impacts of G × E × M interactions
35
36 689 on NUE. In other words, controlling for this G × E × M effect represents an additional requirement
37
38 690 when evaluating and interpreting NUE above and beyond the previously known requirements of
39
40 691 controlling for both NNI and biomass (Barraclough et al., 2010; Caviglia et al., 2014; Sadras &
41
42 692 Lemaire, 2014; Gastal et al., 2015; Lemaire & Ciampitti, 2020).
43
44
45
46
47

48
49
50 693 Following from the above discussion of the CNUtEC and the findings of Giletto et al. (2020), G ×
51
52 694 E × M effects that increase the relative proportion of biomass partitioned to tubers and reduce the
53
54 695 time to tuber initiation will both decrease the %N_c and increase the NUtE_c values. Therefore, future
55
56 696 efforts to systematically improve NUE in potato through either management practices (e.g.,
57
58 697 Bohman et al. (2021)) or crop breeding (e.g., Tiwari et al. (2018); Jones et al. (2021); Stefaniak et
59
60
61
62
63
64
65

1
2
3
4 698 al. (2021)) should focus on identifying $G \times E \times M$ interactions that result in an increased proportion
5
6 699 of biomass partitioned to tubers or result in earlier timing of tuber initiation.
7
8
9

10 700 *4.3. Uncertainty in Critical N Concentration*
11
12

13 701 4.3.1. Communicating Uncertainty in Critical N Concentration
14
15

16
17 702 This study as well as others that implemented Bayesian statistical methods to derive critical N
18
19 703 dilution curves (Makowski et al., 2020; Ciampitti et al., 2021; Yao et al., 2021) clearly indicate
20
21 704 that there is meaningful uncertainty in $\%N_c$ values. Therefore, the use of $\%N_c$ in subsequent
22
23 705 calculations should include this inherent uncertainty. However, the direct use of the credible region
24
25 defined from posterior distribution of the fitted Bayesian hierarchical model in subsequent
26
27 706 calculations is impractical, and a method to concisely and accurately communicate the credible
28
29 707 region remains necessary.
30
31
32

33
34
35 709 Our finding that the credible region can be satisfactorily estimated using an equation of the same
36
37 710 form as the CNDC (Figure 5) suggests that an additional pair of negative exponential curves
38
39 711 representing the upper and lower boundary of the credible region for $\%N_c$ (i.e., $CNDC_{lo}$ and
40
41 712 $CNDC_{up}$) should be reported in future studies. In this manner, the median value and credible region
42
43 713 for $\%N_c$ is defined by a set of three, two-parameter curves (i.e., $CNDC - a, b$; $CNDC_{up} - a_{up}, b_{up}$;
44
45 714 $CNDC_{lo} - a_{lo}, b_{lo}$) which can be easily communicated and used in subsequent computations (Table
46
47 715 5).
48
49
50

51
52
53 716 4.3.2. Computing Uncertainty of Derived Parameters
54
55
56

57 717 Critical N concentration and the associated CNDC parameters are commonly used to derive and
58
59 718 calculate other related parameters. For example, the calculation of NNI depends on both $\%N_{Plant}$
60
61
62

1
2
3
4 719 and %N_c. (Eq. [1] and Eq. [2]). However, to properly account for the uncertainty in %N_c when
5
6 720 computing NNI, the upper [%N_{c,up}] and lower [%N_{c,lo}] bounds of the credible interval for %N_c
7
8 721 should also be used to determine the upper [NNI_{up}] and lower [NNI_{lo}] bounds of the credible
9 interval for NNI, where %N_{c,up} and %N_{c,lo} are calculated using the CNDC_{up} and CNDC_{lo},
10
11 722 respectively:
12
13
14 723
15
16

17 724 $\text{NNI}_{\text{up}} = \% \text{N}_{\text{Plant}} / \% \text{N}_{c,\text{up}} = \% \text{N}_{\text{Plant}} / (a_{\text{up}} W^{-b_{\text{up}}})$ [12]
18
19
20

21 725 $\text{NNI}_{\text{lo}} = \% \text{N}_{\text{Plant}} / \% \text{N}_{c,\text{lo}} = \% \text{N}_{\text{Plant}} / (a_{\text{lo}} W^{-b_{\text{lo}}})$ [13]
22
23

24 726 This has important practical implications for interpreting NNI values. For example, in a case where
25
26 727 NNI is less than 1 but NNI_{up} is greater than 1, it follows that crop N status would not be considered
27
28 728 deficient (i.e., NNI is not significantly different from 1). In contrast, when both NNI and NNI_{lo} are
29
30 729 greater than 1, it follows that crop N status would be considered surplus (i.e., NNI is significantly
31
32 730 greater than 1). However, the threshold for considering significant differences in NNI will
33
34 731 necessarily depend upon the threshold used for calculating %N_{c,lo} and %N_{c,up} (e.g., 90%
35
36 732 confidence region). For example, the conclusions of a small-plot trial evaluating the effect of
37
38 733 various N fertilizer treatments on yield and biomass (e.g., Bohman et al. (2021)) may draw
39
40 734 different conclusions when uncertainty in calculated NNI values is explicitly considered (e.g., N
41
42 735 treatments were or were not limiting).
43
44
45
46
47

48
49
50 736 Additionally, the parameters of the CNDC (i.e., a , b) are also used to parameterize other related
51
52 737 curves such as the critical N uptake curve [CNUC] or the critical N utilization efficiency curve
53
54 738 [CNUtEC] (Bohman et al., 2021). When computing the critical N uptake [N_c] or critical N
55
56 739 utilization efficiency [NUtE_c] values defined by these curves, respectively, the parameters from
57
58 740 the CNDC_{lo} (i.e., a_{lo} , b_{lo}) and CNDC_{up} (i.e., a_{up} , b_{up}) should be used to calculate the upper and
59
60
61
62
63
64
65

1
2
3
4 741 lower bounds of these derived values. In general, any calculation depending on either %N_c or any
5
6 equation that uses the parameters of the CNDC, should also additionally use the CNDC_{lo} and
7
8 CNDC_{up} to account for uncertainty in %N_c.
9
10
11
12
13 744 *4.4. Evaluating Differences between Statistical Methods*
14
15
16 745 While the occurrence of differences between CNDCs derived using the Bayesian hierarchical
17
18 model compared to the conventional statistical methods (Figure 6) is itself notable, the magnitude
19
20 of the differences found in the present study is especially remarkable for the following reasons.
21
22
23
24 748 Because of its strong theoretical underpinning, %N_c and NNI are typically considered to be high
25
26 fidelity measurements of crop N status, not affected by the subjectivity or relativity found in most
27
28 other methods (Lemaire et al., 2019). However, the findings of the present study strongly suggest
29
30 that this conception of the NNI framework must be qualified within a particular application by the
31
32 statistical methods used to derive the CNDC for a given experimental dataset.
33
34
35
36
37
38 753 Unfortunately, the direct evaluation of different statistical methods to calculate the CNDC from
39
40 the same experimental dataset cannot directly answer the question of which statistical method or
41
42 resulting CNDC is “correct” (i.e., most accurate, least biased). However, we can reasonably
43
44 conclude from both deduction and from the findings of the present study that a Bayesian
45
46 hierarchical model utilizing the linear-plateau method and leveraging partial pooling across effect
47
48 levels will result in inference that is less subjected to potential bias in the experimental data set
49
50 compared to the conventional statistical methods. Additionally, it extracts the greatest amount of
51
52 information from a given dataset, as no data are excluded from the fitting of the total model.
53
54
55
56
57
58
59
60
61
62
63
64
65

1
2
3
4 761 Therefore, it appears preferable for the future development of CNDCs to utilize the Bayesian
5 hierarchical method to both quantify uncertainty and reduce bias in %N_c. Without addressing these
6
7 762 limitations (i.e., bias and uncertainty), both directly resulting from the statistical methods used, the
8
9 763 NNI framework cannot fulfill its core objective of providing an absolute reference of crop N status.
10
11 764
12
13
14
15 765 Additionally, with further development of standardized tools for this scientific computing task, the
16
17 766 implementation of the partially-pooled Bayesian hierarchical framework for deriving the CNDC
18 can be made trivial and may enable the development of CNDCs from existing but unutilized
19 experimental datasets. Therefore, the development of a dedicated software library to implement
20
21 767 the partially-pooled Bayesian hierarchical method developed in the present study is a priority for
22
23 768 future research efforts because it will enable other researchers to implement this preferred method
24
25 769 of deriving CNDCs. This is of timely importance given the increased availability of high-quality,
26
27 770 consolidated datasets suitable for fitting CNDCs across G × E × M effects (Ciampitti, et al., 2022).
28
29
30 771
31
32 772
33
34 773 Given the increased availability of data, future research should expand the partially-pooled
35
36 774 Bayesian hierarchical method to fit models simultaneously using data from multiple crop species.
37
38
39
40 775 Finally, having sufficient quantity and quality of experimental data remains an essential criterion
41
42
43 776 to consider when deriving a CNDC independent of the statistical method used (Fernández et al.,
44
45 777 2021; Fernández et al., 2022). Even with the advantages of the partially-pooled Bayesian
46
47 778 hierarchical method, insufficient experimental data quality and quantity may still result in
48
49 779 inferential bias of the CNDC for an individual G × E × M interaction level. Given the limitations
50
51 780 of the quantity and quality of experimental data used in this study (i.e., bias towards N limiting
52
53 781 conditions for Argentina, bias towards non-N limiting conditions for Belgium and Minnesota), it
54
55 782 is plausible that estimates of CNDCs from this study are biased relative to estimates of CNDCs
56
57 783 derived using an “ideal” experimental dataset and identical statistical methods. Therefore, future
58
59
60 784
61
62
63
64
65

1
2
3
4 784 studies utilizing the partially-pooled Bayesian hierarchical method should ensure that the
5 experimental dataset for each $G \times E \times M$ interaction level meets the sufficiency criteria identified
6 by Fernández et al. (2022) (i.e., at least eight experimental trials containing at least three N
7 treatments and at least three sampling dates).
8
9
10
11
12
13
14
15

16 788 **5. Conclusions**
17
18
19
20 789 First, this study demonstrated that there are significant differences between CNDCs developed
21 across $G \times E \times M$ effects for potato. Therefore, any application of $\%N_c$ must use an appropriate
22 CNDC (i.e., not significantly different) for the $G \times E \times M$ interaction being considered. Second,
23 this study developed an approach to communicate uncertainty in $\%N_c$ through the concise set of
24 six parameters defined by the CNDC (i.e., a, b), $CNDC_{lo}$ (i.e., a_{lo}, b_{lo}), and $CNDC_{up}$ (i.e., a_{up}, b_{up}),
25 and the $\%N_c$ value computed from these three curves should be used in all subsequent
26 computations to propagate uncertainty. Third, this study demonstrated that the statistical method
27 used to derive CNDCs affects the inferred $\%N_c$ values, and that the partially-pooled hierarchical
28 Bayesian framework is less susceptible to bias due to insufficient quantity and quality of
29 experimental data than the conventional statistical methods. Therefore, future efforts to derive
30 CNDCs should utilize the partially-pooled hierarchical Bayesian framework whenever possible.
31
32 794 Fourth, the findings of this study suggest that variation in $\%N_c$ across $G \times E \times M$ interactions
33 necessarily extends to NUE, via the relationship between the CNDC and the CNUtEC. Therefore,
34 795 NUE is dependent on the mechanisms that control N dilution (i.e., biomass partitioning), and future
35 efforts to improve NUE should explicitly consider how $G \times E \times M$ interactions affect N dilution.
36
37 796
38
39 797
40
41 798
42
43 799
44
45 800
46
47 801
48
49 802
50
51 803
52
53
54 804
55
56
57
58
59
60
61
62
63
64
65

1
2
3
4 805 **6. Acknowledgements**
5
6
7 806 Research funding for this project was provided by Minnesota Area II Potato Growers Research
8 807 and Promotion Council, and the Clean Water Land and Legacy Amendment with funding
9 808 administered through the Minnesota Department of Agriculture.
10 809
11
12
13
14
15
16
17
18
19
20
21
22
23
24
25
26
27
28
29
30
31
32
33
34
35
36
37
38
39
40
41
42
43
44
45
46
47
48
49
50
51
52
53
54
55
56
57
58
59
60
61
62
63
64
65

1
2
3
4 810 7. References
5
6

- 7 811 AHDB. (2015). Charlotte: Agriculture and Horticulture Development Board. Retrieved from
8 812 <https://varieties.ahdb.org.uk/varieties/view/CHARLOTTE>
9 813 Allen, E.J., and R.K. Scott. (1980). An Analysis of Growth of the Potato Crop. *J. Agr. Sci.*, 94(3),
10 814 583-606. <https://doi.org/10.1017/S0021859600028598>.
11 815 Barraclough, P.B., J.R. Howarth, J. Jones, R. Lopez-Bellido, S. Parmar, C.E. Shepherd, and M.J.
12 816 Hawkesford. (2010). Nitrogen Efficiency of Wheat: Genotypic and Environmental
13 817 Variation and Prospects for Improvement. *Eur. J. Agron.*, 33(1), 1-11.
14 818 <https://doi.org/10.1016/j.eja.2010.01.005>.
15 819 Bates, D.M. (2010). *Lme4: Mixed-Effects Modeling with R*.
16 820 Bélanger, G., J.R. Walsh, J.E. Richards, P.H. Milburn, and N. Ziadi. (2000). Yield Response of
17 821 Two Potato Culivars to Supplemental Irrigation and N Fertilization in New Brunswick.
18 822 *Am. J. Potato Res.*, 77(1), 11-21. <https://doi.org/10.1007/BF02853657>.
19 823 Bélanger, G., J.R. Walsh, J.E. Richards, P.H. Milburn, and N. Ziadi. (2001a). Critical Nitrogen
20 824 Curve and Nitrogen Nutrition Index for Potato in Eastern Canada. *Am. J. Potato Res.*,
21 825 78(5), 355-364. <https://doi.org/10.1007/BF02884344>.
22 826 Bélanger, G., J.R. Walsh, J.E. Richards, P.H. Milburn, and N. Ziadi. (2001b). Tuber Growth and
23 827 Biomass Partitioning of Two Potato Cultivars Grown under Different N Fertilization Rates
24 828 with and without Irrigation. *Am. J. Potato Res.*, 78(2), 109-117.
25 829 <https://doi.org/10.1007/BF02874766>.
30 830 Ben Abdallah, F., M. Olivier, J.P. Goffart, and O. Minet. (2016). Establishing the Nitrogen
31 831 Dilution Curve for Potato Cultivar Bintje in Belgium. *Potato Res.*, 59(3), 241-258.
32 832 <https://doi.org/10.1007/s11540-016-9331-y>.
33 833 Bennett, S.M., T.W. Tibbitts, and W. Cao. (1991). Diurnal Temperature Fluctuation Effects on
34 834 Potatoes Grown with 12 Hr Photoperiods. *Am. Potato J.*, 68, 81-86.
35 835 <https://doi.org/10.1007/BF02853925>.
36 836 Benoit, G.R., W.J. Grant, and O.J. Devine. (1986). Potato Top Growth as Influenced by Day-Night
37 837 Temperature Differences. *Agron. J.*, 78(2), 264-269.
38 838 <https://doi.org/10.2134/agronj1986.00021962007800020010x>.
39 839 Bohman, B.J., M. McNearney, J. Crants, and C.J. Rosen. (2020). A Novel Approach to Manage
40 840 Nitrogen Fertilizer for Potato Production Using Remote Sensing. *Research Reports – 2020*.
41 841 Fargo, ND: Minnesota Area II Potato Research and Promotion Council and Northern Plains
42 842 Potato Growers Association. Retrieved from
43 843 <https://www.ag.ndsu.edu/potatoextension/research/2020ResearchBooks.pdf>
44 844 Bohman, B.J., C.J. Rosen, and D.J. Mulla. (2021). Relating Nitrogen Use Efficiency to Nitrogen
45 845 Nutrition Index for Evaluation of Agronomic and Environmental Outcomes in Potato.
46 846 *Field Crops Res.*, 262. <https://doi.org/10.1016/j.fcr.2020.108041>.
47 847 Bremner, P.M., and M.A. Taha. (1966). Studies in Potato Agronomy. I. The Effects of Variety,
48 848 Seed Size and Spacing on Growth, Development and Yield. *The Journal of Agricultural
49 849 Science*, 66(2), 241-252. <https://doi.org/10.1017/s0021859600062651>.
50 850 Bürkner, P.-C. (2017). Brms: An R Package for Bayesian Multilevel Models Using Stan. *J. Stat.
51 851 Softw.*, 80(1). <https://doi.org/10.18637/jss.v080.i01>.
52 852 Bürkner, P.-C. (2018). Advanced Bayesian Multilevel Modeling with the R Package Brms. *R J.*,
53 853 10(1), 395-411. <https://doi.org/10.32614/RJ-2018-017>.

- 1
2
3
- 4 854 Carpenter, B., A. Gelman, M.D. Hoffman, D. Lee, B. Goodrich, M. Betancourt, M. Brubaker, J.
5 855 Guo, P. Li, and A. Riddell. (2017). Stan: A Probabilistic Programming Language. *J. Stat.*
6 856 *Softw.*, 76(1). <https://doi.org/10.18637/jss.v076.i01>.
- 7 857 Caviglia, O.P., R.J.M. Melchiori, and V.O. Sadras. (2014). Nitrogen Utilization Efficiency in
8 858 Maize as Affected by Hybrid and N Rate in Late-Sown Crops. *Field Crops Res.*, 168, 27-
9 859 37. <https://doi.org/10.1016/j.fcr.2014.08.005>.
- 10 860 CFIA. (2013). Bintje: Canadian Food Inspection Agency. Retrieved from
11 861 [https://inspection.canada.ca/plant-varieties/potatoes/potato-](https://inspection.canada.ca/plant-varieties/potatoes/potato-varieties/bintje/eng/1312587385655/1312587385656)
12 862 [varieties/bintje/eng/1312587385655/1312587385656](#)
- 13 863 Ciampitti, I.A., J. Fernandez, S. Tamagno, B. Zhao, G. Lemaire, and D. Makowski. (2021). Does
14 864 the Critical N Dilution Curve for Maize Crop Vary across Genotype X Environment X
15 865 Management Scenarios? - a Bayesian Analysis. *Eur. J. Agron.*, 123, 126202.
16 866 <https://doi.org/10.1016/j.eja.2020.126202>.
- 17 867 Ciampitti, I., E. van Versendaal, J.F. Rybecky, J. Lacasa, J. Fernandez, D. Makowski, and G.
18 868 Lemaire. (2022). A Global Dataset to Parametrize Critical Nitrogen Dilution Curves for
19 869 Major Crop Species. *Sci. Data*, 9(1), 277. <https://doi.org/10.1038/s41597-022-01395-2>.
- 20 870 Crants, J., C. Rosen, M. McNearney, and L. Sun. (2017). The Use of Chlorophyll Meters for
21 871 Nitrogen Management in Potatoes. *Research Reports – 2017*. Fargo, ND: Minnesota Area
22 872 II Potato Research and Promotion Council and Northern Plains Potato Growers
23 873 Association. Retrieved from <https://www.ag.ndsu.edu/potatoextension/research>
- 24 874 Duchenne, T., J.M. Machet, and M. Martin. (1997). Potatoes. In G. Lemaire (Ed.), *Diagnosis of
25 875 the Nitrogen Status in Crops* (pp. 119-130). Berlin: Springer.
- 26 876 Egel, D.S. (2017). Midwest Vegetable Production Guide for Commercial Growers. *BU-07094-S*:
27 877 University of Minnesota Extension. Retrieved from <https://ag.purdue.edu/btny/midwest-vegetable-guide/Pages/default.aspx>
- 28 878 Errebbi, M., C.J. Rosen, S.C. Gupta, and D.E. Birong. (1998). Potato Yield Response and Nitrate
29 879 Leaching as Influenced by Nitrogen Management. *Agron. J.*, 90, 10-15.
30 880 <https://doi.org/10.2134/agronj1998.00021962009000010003x>.
- 31 881 Ewing, E.E., and P.C. Struik. (1992). Tuber Formation in Potato: Induction, Initiation, and Growth.
32 882 In J. Janick (Ed.), *Horticultural Reviews, Volume 14* (pp. 89-198): John Wiley & Sons.
- 33 883 Fernández, J.A., G. Lemaire, G. Bélanger, F. Gastal, D. Makowski, and I.A. Ciampitti. (2021).
34 884 Revisiting the Critical Nitrogen Dilution Curve for Tall Fescue: A Quantitative Synthesis.
35 885 *Eur. J. Agron.*, 131, 126380. <https://doi.org/10.1016/j.eja.2021.126380>.
- 36 886 Fernandez, J.A., E. van Versendaal, J. Lacasa, D. Makowski, G. Lemaire, and I.A. Ciampitti.
37 887 (2022). Dataset Characteristics for the Determination of Critical Nitrogen Dilution Curves:
38 888 From Past to New Guidelines. *Eur. J. Agron.*, 139, 126568.
39 889 <https://doi.org/10.1016/j.eja.2022.126568>.
- 40 890 Franzen, D., A. Robinson, and C. Rosen. (2018). Fertilizing Potato in North Dakota. *SF715*. Fargo,
41 891 ND: North Dakota State University. Retrieved from
42 892 <https://www.ag.ndsu.edu/publications/crops/fertilizing-potato-in-north-dakota>
- 43 893 Gastal, F., G. Lemaire, J.-L. Durand, and G. Louarn. (2015). Quantifying Crop Responses to
44 894 Nitrogen and Avenues to Improve Nitrogen-Use Efficiency. In *Crop Physiology* (Second
45 895 ed., pp. 161-206).
- 46 896 Gelaro, R., W. McCarty, M.J. Suarez, R. Todling, A. Molod, L. Takacs, C. Randles, A. Darmenov,
47 897 M.G. Bosilovich, R. Reichle, K. Wargan, L. Coy, R. Cullather, C. Draper, S. Akella, V.
48 898 Buchard, A. Conaty, A. da Silva, W. Gu, G.K. Kim, R. Koster, R. Lucchesi, D. Merkova,
49 899
- 50 900
- 51 901
- 52 902
- 53 903
- 54 904
- 55 905
- 56 906
- 57 907
- 58 908
- 59 909
- 60 910
- 61 911
- 62 912
- 63 913
- 64 914
- 65 915

- 1
2
3
- 4 900 J.E. Nielsen, G. Partyka, S. Pawson, W. Putman, M. Rienecker, S.D. Schubert, M.
5 901 Sienkiewicz, and B. Zhao. (2017). The Modern-Era Retrospective Analysis for Research
6 902 and Applications, Version 2 (Merra-2). *J Clim, Volume 30*(Iss 13), 5419-5454.
7 903 <https://doi.org/10.1175/JCLI-D-16-0758.1>.
- 8 904 Giletto, C.M., and H.E. Echeverría. (2015). Critical Nitrogen Dilution Curve in Processing Potato
9 905 Cultivars. *Am. J. Plant Sci.*, 06(19), 3144-3156. <https://doi.org/10.4236/ajps.2015.619306>.
- 10 906 Giletto, C.M., N.I. Reussi Calvo, P. Sandaña, H.E. Echeverría, and G. Bélanger. (2020). Shoot-
11 907 and Tuber-Based Critical Nitrogen Dilution Curves for the Prediction of the N Status in
12 908 Potato. *Eur. J. Agron.*, 119. <https://doi.org/10.1016/j.eja.2020.126114>.
- 13 909 Greenwood, D.J., G. Lemaire, G. Gosse, P. Cruz, A. Draycott, and J.J. Neeteson. (1990). Decline
14 910 in Percentage N of C3 and C4 Crops with Increasing Plant Mass. *Ann. Bot.*, 66(4), 425-
15 911 436. <https://doi.org/10.1093/oxfordjournals.aob.a088044>.
- 16 912 Greenwood, D.J., J.J. Neeteson, and A. Draycott. (1986). Quantitative Relationships for the
17 913 Dependence of Growth Rate of Arable Crops on Their Nitrogen Content, Dry Weight and
18 914 Aerial Environment. *Plant Soil*, 91(3), 281-301. <https://doi.org/10.1007/BF02198111>.
- 19 915 Gupta, S., and C.J. Rosen. (2019). Nitrogen Fertilization Rate and Cold-Induced Sweetening in
20 916 Potato Tubers During Storage. *Research Reports – 2019*. Fargo, ND: Minnesota Area II
21 917 Potato Research and Promotion Council and Northern Plains Potato Growers Association.
22 918 Retrieved from
23 919 <https://www.ag.ndsu.edu/potatoextension/research/2019RESEARCHREPORTS.pdf>
- 24 920 Gupta, S.K., J. Crants, M. McNearney, and C.J. Rosen. (2020). Evaluation of a Promising
25 921 Minnesota Clone for N Response, Agronomic Traits & Storage Quality. *Research Reports*
26 922 – 2020. Fargo, ND: Minnesota Area II Potato Research and Promotion Council and
27 923 Northern Plains Potato Growers Association. Retrieved from
28 924 <https://www.ag.ndsu.edu/potatoextension/research/2020ResearchBooks.pdf>
- 29 925 Hansen, B., and A.G. Giencke. (1988). Sand Plains Research Farm Soil Report. St. Paul, MN:
30 926 University of Minnesota
- 31 927 Herrmann, A., and F. Taube. (2004). The Range of the Critical Nitrogen Dilution Curve for Maize
32 928 (*Zea Mays L.*) Can Be Extended until Silage Maturity. *Agron. J.*, 96(4), 1131-1138.
33 929 <https://doi.org/10.2134/agronj2004.1131>.
- 34 930 Horneck, D.A., and R.O. Miller. (1998). Determination of Total Nitrogen in Plant Tissue. In Y. P.
35 931 Kalra (Ed.), *Handbook of Reference Methods for Plant Analysis* (pp. 75-84). Boston: CRC
36 932 Press.
- 37 933 Horwitz, W., P. Chichilo, and H. Reynolds. (1970). *Official Methods of Analysis of the Association*
38 934 *of Official Analytical Chemists*. (11th ed.). Washington, DC: Association of Official
39 935 Analytical Chemists.
- 40 936 Houlès, V., M. Guérif, and B. Mary. (2007). Elaboration of a Nitrogen Nutrition Indicator for
41 937 Winter Wheat Based on Leaf Area Index and Chlorophyll Content for Making Nitrogen
42 938 Recommendations. *Eur. J. Agron.*, 27(1), 1-11. <https://doi.org/10.1016/j.eja.2006.10.001>.
- 43 939 Ifenkwe, O.P., and E.J. Allen. (1978). Effects of Row Width and Planting Density on Growth and
44 940 Yield of Two Maincrop Potato Varieties. 1. Plant Morphology and Dry-Matter
45 941 Accumulation. *The Journal of Agricultural Science*, 91(2), 265-278.
46 942 <https://doi.org/10.1017/s0021859600046359>.
- 47 943 Jones, C.R., T.E. Michaels, C.S. Carley, C.J. Rosen, and L.M. Shannon. (2021). Nitrogen Uptake
48 944 and Utilization in Advanced Fresh-Market Red Potato Breeding Lines. *Crop Sci.*, 61, 878-
49 945 895. <https://doi.org/10.1002/csc2.20297>.
- 50
51
52
53
54
55
56
57
58
59
60
61
62
63
64
65

- 1
2
3
- 4 946 Justes, E., B. Mary, J.-M. Meynard, J.-M. Machet, and L. Thelier-Huche. (1994). Determination
5 947 of a Critical Nitrogen Dilution Curve for Winter Wheat Crops. *Ann. Bot.*, 74(4), 397-407.
6 948 https://doi.org/10.1006/anbo.1994.1133.
- 7 949 Kim, Y.U., and B.W. Lee. (2019). Differential Mechanisms of Potato Yield Loss Induced by High
8 950 Day and Night Temperatures During Tuber Initiation and Bulking: Photosynthesis and
9 951 Tuber Growth. *Front. Plant Sci.*, 10, 300. https://doi.org/10.3389/fpls.2019.00300.
- 10 952 Kleinkopf, G.E., D.T. Westermann, and R.B. Dwelle. (1981). Dry Matter Production and Nitrogen
11 953 Utilization by Six Potato Cultivars. *Agron. J.*, 73(5), 799-802.
12 954 https://doi.org/10.2134/agronj1981.00021962007300050013x.
- 13 955 Lemaire, G., and I. Ciampitti. (2020). Crop Mass and N Status as Prerequisite Covariates for
14 956 Unraveling Nitrogen Use Efficiency across Genotype-by-Environment-by-Management
15 957 Scenarios: A Review. *Plants*, 9(10). https://doi.org/10.3390/plants9101309.
- 16 958 Lemaire, G., and F. Gastal. (1997). N Uptake and Distribution in Plant Canopies. In G. Lemaire
17 959 (Ed.), *Diagnosis of the Nitrogen Status in Crops* (pp. 3-43). Berlin: Springer.
- 18 960 Lemaire, G., T. Sinclair, V. Sadras, and G. Bélanger. (2019). Allometric Approach to Crop
19 961 Nutrition and Implications for Crop Diagnosis and Phenotyping. A Review. *Agron. Sustain. Dev.*, 39(2). https://doi.org/10.1007/s13593-019-0570-6.
- 20 962 Li, D., Y. Miao, S.K. Gupta, C.J. Rosen, F. Yuan, C. Wang, L. Wang, and Y. Huang. (2021).
21 963 Improving Potato Yield Prediction by Combining Cultivar Information and Uav Remote
22 964 Sensing Data Using Machine Learning. *Remote Sens.*, 13(16).
23 965 https://doi.org/10.3390/rs13163322.
- 24 966 Lindstrom, M.J., and D.M. Bates. (1990). Nonlinear Mixed Effects Models for Repeated Measures
25 967 Data. *Biometrics*, 46(3), 673-687. https://doi.org/10.2307/2532087.
- 26 968 Lizana, X.C., A. Avila, A. Tolaba, and J.P. Martinez. (2017). Field Responses of Potato to
27 969 Increased Temperature During Tuber Bulking: Projection for Climate Change Scenarios,
28 970 at High-Yield Environments of Southern Chile. *Agric. For. Meteorol.*, 239, 192-201.
29 971 https://doi.org/10.1016/j.agrformet.2017.03.012.
- 30 972 Makowski, D., B. Zhao, S.T. Ata-Ul-Karim, and G. Lemaire. (2020). Analyzing Uncertainty in
31 973 Critical Nitrogen Dilution Curves. *Eur. J. Agron.*, 118.
32 974 https://doi.org/10.1016/j.eja.2020.126076.
- 33 975 McElreath, R. (2020). *Statistical Rethinking: A Bayesian Course with Examples in R and Stan* (2nd
34 976 ed.). Boca Raton: Chapman and Hall/CRC.
- 35 977 Menzel, C.M. (1985). Tuberization in Potato at High Temperatures: Interaction between
36 978 Temperature and Irradiance. *Ann. Bot.*, 55(1), 35-39.
37 979 https://doi.org/10.1093/oxfordjournals.aob.a086875.
- 38 980 Monteith, J.L. (1977). Climate and the Efficiency of Crop Production in Britain. *Phil. Trans. R. Soc. Lond. B*, 281, 277-294. https://doi.org/10.1098/rstb.1977.0140.
- 39 981 Morier, T., A.N. Cambouris, and K. Chokmani. (2015). In-Season Nitrogen Status Assessment
40 982 and Yield Estimation Using Hyperspectral Vegetation Indices in a Potato Crop. *Agron. J.*, 107(4), 1295-1309. https://doi.org/10.2134/agronj14.0402.
- 41 983 Morris, T.F., T.S. Murrell, D.B. Beegle, J.J. Camberato, R.B. Ferguson, J. Grove, Q. Ketterings,
42 984 P.M. Kyveryga, C.A.M. Laboski, J.M. McGrath, J.J. Meisinger, J. Melkonian, B.N.
43 985 Moebius-Clune, E.D. Nafziger, D. Osmond, J.E. Sawyer, P.C. Scharf, W. Smith, J.T.
44 986 Spargo, H.M. van Es, and H. Yang. (2018). Strengths and Limitations of Nitrogen Rate
45 987 Recommendations for Corn and Opportunities for Improvement. *Agron. J.*, 110(1), 1.
46 988 https://doi.org/10.2134/agronj2017.02.0112.

1
2
3

- 4 992 OSU. (2021). Potato Variety Identification and Ownership Table: Oregon State University –
5 993 Oregon Seed Certification Service. Retrieved from
6 994 https://seedcert.oregonstate.edu/sites/seedcert.oregonstate.edu/files/potato_varietyratingkey.pdf
7 995
8 996 Plénet, D., and G. Lemaire. (2000). Relationships between Dynamics of Nitrogen Uptake and Dry
9 997 Matter Accumulation in Maize Crops. Determination of Critical N Concentration. *Plant*
10 998 *Soil*, 216(1/2), 65-82. <https://doi.org/10.1023/a:1004783431055>.
11 999 Plummer, M. (2013). Jags: Just Another Gibbs Sampler. Retrieved from <http://mcmc-jags.sourceforge.net/>.
12 1000
13 1001 Plummer, M. (2019). Rjags: Bayesian Graphical Models Using Mcmc. Retrieved from
14 1002 <https://CRAN.R-project.org/package=rjags>
15 1003 Porter, G. (2014). 201400091. USDA PVPO.
16 1004 R Core Team. (2021a). R: A Language and Environment for Statistical Computing. Vienna,
17 1005 Austria: R Foundation for Statistical Computing. Retrieved from <https://www.R-project.org/>
18 1006
19 1007 R Core Team. (2021b). "Stats": The R Stats Package. Retrieved from <https://CRAN.R-project.org/package=stats>
20 1008
21 1009 Rosen, C., D. Birong, and M. Zumwinkle. (1992). Nitrogen Fertilization Studies on Irrigated
22 1010 Potatoes: Nitrogen Use, Soil Nitrate Movement, and Petiole Sap Nitrate Analysis for
23 1011 Predicting Nitrogen Needs. *Field Research in Soil Science – Soil Series #134*. St. Paul,
24 1012 MN: University of Minnesota. Retrieved from
25 1013 <https://conservancy.umn.edu/handle/11299/121705>
26 1014 Rosen, C., J. Crants, B. Bohman, and M. McNearney. (2021). Effects of Banded Versus Broadcast
27 1015 Application of Esn, Turkey Manure, and Different Approaches to Measuring Plant N Status
28 1016 on Tuber Yield and Quality in Russet Burbank Potatoes. *Reserach Reports – 2021*. Fargo,
29 1017 ND: Minnesota Area II Potato Research and Promotion Council and Northern Plains Potato
30 1018 Growers Association. Retrieved from
31 1019 https://www.ag.ndsu.edu/potatoextension/research/research_reports_114_4126022392.pdf
32 1020
33 1021 Rosen, C., M. Errebhi, J. Moncrief, S. Gupta, H.H. Cheng, and D. Birong. (1993). Nitrogen
34 1022 Fertilization Studies on Irrigated Potatoes: Nitrogen Use, Soil Nitrate Movement, and
35 1023 Petiole Sap Nitrate Analysis for Predicting Nitrogen Needs. *Field Research in Soil Science*
36 1024 – *Soil Series #136*. St. Paul, MN: University of Minnesota. Retrieved from
37 1025 <https://conservancy.umn.edu/handle/11299/121706>
38 1026 Rosen, C.J. (2018). Potato Fertilization on Irrigated Soils: University of Minnesota Extension.
39 1027 Retrieved from <https://extension.umn.edu/crop-specific-needs/potato-fertilization-irrigated-soils>
40 1028
41 1029 Sadras, V.O., and G. Lemaire. (2014). Quantifying Crop Nitrogen Status for Comparisons of
42 1030 Agronomic Practices and Genotypes. *Field Crops Res.*, 164, 54-64.
43 1031 <https://doi.org/10.1016/j.fcr.2014.05.006>.
44 1032 Schad, D.J., M. Betancourt, and S. Vasishth. (2021). Toward a Principled Bayesian Workflow in
45 1033 Cognitive Science. *Psychol Methods*, 26(1), 103-126. <https://doi.org/10.1037/met0000275>.
46 1034 Sinclair, T.R., and R.C. Muchow. (1999). Radiation Use Efficiency. In D. L. Sparks (Ed.),
47 1035 *Advances in Agronomy, Volume 65* (Vol. 65, pp. 215-265).
48 1036 Slater, J.W. (1968). The Effect of Night Temperature on Tuber Initiation of the Potato. *European*
49 1037 *Potato Journal*, 11(1), 14-22. <https://doi.org/10.1007/BF02365158>.
50
51
52
53
54
55
56
57
58
59
60
61
62
63
64
65

1
2
3

- 4 1038 Stark, J.C., A.L. Thompson, R. Novy, and S.L. Love. (2020). Variety Selection and Management.
5 1039 In J. C. Stark, M. Thornton, and P. Nolte (Eds.), *Potato Production Systems* (pp. 35-64).
6 1040 Steele, D.D., T.F. Scherer, J. Wright, D.G. Hopkins, S.R. Tuscherer, and J. Wright. (2010).
7 1041 Spreadsheet Implementation of Irrigation Scheduling by the Checkbook Method for North
8 1042 Dakota and Minnesota. *Appl. Eng. Agric.*, 26, 983-996.
9 1043 <https://doi.org/10.13031/2013.35914>.
10 1044 Stefaniak, T.R., S. Fitzcollins, R. Figueroa, A.L. Thompson, C. Schmitz Carley, and L.M.
11 1045 Shannon. (2021). Genotype and Variable Nitrogen Effects on Tuber Yield and Quality for
12 1046 Red Fresh Market Potatoes in Minnesota. *Agronomy*, 11, 255.
13 1047 <https://doi.org/10.3390/agronomy11020255>.
14 1048 Sun, N. (2017). *Agronomic and Storage Factors Affecting Acrylamide Formation in Processed*
15 1049 *Potatoes*. (Ph.D.). University of Minnesota, St. Paul, MN. Retrieved from
16 1050 <https://conservancy.umn.edu/handle/11299/190488>
17 1051 Sun, N., Y. Wang, S.K. Gupta, and C.J. Rosen. (2019). Nitrogen Fertility and Cultivar Effects on
18 1052 Potato Agronomic Properties and Acrylamide-Forming Potential. *Agron. J.*, 111(1), 408.
19 1053 <https://doi.org/10.2134/agronj2018.05.0350>.
20 1054 Sun, N., Y. Wang, S.K. Gupta, and C.J. Rosen. (2020). Potato Tuber Chemical Properties in
21 1055 Storage as Affected by Cultivar and Nitrogen Rate: Implications for Acrylamide
22 1056 Formation. *Foods*, 9(3). <https://doi.org/10.3390/foods9030352>.
23 1057 Thompson, A. (2013). 201300475. USDA PVPO.
24 1058 Thornton, M. (2020). Potato Growth and Development. In J. C. Stark, M. Thornton, and P. Nolte
25 1059 (Eds.), *Potato Production Systems* (pp. 19-33).
26 1060 Tiwari, J.K., D. Plett, T. Garnett, S.K. Chakrabarti, and R.K. Singh. (2018). Integrated Genomics,
27 1061 Physiology and Breeding Approaches for Improving Nitrogen Use Efficiency in Potato:
28 1062 Translating Knowledge from Other Crops. *Funct. Plant Biol.*, 45(6), 587.
29 1063 <https://doi.org/10.1071/fp17303>.
30 1064 USDA. (1997). United States Standards for Grades of Potatoes for Processing. Retrieved from
31 1065 https://www.ams.usda.gov/sites/default/files/media/Potatoes_for_Processing_Standard%5B1%5D.pdf
32 1066
33 1067 USDA NRCS. (2013). Soil Series Classification Database – Hubbard Series: United States
34 1068 Department of Agriculture. Retrieved from
35 1069 https://soilseries.sc.egov.usda.gov/OSD_Docs/H/HUBBARD.html
36 1070 Ushey, K. (2021). Renv: Project Environments. Retrieved from <https://CRAN.R-project.org/package=renv>
37 1071
38 1072 Vander Zaag, P., A.L. Demagante, and E.E. Ewing. (1990). Influence of Plant Spacing on Potato
39 1073 (*Solanum Tuberosum L.*) Morphology, Growth and Yield under Two Contrasting
40 1074 Environments. *Potato Res.*, 33(313–323). <https://doi.org/10.1007/BF02359305>.
41 1075 Vehtari, A., A. Gelman, D. Simpson, B. Carpenter, and P.-C. Bürkner. (2021). Rank-
42 1076 Normalization, Folding, and Localization: An Improved R-Hat for Assessing Convergence
43 1077 of MCMC (with Discussion). *Bayesian Anal.*, 16(2), 667-718. <https://doi.org/10.1214/20-BA1221>.
44 1078
45 1079 Weather Spark. (2021). Compare the Climate and Weather in Becker, Saint-Léonard, Balcarce,
46 1080 and Gembloix. Retrieved from
47 1081 <https://weatherspark.com/compare/y/10443~27617~28950~51092/Comparison-of-the-Average-Weather-in-Becker-Saint-L%C3%A9onard-Balcarce-and-Gembloix>
48 1082
49
50
51
52
53
54
55
56
57
58
59
60
61
62
63
64
65

1
2
3
4 1083 Wright, J. (2002). Irrigation Scheduling Checkbook Method. *BU-FO-01322*. St. Paul, MN:
5
6 University of Minnesota. Retrieved from <https://extension.umn.edu/irrigation/irrigation-scheduling-checkbook-method>
7
8 1086 Yao, B., X. Wang, G. Lemaire, D. Makowski, Q. Cao, X. Liu, L. Liu, B. Liu, Y. Zhu, W. Cao, and
9
10 1088 L. Tang. (2021). Uncertainty Analysis of Critical Nitrogen Dilution Curves for Wheat. *Eur.
11 J. Agron.*, 128, 126315. <https://doi.org/10.1016/j.eja.2021.126315>.

12 1089
13
14
15
16
17
18
19
20
21
22
23
24
25
26
27
28
29
30
31
32
33
34
35
36
37
38
39
40
41
42
43
44
45
46
47
48
49
50
51
52
53
54
55
56
57
58
59
60
61
62
63
64
65

[Click here to view linked References](#)

1 **Quantifying critical N dilution curves across G × E × M effects for potato using a partially-**
2 **pooled Bayesian hierarchical method**

3 Brian J. Bohman^{1*}, Michael J. Culshaw-Maurer², Feriel Ben Abdallah³, Claudia Giletto⁴, Gilles
4 Bélanger⁵, Fabián G. Fernández¹, Yuxin Miao¹, David J. Mulla¹, and Carl J. Rosen¹

5 1. Department of Soil, Water, and Climate, University of Minnesota. 1991 Upper Buford
6 Circle, St. Paul MN 55108

7 2. CyVerse, University of Arizona, Tuscon, AZ

8 3. Productions in Agriculture Department, Crop Production Unit, Walloon Agricultural
9 Research Centre (CRA-W), Gembloux, Belgium

10 4. Unidad Integrada Balcarce, Facultad de Ciencias Agrarias (UNMdP)-INTA Balcarce. Ruta
11 226 km 73,5 (7620) Balcarce, Buenos Aires, Argentina

12 5. Science and Technology Branch, Agriculture and Agri-Food Canada, Québec City, Canada

13 * Corresponding Author: bohm0072@umn.edu

14

15 **Abstract:** Multiple critical N dilution curves [CNDCs] have been previously developed for potato;
16 however, attempts to directly compare differences in CNDCs across genotype [G], environment
17 [E], and management [M] interactions have been confounded by non-uniform statistical methods,
18 biased experimental data, and lack of proper quantification of uncertainty in the critical N
19 concentration [%N_c]. This study implements a partially-pooled Bayesian hierarchical method to
20 develop CNDCs for previously published and newly reported experimental data, systematically
21 evaluates the difference in %N_c [$\Delta\%N_c$] across G × E × M effects, and directly compare CNDCs
22 from the Bayesian framework to CNDCs from conventional statistical methods. The partially-
23 pooled Bayesian hierarchical method implemented in this study has the advantage of being less
24 susceptible to inferential bias at the level of individual G × E × M interactions compared to
25 alternative statistical methods that result from insufficient quantity and quality of experimental
26 datasets (e.g., unbalanced distribution of N limiting and non-N limiting observations). This method
27 also allows for a direct statistical comparison of differences in %N_c across levels of the G × E ×
28 M interactions. Where found to be significant, $\Delta\%N_c$ was hypothesized to be related to variation
29 in the timing of tuber initiation (e.g., maturity class) and the relative rate of tuber bulking (e.g.,
30 planting density) across G × E × M interactions. In addition to using the median value for %N_c
31 (i.e., CNDC), the lower and upper boundary values for the credible region (i.e., CNDC_{lo} and
32 CNDC_{up}) derived using the Bayesian framework should be used in calculation of N nutrition index
33 (and other calculations) to account for uncertainty in %N_c. Overall, this study provides additional
34 evidence that %N_c is dependent upon G × E × M interactions; therefore, evaluation of crop N status
35 or N use efficiency must account for variation in %N_c across G × E × M interactions.

36 **Keywords:** critical N concentration; critical nitrogen dilution curve; nitrogen nutrition index;
37 nitrogen use efficiency; potato; Bayesian; genotype-by-environment-by-management interactions

38

39 **Abbreviations:** NUE, nitrogen use efficiency; NUpE, nitrogen uptake efficiency; NUtE, nitrogen
40 utilization efficiency; NNI, nitrogen nutrition index; CNDC, critical nitrogen dilution curve;
41 CNUC, critical nitrogen uptake curve; CNUtEC, critical nitrogen utilization efficiency curve; W,
42 total dry weight plant biomass; N_{Plant} , plant nitrogen content, $\%N_{Plant}$, plant nitrogen concentration;
43 $\%N_c$, critical plant nitrogen concentration; $NUtE_c$, critical nitrogen utilization efficiency; $\Delta\%N_c$,
44 difference in critical nitrogen concentration; $\%N_{c,up}$, upper bounds of credible interval for critical
45 nitrogen concentration; $\%N_{c,lo}$, lower bounds of credible interval for critical nitrogen
46 concentration; NNI_{up} , upper bound of credible interval for nitrogen nutrition index value; NNI_{lo} ,
47 lower bound of credible interval for nitrogen nutrition index value; $CNDC_{lo}$, lower boundary of
48 credible region for critical nitrogen dilution curve; $CNDC_{up}$, upper boundary of credible region for
49 critical nitrogen dilution curve; G, genotype; E, environment; M, management; EONR,
50 economically optimum nitrogen rate

51

52 **1. Introduction**

53 Identifying optimal crop nitrogen [N] status to maximize growth and yield production is an elusive
54 goal. Traditionally, either the yield-goal approach or rate-response curves have been used to
55 identify optimal N fertilizer application rate (Morris et al., 2018). The N nutrition index [NNI] is
56 an alternative approach to the current paradigm and comprises a well-developed framework to
57 determine optimal crop N status (Lemaire et al., 2019). Typically, NNI is used to determine crop
58 N status using whole plant analysis and to direct adaptive N management within a growing season
59 (Houlès et al., 2007; Morier et al., 2015). The NNI framework has conventionally been considered
60 generalizable across E × M effects (e.g., year-to-year, geographic, or cultural practices variability)
61 and can be defined for any particular G effect (e.g., crop species or cultivar). In this manner, NNI
62 reflects intrinsic physiological properties and reflects absolute crop N status across variation in
63 environmental conditions (e.g., net soil N supply) or management practices (e.g., rate, source,
64 timing, and placement of N fertilizer) (Sadras & Lemaire, 2014).

65 The NNI approach is defined based on the allometric relationship of declining plant N
66 concentration [%N_{Plant}] with increasing plant biomass, referred to as the critical N dilution curve
67 [CNDC], which defines the critical N concentration [%N_c] below which relative growth rate is
68 reduced (Gastal et al., 2015):

$$69 \quad \%N_c = a W^{-b} \quad [1]$$

70 where W represents dry weight plant biomass, and *a* and *b* are empirically fitted parameters.
71 Parameter *a* is numerically equivalent to %N_c expressed in units of g N 100 g⁻¹ when W is equal
72 to 1 Mg ha⁻¹, and parameter *b* represents the ratio of the relative rate of decline in %N_c to the

73 relative rate of increase in W. Using the CNDC, NNI values are then calculated as ratio of %N_{Plant}
74 and %N_c:

75 $\text{NNI} = \% \text{N}_{\text{Plant}} / \% \text{N}_c$ [2]

76 When NNI is greater than 1.0, crop N status is said to be in excess, and crop growth is not limited
77 by N, while when NNI is less than 1.0, crop N status is deficient, and crop growth is limited by N.
78 At NNI equal to 1.0, crop N status is optimal (Lemaire & Gastal, 1997).

79 A robust theoretical framework has been developed to explain decline in N concentration as
80 biomass increases, but the application of this theory is most commonly restricted to the vegetative
81 period where only metabolic and structural tissues are present (Greenwood et al., 1990; Justes et
82 al., 1994; Sadras & Lemaire, 2014). Dilution of N in vegetative tissue occurs in relationship to an
83 increasing proportion of structural biomass, with low N concentration, relative to metabolic (i.e.,
84 photosynthetic) biomass, with high N concentration (Lemaire & Gastal, 1997; Gastal et al., 2015).

85 Multiple previous studies have extended and empirically validated the CNDC relationships beyond
86 its typical applications to describe declining N concentration over the entire crop growth cycle,
87 including periods of reproductive growth, by including consideration of storage tissues in addition
88 to structural and metabolic tissues (Greenwood et al., 1986; Duchenne et al., 1997; Plénet &
89 Lemaire, 2000; Herrmann & Taube, 2004). Acceleration of N dilution beyond the vegetative
90 period primarily occurs as low N biomass (i.e., starch) accumulates in storage tissues such as grain
91 or tubers where the rate of decline is determined by the relative N concentration in storage biomass
92 compared to vegetative biomass (Duchenne et al., 1997; Plénet & Lemaire, 2000). Duchenne et al.
93 (1997) observed that as an increasing proportion of biomass accumulates in tubers, the rate of
94 decline in N concentration increases with increasing biomass. Certain crops, such as potato,

95 exclusively use a CNDC based on whole plant biomass due to the complex relationship between
96 vine growth and tuber production (Duchenne et al., 1997; Bélanger et al., 2001a; Giletto &
97 Echeverría, 2015; Ben Abdallah et al., 2016). Despite the validity of this approach, interpreting
98 variation in CNDC observed between cultivars and geographies has been challenging.

99 However, recent work by Giletto et al. (2020) identified a mechanistic relationship underpinning
100 the observed empirical relationships in N dilution for potato. The CNDC based on whole plant
101 biomass reflects dilution in both the tuber and vine biomass, individually, and the increasing
102 proportion of biomass allocated to low concentrations of N in biomass (i.e., tubers) as whole plant
103 biomass increases. Giletto et al. (2020) also observed that varieties and locations with a greater
104 proportion of biomass allocated to tubers have a greater value for parameter b of the CNDC, where
105 parameter b of the CNDC represents the relative rate of decline in $\%N_c$ as biomass increases.

106 Based on this framework developed by Giletto et al. (2020), it is reasonable to expect that variation
107 in CNDC for potato would occur due to variation in total biomass and harvest index (i.e., timing
108 of tuber initiation, relative rate of tuber bulking) across $G \times E \times M$ gradients. Understanding the
109 effects of $G \times E \times M$ interactions on crop N requirements and status is critical to improving
110 agronomic outcomes and N use efficiency [NUE] within cropping systems (Lemaire & Ciampitti,
111 2020).

112 Previous CNDCs for potato have been developed with different statistical methods and limited
113 quantification of their uncertainty (Duchenne et al., 1997; Bélanger et al., 2001a; Giletto &
114 Echeverría, 2015; Ben Abdallah et al., 2016). This makes it difficult to ascertain whether observed
115 differences in CNDCs result from underlying $G \times E \times M$ effects, are confounded by the limitations

116 of the statistical approach, or biased due to insufficient quantity or quality of experimental data
117 (e.g., unbalanced distribution of N limiting and non-N limiting observations).

118 The conventional approach to fit a CNDC consists of a two-step process: first, the critical points
119 from the relationship of %N_{Plant} as a function of biomass are selected using statistical criteria;
120 second, a negative exponential curve is fit to the subset of critical points using non-linear
121 regression. There are two commonly used statistical approaches to identify critical points: (1)
122 linear-plateau curve fit and (2) ANOVA and protected multiple comparison. Using a linear-plateau
123 curve to derive critical points was originally suggested by Justes et al. (1994). This approach is
124 rigorous and requires sufficient empirical data such that a linear-plateau curve can be identified
125 (i.e., at least one N limiting and at least two non-N limiting data points) for each observation date.
126 Therefore, this approach can be difficult or impossible to implement due to potential limitations
127 of the experimental data used such as insufficient levels of N treatments (i.e., fewer than three
128 treatment levels) or interactions between management practices and environmental conditions (i.e.,
129 all observations are either N limiting or non-N limiting). In contrast, many studies use methods
130 similar to Ben Abdallah et al. (2016) where critical points are determined using a simplified
131 statistical method. In this approach, ANOVA is first used to identify experimental dates where
132 variation in biomass is statistically significant. Subsequently, a protected multiple comparisons
133 analysis is used to identify which experimental treatments had the highest level of biomass – the
134 treatment level with the significantly greatest level of biomass is then defined as the critical point.
135 While this statistical method is more flexible to implement, it cannot resolve deficiencies in the
136 underlying empirical data (e.g., insufficient level of N treatments, interactions with environmental
137 conditions). Therefore, the critical points selected using the simplified method may be biased due
138 to inherent deficiencies of the underlying experimental data used.

139 Novel statistical methods developed first by Makowski et al. (2020) provide a framework which
140 allows for standardization in statistical approach and quantification of uncertainty for deriving in
141 CNDCs which enables comparison of $\%N_c$ across $G \times E \times M$ interactions. In short, this framework
142 implements a hierarchical Bayesian model which simultaneously identifies critical points using
143 the linear-plateau method (e.g., Justes et al. (1994)) while fitting the negative exponential curve
144 which defines $\%N_c$. The advantage of this method is that it fits the CNDC from the entire set of
145 experimental data for a given $G \times E \times M$ interaction level and removes the arbitrary intermediate
146 step of separately identifying critical points. This approach has already been successfully used by
147 Ciampitti et al. (2021), Yao et al. (2021), and Fernández et al. (2021) to evaluate differences in
148 CNDCs across $G \times E \times M$ interactions for maize, wheat, and tall fescue cropping systems,
149 respectively. Through this single-step process, the Bayesian hierarchical method both eliminates
150 the need to separately identify critical points and implements the theoretically preferred method
151 (e.g., linear-plateau curve fit) to select critical points.

152 The Bayesian hierarchical method, however, remains subject to inferential bias due to both limited
153 quantity and quality of experimental data (Fernández et al., 2021; Fernandez et al., 2022). With
154 respect to quantity, having an insufficient number of observations from a limited number of
155 experimental trials to derive an individual CNDC will result in increased bias in $\%N_c$. With respect
156 to quality, using experimental data that does not reflect a full range of biomass values or does not
157 sufficiently represent both limiting and non-limiting N conditions will result in increased bias in
158 $\%N_c$. Datasets used to derive the CNDC using the Bayesian hierarchical method should contain at
159 least eight experimental trials containing at least three N treatments and at least three sampling
160 dates (Fernández et al., 2022).

161 However, there are multiple approaches to pooling across $G \times E \times M$ interactions within the
162 Bayesian hierarchical method to address this bias due to experimental data limitations: no pooling,
163 full pooling, and partial pooling. The no pooling approach treats each experimental data level
164 independently where experimental data from one level is not used in inference for any other level
165 (McElreath, 2020). The no pooling approach was used by Makowski et al. (2020), Ciampitti et al.
166 (2021), Yao et al. (2021), and Fernández et al. (2021) to develop independent models for each G
167 $\times E \times M$ interaction. For the Bayesian hierarchical method, the no pooling approach is directly
168 limited by the quantity and quality of experimental data for each $G \times E \times M$ interaction level. The
169 full pooling approach, in contrast, treats each experimental data level in an equivalent manner
170 where the experimental data from all levels are used simultaneously for inference (McElreath,
171 2020). The full pooling approach was used by Fernández et al. (2021) to develop a single model
172 across $G \times E \times M$ interaction levels. While this approach was found by Fernández et al. (2021) to
173 potentially reduce inferential bias from the Bayesian hierarchical method (i.e., by increasing the
174 combined quantity and quality of data used to fit a given CNDC), the fully pooled approach has
175 the explicit tradeoff that inference at individual levels of $G \times E \times M$ interactions is not possible.
176 The partial pooling approach balances the tradeoffs between fitting a single population-level model
177 (i.e., full pooling) and fitting multiple independent group-level models (i.e., no pooling) by using
178 the entire set of experimental data to fit a single model with where the data from all other levels of
179 an effect influence the inference for a particular level and reduce inferential bias (McElreath,
180 2020). In this manner, individual effect levels are said to be “borrowing strength” through the
181 process of “shrinkage”, where more extreme values are pulled toward the average (Lindstrom &
182 Bates, 1990; Bates, 2010). Therefore, using a partially-pooled Bayesian hierarchical method
183 should reduce the inferential bias for a given $G \times E \times M$ interaction level where the quantity and

184 quality of experimental data are not otherwise sufficient and enable inference for each individual
185 G × E × M interaction level. However, the partial pooling approach has not yet been implemented
186 within in the Bayesian hierarchical method to derive CNDCs.

187 Building upon previous work, the objectives of this study are to 1) develop CNDCs using the
188 hierarchical Bayesian framework for potato varieties in Minnesota (from both previously
189 published and unpublished experimental data) and for potato varieties in Argentina (Giletto &
190 Echeverría, 2015), Canada (Bélanger et al., 2001a), and Belgium (Ben Abdallah et al., 2016) (from
191 previously published experimental data), 2) extend the implementation of the hierarchical
192 Bayesian framework using a partial pooling approach to compare CNDCs across G × E × M
193 interactions based on the uncertainty in %N_c and curve parameters *a* and *b*, 3) identify the optimal
194 methods to determine uncertainty in %N_c for use in calculating NNI and other derivative metrics,
195 and 4) compare CNDCs developed with the hierarchical Bayesian framework methods to
196 previously published CNDCs for the same data with different statistical methods.

197 **2. Materials and Methods**

198 *2.1. Experimental Data*

199 This study combines experimental data from both newly reported and previously published sources
200 (Ben Abdallah et al., 2016; Giletto et al., 2020). The data used for analysis in this study are
201 summarized in Table 1 and the relevant methods related to the experimental trials are reported
202 below. All individual experimental observations used in this study are presented in the
203 Supplemental Materials (Table S1).

Table 1. Summary of experimental data used in this study.

Study	Location	Variety	Site-Years	Sampling Dates	Samples
Present Study	Minnesota	Clearwater	2	10	30
		Dakota Russet	2	14	70
		Easton	2	14	70
		Russet Burbank	9	52	328
		Umatilla Russet	2	10	30
Giletto et al. (2020)	Argentina	Bannock Russet	3	13	52
		Gem Russet	4	18	72
		Innovator	4	18	72
		Markies Russet	2	9	36
		Umatilla Russet	3	14	56
Ben Abdallah et al. (2016)	Canada	Russet Burbank	4	30	104
		Shepody	4	30	105
204	Belgium	Bintje	17	49	238
		Charlotte	7	24	114

204

205 2.1.1. Newly Reported Data – Minnesota

206 Six individual plot-scale field experiments were conducted over a total of eight years (MN-1:
207 1991–1992; MN-2: 2014-2015, MN-3: 2016, MN-4: 2018-2019, MN-5: 2019, MN-6: 2020) at the
208 Sand Plain Research Farm [SPRF] in Becker, MN ($45^{\circ} 23' N$, $93^{\circ} 53' W$). A summary of the
209 treatments and sampling design for each experiment is presented in Table 2, and a summary of key
210 experimental factors across G, E, and M effects are presented in Table 3.

211 A randomized complete block design with three or four replicates was used in each field
212 experiment. All experiments evaluated at least three N rates ($0 - 400 \text{ kg N ha}^{-1}$) for Russet Burbank
213 potato [*Solanum tuberosum* (L.)], with some studies evaluating additional potato varieties (Table
214 2). Nitrogen fertilizer was applied using various source and timing regimes including polymer
215 coated urea applied at planting and/or emergence, split-applied urea and urea-ammonium nitrate
216 at emergence and/or post-emergence, ammonium nitrate at planting, emergence, and/or post-
217 emergence. Experiments that evaluated multiple varieties had either a factorial design, or split-plot
218 design with variety treatment as the whole-plot and N treatment as the split-plot. Plots in these

219 studies were between 5.4 – 6.4 m wide (6 or 7 × 0.9 m rows) and 6.1 – 9.1 m long. Experiments
 220 were planted each year in late-April to early-May and were mechanically harvested in mid-
 221 September with vines terminated one to two weeks prior to harvest. Apart from experimental N
 222 and variety treatments, all management and cultural practices were managed by the staff at the
 223 SPRF in accordance with common practices for the region (Egel, 2017). Nutrients were applied
 224 based on soil samples and University recommendations (Franzen et al., 2018; Rosen, 2018), and
 225 supplemental irrigation was applied based on the University recommended checkbook method
 226 (Wright, 2002; Steele et al., 2010). Additional details on experimental procedures for these studies
 227 have been previously reported (Table 2).

Table 2. Summary of newly reported experimental small-plot trials in Minnesota, USA

Experiment	Year	N trts. [†]	N rates [kg ha ⁻¹]	Varieties	Sampling Dates	Reference
MN-1	1991	10	0, 135, 180, 225, 270	Russet Burbank	12 June, 24 June, 2 July, 16 July, 30 July, 13 Aug., 10 Sept.	Rosen et al. (1992); Rosen et al. (1993); Errebbi et al. (1998)
			0, 135, 180, 225, 270		10 June, 25 June, 17 July, 5 Aug., 26 Aug., 15 Sept.	
MN-2	2014	5	135, 200, 270, 335, 400	Russet Burbank, Dakota Russet, Easton	30 June, 15 July, 24 July, 11 Aug., 26 Aug., 8 Sept., 15 Sept.	Sun (2017); Sun et al. (2019); Sun et al. (2020)
			135, 200, 270, 335, 400	Russet Burbank, Dakota Russet, Easton	23 June, 7 July, 21 July, 4 Aug., 17 Aug., 1 Sept., 16 Sept.	
MN-3	2016	4	45, 180, 245, 335	Russet Burbank	28 June, 13 July, 26 July, 3 Aug., 10 Aug., 13 Sept.	Crants et al. (2017)
MN-4	2018	3	135, 270, 400	Russet Burbank, Clearwater, Umatilla Russet	26 June, 10 July, 18 July, 1 Aug., 13 Sept.	Gupta and Rosen (2019); Gupta et al. (2020); Li et al. (2021)
			135, 270, 400	Russet Burbank, Clearwater, Umatilla Russet	26 June, 11 July, 24 July, 7 Aug., 16 Sept.	
MN-5	2019	8	45, 155, 245, 290, 335	Russet Burbank	25 June, 9 July, 23 July, 6 Aug., 21 Aug., 16 Sept	Bohman et al. (2020)
MN-6	2020	8	55, 155, 245, 270, 290, 335	Russet Burbank	24 June, 7 July, 22 July, 4 Aug., 16 Sept.	Rosen et al. (2021)

[†] Including N source, timing, and placement combinations occurring at an equivalent N rate

228 Samples of vine biomass were harvested immediately prior to mechanical termination for
229 determination of fresh weight vine yield. Harvested tubers were mechanically sorted into weight
230 classes and graded (USDA, 1997), and fresh weight tuber yield was determined as the sum of all
231 weight classes and tuber grades. Harvested biomass was oven dried at 60°C to determine dry matter
232 content of vines and tubers. Dry weight tuber and vine biomass was calculated as the product of
233 fresh weight and dry matter content for each tissue respectively. Total N concentration of vines
234 and tubers was determined from subsamples of plant tissues with either combustion analysis
235 (Elementar Vario EL III, Elementar Americas Inc., Mt. Laurel, NJ) using standard methods
236 (Horneck & Miller, 1998), or with the salicylic Kjeldahl method (Horwitz et al., 1970). Total N
237 content of vines and tubers was calculated as the product of N concentration and dry weight
238 biomass for each tissue respectively. Total plant N content [N_{Plant}] (kg N ha^{-1}) was calculated from
239 the sum of tuber and vine N content. Total plant dry weight biomass [W] ($\text{Mg dry wt. ha}^{-1}$) was
240 calculated from the sum of vine and tuber dry weight biomass. Plant N concentration [% N_{Plant}] (g
241 N 100 g^{-1} dry wt.) was calculated as the ratio of N_{Plant} to W.

242 Whole-plant samples were also regularly collected during the period of late-May to early-
243 September (Table 2). Two to three plants were harvested from each plot on four to six dates each
244 year with vines, roots, and tubers each measured separately. Dry weight biomass, N concentration,
245 and N content for vines and tubers were determined for these in-season plant tissue samples using
246 the methods described above. Calculations for W, N_{Plant} , and % N_{Plant} were the same as methods
247 previously described above.

248 2.1.2. Previously Published Data – Belgium, Argentina, and Canada

249 Data reported in two previous studies, Giletto et al. (2020) and Ben Abdallah et al. (2016), were
250 included in the analysis conducted for the present study. The data from Giletto et al. (2020)
251 comprises two separate experimental data sets from small-plot experiments conducted in Balcarce
252 in the province of Buenos Aires, Argentina ($37^{\circ} 45' S$; $58^{\circ} 18' W$) (Giletto & Echeverría, 2015)
253 and in the upper St. John River Valley of New Brunswick, Canada ($47^{\circ} 03' N$; $67^{\circ} 45' W$)
254 (Bélanger et al., 2000, 2001a, 2001b). All data from the Giletto et al. (2020) study used in the
255 present analysis was included in this previous publication.

256 The data from Ben Abdallah et al. (2016) represents multiple experimental data set from small-
257 plot experiments were conducted in Gembloux, Belgium ($50^{\circ} 33' N$; $4^{\circ} 43' E$). Only a portion of
258 the data from the Ben Abdallah et al. (2016) study used in the present analysis was included in this
259 previous publication – while the dry weight biomass data were previously reported, the N
260 concentration data from the Ben Abdallah et al. (2016) experiment is reported for the first time in
261 this work.

262 A summary of experimental data from each trial used in the present study is presented in Table 1,
263 and a summary of key experimental factors across G, E, and M effects is presented in Table 3.

264

Table 3. Comparison of key experimental factors including for Genotype [G]: variety maturity class [Maturity Class]; Environment [E]: soil texture classification [Soil Texture], dates of typical growing season [Growing Season], soil organic matter content [OM], growing season mean daily temperature [T_{Mean}], growing season cumulative precipitation [Precip.], growing season mean diurnal temperature difference [$\Delta T_{Diurnal}$] calculated as the average of daily diurnal temperature difference (i.e., difference between daily max temperature and daily minimum temperature), growing season cumulative growing degree days [GDD] calculated with base temperature of 7 °C and maximum temperature of 30 °C, growing season mean daily incident solar radiation [Sol. Rad.]; and Management [M]: planting density [Density], N fertilizer application source and timing [N Source & Timing], and use of supplemental irrigation [Irr.].

Location	Variety	G		E							M		
		Maturity Class [†]	Soil Texture [‡]	OM [%]	Growing Season [§]	T_{Mean} [°C]	Precip. [mm]	$\Delta T_{Diurnal}$ [°C]	GDD [°C d]	Sol. Rad. [MJ m ⁻²]	Density [plants ha ⁻¹]	N Source & Timing [¶]	Irr.
Argentina	Bannock Russet	L to VL	L	4.2 – 5.2	1 June – 10 Oct.	18.4	428	13.6	1739	25.5	59,000	Urea @ PL	Yes
	Gem Russet	M to L											
	Innovator	E to M											
	Markies Russet	L to VL											
	Umatilla Russet	ML to L											
Belgium	Bintje	L	SiCL, SiL, L, SL	1.3 – 2.6	10 Oct. – 10 Mar.	15.5	244	8.3	1313	20.0	38,000	AN @ PL	No
	Charlotte	M											
Canada	Russet Burbank	L to VL	CL, L	2.6 – 3.0	20 Apr – 20 Sept.	15.7	371	10.0	1150	19.1	29,000 44,000	AN @ PL	Yes
	Shepody	E to ME											
Minnesota	Clearwater	ML	LS	1.3 – 2.5	1 May – 15 Sept.	18.9	383	11.6	1638	22.7	36,000*	AN, Urea, UAN, and/or PCU @ PL, EM, and/or P-EM	Yes
	Dakota Russet	ML											
	Easton	L											
	Russet Burbank	L to VL											
	Umatilla Russet	ML to L											

† Early [E], medium-early [ME], medium [M], medium-late [ML], late [L], very late [VL] as classified by Stark et al. (2020), OSU (2021), Giletto & Echeverría (2015), CFIA (2013), AHDB (2015), Thompson (2013), and Porter (2014)

‡ Silty clay loam [SiCL], clay loam [CL], silt loam [SiL], loam [L], sandy loam [SL], loamy sand [LS]

§ Summary weather data based on typical growing season dates and historical climate reconstruction for the period of 1980-2016 (Gelaro et al., 2017; Weather Spark, 2021)

¶ Ammonium nitrate [AN], urea-ammonium nitrate [UAN], polymer-coated urea [PCU], planting [PL], emergence [EM], post-emergence [P-EM]

* Russet Burbank in MN-1 was planted at a density of 48,000 plants ha⁻¹

269 2.2. Statistical Methods

270 Based on the general approach outlined by Makowski et al. (2020), this study implemented a
271 partially-pooled Bayesian hierarchical framework to infer CNDC parameters for each location and
272 variety within location, assess the uncertainty in model parameters and %N_c, and compare fitted
273 CNDCs across the effects of location and variety.

274 The Bayesian hierarchical framework outlined by Makowski et al. (2020) was extended to
275 explicitly include the G × E × M interaction levels within the fitted model using a partial pooling
276 approach. Experimental data were nested according to location and variety within location, where
277 the linear-plateau curve fitted for each experimental sampling date is nested within a given level
278 of variety within location (Figure 1). This model structure leverages the advantages of partial
279 pooling to addresses the limitations identified by Fernández et al. (2021) that a sufficient quantity
280 and quality of experimental data are required while still enabling direct inference on the individual
281 G × E × M interaction levels. Using *R* (R Core Team, 2021a), the *brms* package (Bürkner, 2017,
282 2018) was used to implement the statistical framework outlined by Makowski et al. (2020) with
283 the modifications as previously described (Figure 1). The *brms* package, an interface to *Stan*
284 (Carpenter et al., 2017), was chosen due to the ability to include group-level effects (i.e., random
285 effects) which allows for the fit of this particular partially-pooled Bayesian hierarchical model.
286 The *brms* package includes a user-friendly modeling language, robust documentation, and a
287 diverse set of tools to analyze and assess models.

288

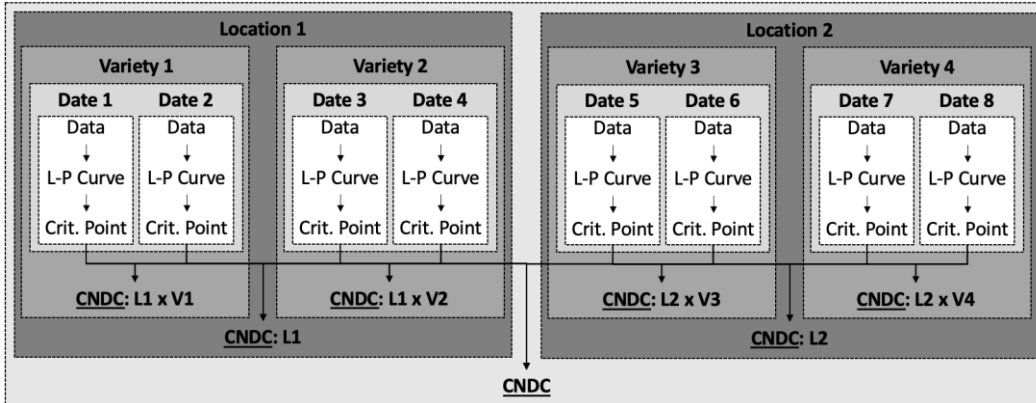


Figure 1. Flowchart showing nested structure used to fit critical N dilution curves [CNDC] using the hierarchical Bayesian method based on Makowski et al. (2020). Linear-plateau (L-P) curves and critical points (i.e., the fitted join point of each linear-plateau curve) are identified at the level of each experimental sampling date and pooled at various levels of location and variety within location to determine the CNDC for that level. This hierarchical model structure simultaneously fits all individual levels of location and variety within location, as well as for the global level of all experimental data, which allows for direct comparison across levels.

289

290 A non-linear *brms* model was defined by combining the two separate expressions used by
 291 Makowski et al. (2020) to parameterize the Bayesian hierarchical model as previously
 292 implemented with *rjags* (Plummer, 2019) and *JAGS* statistical software (Plummer, 2013).

293 The first expression from Makowski et al. (2020) represents the linear-plateau component:

294
$$W = \min(W_{Max,i} + S_i \cdot (\%N_{Plant} - \%N_c), W_{Max,i}) \quad [3]$$

295 where S_i and $W_{Max,i}$ are the slope of the linear-plateau curve and the maximum value of biomass
 296 (i.e., plateau) for a given date [i], respectively, \min represents the minima function (i.e., the plateau
 297 component), and W , $\%N_{Plant}$, and $\%N_c$ have the same meaning as previously defined in this present
 298 study. This linear-plateau curve is defined with N concentration as the independent variable and
 299 biomass as the dependent variable and is written in point-slope form where the reference point
 300 used is the critical point.

301 The second expression from Makowski et al. (2020) represents the CNDC component:

302 $\%N_c = a W_{Max,i}^{-b}$ [4]

303 where a and b are the parameters that define the negative exponential curve and $\%N_c$ and $W_{Max,i}$
304 have the same meanings as defined above.

305 Using algebraic substitution (i.e., for $\%N_c$), these two expressions (Eq. [3] and Eq. [4]) were
306 combined to produce following non-linear *brms* model formula:

307 $W \sim min(W_{Max,i} + S_i (\%N_{Plant} - (a W_{Max,i}^{-b})), W_{Max,i})$ [5]

308 Two group-level (i.e., random) effects were specified for this *brms* model to parameterize the
309 nested structure (Figure 1). First, the parameters S and W_{Max} included group-level effects to fit a
310 linear-plateau curve to each experimental sampling date:

311 $W_{Max} + S \sim 1 + (1 | index)$ [6]

312 where *index* represents the unique level of each experimental sampling date, nested within a given
313 level of variety within location. Second, the parameters a and b included group-level effects to fit
314 the CNDC:

315 $a + b \sim 1 + (1 | location) + (1 | location:variety)$ [7]

316 where *location* and *location:variety* represents the unique effect level for location and variety
317 within location, respectively. Models were fit using treatment-level means (i.e., an effect of
318 *replicate* was not included in the model).

319 The *brms* model was fitted using 4 chains and 10000 iterations with 3000 warmups per chain.
320 Model convergence was verified by determining that all parameters had satisfactory R-hat values
321 of less than 1.01 with bulk-ESS and tail-ESS values of at least 100 samples per chain (Vehtari et

322 al., 2021). The priors for this model were chosen based on expert knowledge (i.e., previously
 323 reported values), empirical observations (i.e., summary values from the data set), and inspection
 324 of the joint prior predictive distribution. Evaluating the joint prior predictive distribution is
 325 particularly important for hyperparameters dealing with the standard deviation between groups in
 326 a hierarchical model due to the propagation of variance throughout model levels. If a set of
 327 relatively uninformative priors led to biologically or physically impossible predictions which
 328 prevented model convergence, the prior ranges were narrowed (Schad et al., 2021). In particular,
 329 a positive value for S is required to represent the positive physiological relationship between W
 330 and $\%N_{Plant}$ (i.e., linear-plateau curve where W increases as $\%N_{Plant}$ up to W_{max} at $\%N_c$). Similarly,
 331 having non-positive value for W_{max} is physically impossible. A summary of the prior values used
 332 in this model is given below (Table 4).

Table 4. Priors used in fitting the hierarchical Bayesian model with *brms*.

Parameter	Distribution	Bounds	
		Lower	Upper
a	Normal (5.3, 0.1)	0	∞
$\sigma(a_{location})$	Normal (0.10, 0.02)	$-\infty$	∞
$\sigma(a_{location:variety})$	Normal (0.05, 0.01)	$-\infty$	∞
b	Normal (0.40, 0.01)	0	1
$\sigma(b_{location})$	Normal (0.05, 0.02)	$-\infty$	∞
$\sigma(b_{location:variety})$	Normal (0.02, 0.01)	$-\infty$	∞
W_{max}	Normal (8.0, 0.1)	1	∞
$\sigma(W_{max,index})$	Normal (7.0, 1.0)	$-\infty$	∞
S	Normal (6.0, 0.1)	0	∞
$\sigma(S_{index})$	Normal (1.0, 0.1)	$-\infty$	∞
σ	Student's t (3, 1.0, 0.1)	$-\infty$	∞

333
 334 The entire statistical and data workflow used to generate this analysis is reproducible and available
 335 via GitHub repository (<https://github.com/bohm0072/bayesian-cndc-potato>). The *renv* package
 336 (Ushey, 2021) was used to document the computing environment utilized while conducting this
 337 analysis to ensure code portability and reproducibility.

338 **2.3. Evaluating Uncertainty**

339 2.3.1. Critical N Dilution Curve Parameter Uncertainty

340 After the statistical model was successfully fit to the data (n=28,000 draws), values for parameters
341 a and b of the CNDC were reported at the 0.05, 0.50 (i.e., median) and 0.95 quantiles for the effect
342 levels of *location* and *location:variety* to determine the 90% credible interval for each parameter.
343 The correlation between values for parameters a and b was determined for each effect level of
344 *location:variety* using the fitted parameter values at the level of the individual draws.

345 2.3.2. Critical N Concentration Uncertainty

346 Uncertainty in $\%N_c$ was characterized using three methods: (1) directly modeled 0.05 and 0.95
347 quantile value of posterior distribution of $\%N_c$; (2) parameterized approximation of 0.05 and 0.95
348 quantile value of posterior distribution of $\%N_c$; (3) indirect calculation of $\%N_c$ using 0.05 and 0.95
349 quantile values for a and b .

350 For the directly modeled method, $\%N_c$ for a set of discrete values of W between 1 Mg dry wt. ha⁻¹
351¹ and the maximum observed value of W in the experimental data set was calculated for each
352 individual posterior draw based on the fitted values of parameters a and b for that draw. From the
353 distribution of $\%N_c$ values, the 0.05, 0.50 (i.e., median) and 0.95 quantile values were identified
354 for each effect level of *location:variety* to determine the 90% credible region for $\%N_c$. This
355 approach makes maximal use of the jointly estimated parameters contained in the posterior
356 distribution.

357 For the parameterized approximation method, two negative exponential curve of the same form as
358 the CNDC (i.e., $y = a x^{-b}$) were fit using *nls* (R Core Team, 2021b) to the 0.05 and 0.95 quantile
359 values of the posterior distribution of $\%N_c$ computed using the directly modeled method described

360 above. This approach to derive parameterized approximation of the 90% credible region attempts
361 to simplify the complexity of communicating and propagating uncertainty in $\%N_c$. These
362 parameterized curves approximating the upper and lower boundaries of the credible region for the
363 CNDC are respectively referred to as $CNDC_{up}$ and $CNDC_{lo}$, where parameters a_{up} and b_{up}
364 correspond to $CNDC_{up}$ and parameters a_{lo} and b_{lo} correspond to $CNDC_{lo}$:

365
$$\%N_{c,lo} = a_{lo} W^{-b_{-lo}} \quad [8]$$

366
$$\%N_{c,up} = a_{up} W^{-b_{-up}} \quad [9]$$

367 For the indirect calculation method, an estimate of the 90% credible region for $\%N_c$ was calculated
368 by using the boundary values of the 90% credible interval of parameters a and b . The estimate for
369 the upper boundary of the credible region for $\%N_c$ was determined from the 0.95 quantile value
370 for parameter a and 0.05 quantile value for parameter b ; the estimate for the lower boundary of the
371 credible region of $\%N_c$ was determined from the 0.05 quantile value for parameter a and 0.95
372 quantile value for parameter b . This approach does not account for the joint estimation of
373 parameters offered by the Bayesian approach; therefore, the paired combination for parameters a
374 and b (i.e., 0.05 and 0.95 quantiles, respectively) might not actually occur in the posterior
375 distribution.

376 Difference in critical N concentration [$\Delta\%N_c$] were calculated as the difference between a
377 reference value [$\%N_{c,ref}$] and a comparison value [$\%N_{c,i}$]:

378
$$\Delta\%N_c = \%N_{c,ref} - \%N_{c,i} \quad [10]$$

379 To compare differences between the various methods used to quantify uncertainty in $\%N_c$, $\Delta\%N_c$
380 was calculated (Eq. [10]) where $\%N_{c,ref}$ was set as the median value (i.e., 0.50 quantile) of $\%N_c$

381 from the directly modeled method, while $\%N_{c,i}$ was varied and set as the upper and lower values
382 of $\%N_c$ from the directly modeled, parameterized approximation, and indirect calculation methods
383 as described above.

384 2.3.3. Comparing Critical N Concentration across $G \times E \times M$ Effects

385 Using the directly modeled method described above, $\%N_c$ for each posterior draw was calculated.
386 At the effect level of *location:variety*, $\Delta\%N_c$ was calculated (Eq. [10]) where $\%N_{c,ref}$ is the median
387 $\%N_c$ from the posterior distribution for the reference level and $\%N_{c,i}$ was the median $\%N_c$ from
388 the posterior distribution for each pairwise comparison of all other levels. From this computed set
389 of $\Delta\%N_c$, the 0.05, 0.50 (i.e., median) and 0.95 quantile values were identified for each pairwise
390 comparison of *location:variety* levels to determine the 90% credible region for $\Delta\%N_c$. The
391 comparison curve was considered to be not significantly different from the reference curve when
392 the 90% credible region for $\Delta\%N_c$ contained zero. This approach allows for the direct evaluation
393 of differences in $\%N_c$ across $G \times E \times M$ effects (i.e., *location:variety* levels).

394 2.3.4. Comparing Critical N Concentration across Statistical Methods

395 An analogous method was also used to compare the CNDCs fitted in the present study to the
396 CNDCs published in previous studies (i.e., Ben Abdallah et al. (2016); Giletto et al. (2020)).
397 Specifically, $\Delta\%N_c$ for each level of *location:variety* with previously published CNDC was
398 calculated (Eq. [10]) using where $\%N_{c,ref}$ was set as the median value (i.e., 0.50 quantile) of $\%N_c$
399 from the directly modeled method, and $\%N_{c,i}$ was set as the previously published values of $\%N_c$.
400 If $\Delta\%N_c$ falls outside of the 90% credible region for $\%N_c$ determined from the directly modeled
401 method, then the two curves are determined to be significantly different over the range for which
402 the previous value falls outside of the credible region. This approach allows for direct evaluation

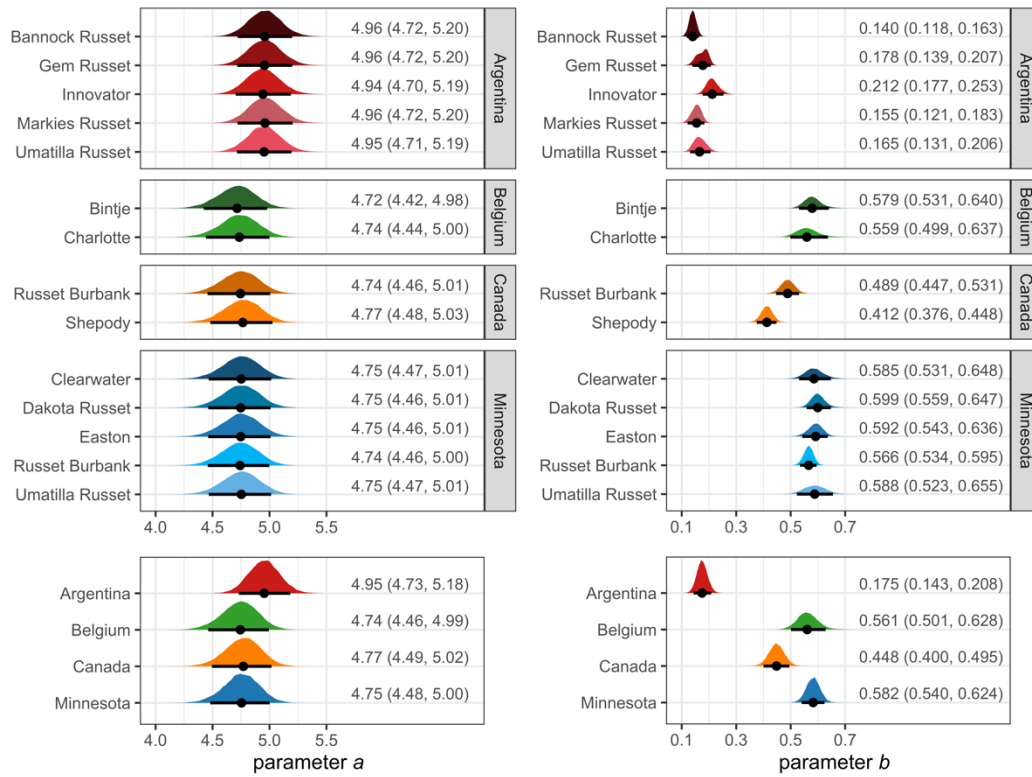
403 of differences in %N_c for CNDCs developed from the same set of data across various statistical
404 methods.

405 **3. Results**

406 *3.1. Fitted Critical N Dilution Curve*

407 The posterior distribution of fitted values for CNDC parameters a and b are presented in Figure 2
408 showing the median value and 90% credible interval (i.e., 0.05 and 0.95 quantile values). For
409 parameter a , there was no significant difference for the effect of location at 90% credible interval
410 threshold (Figure 2a). Although Argentina has a numerically greater value of parameter a (4.95)
411 than the other three locations (4.74 – 4.77), these differences are not significant. Additionally, the
412 variation in parameter a for the variety within location effect is negligible and not statistically
413 significant (Figure 2a).

414



(a)

(b)

Figure 2. Posterior distribution of variety and variety within location effects for (a) parameter a ; and (b) parameter b . Points represent median value and line represents 0.05 and 0.95 quantile range. Values displayed with the figures are the median value with the 90% credible interval boundaries (i.e., 0.05 and 0.95 quantiles) displayed within the parentheses.

415

416 For parameter b , there were significant differences for both the effect of location and variety within
 417 location at a 90% credible interval threshold (Figure 2b). For location, Argentina had the lowest
 418 value for parameter b (0.175), while Canada had a greater value for parameter b (0.448) than
 419 Argentina but lower than either Belgium (0.561) or Minnesota (0.582). The difference between
 420 parameter b for Belgium and Minnesota was not significant. For the variety within location effect,
 421 parameter b significantly varied for varieties in Argentina and Canada, while there were no
 422 significant differences in parameter b within either Belgium or Minnesota. For Argentina,
 423 Innovator had the greatest value for parameter b (0.212), followed by Gem Russet, Umatilla
 424 Russet, Markies Russet, and Bannock Russet (0.178, 0.165, 0.155, and 0.140, respectively). The

425 difference between Innovator and Umatilla Russet, Markies Russet, and Bannock Russet was
 426 significant, while all other differences between varieties were not significant. For Canada, Russet
 427 Burbank had a significantly higher value for parameter b (0.489) than Shepody (0.412).

428 There was a positive correlation found between parameters a and b (Figure 3) which indicates that
 429 quantifying differences in these parameter values independently (Figure 2) is not appropriate to
 430 describe the uncertainty in $\%N_c$ determined by the correlated parameters. Stated alternatively,
 431 significant differences for either parameter a or b do not necessarily imply that differences in $\%N_c$
 432 are also significant.

433

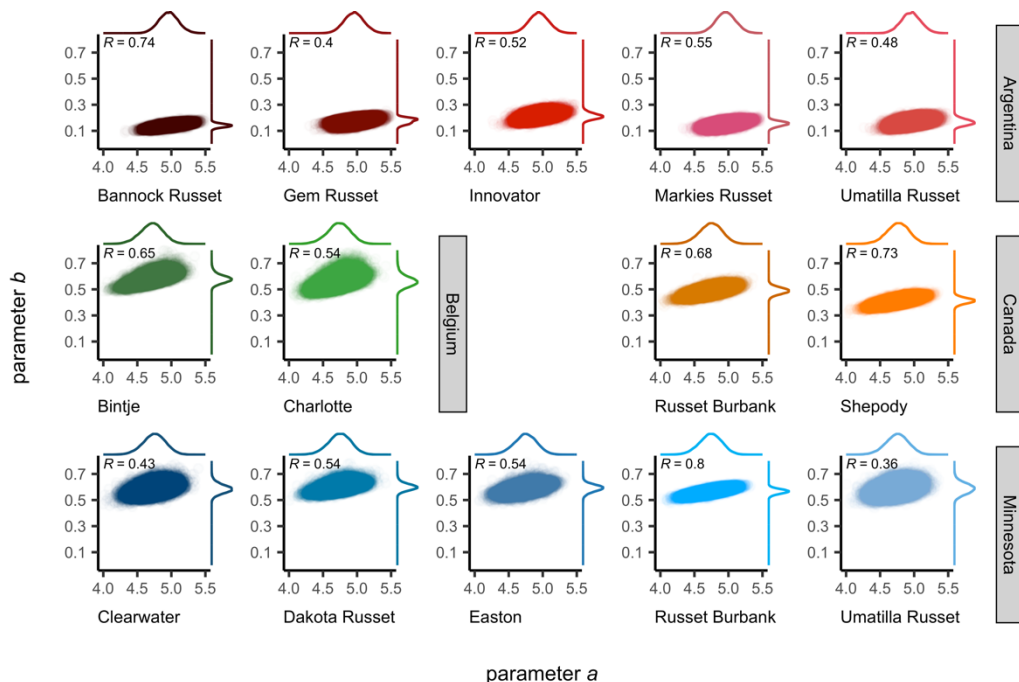


Figure 3. Distribution of posterior values for parameters a and b for each location within variety shown as a scatterplot with marginal density distribution given for each parameter. Pearson correlation coefficient [R] is displayed for the relationship between parameters a and b . Data are shown at the level of individual draws ($n=28,000$).

434
 435 Critical N dilution curves for each variety within location and the experimental data, median linear-
 436 plateau curve for each experimental sampling date, and median value of $\%N_c$ are presented (Figure

437 4). The individual linear-plateau curves fitted for each experimental sampling date nested within
 438 each level of the variety within location effect are presented in the Supplemental Materials (Figure
 439 S1).

440

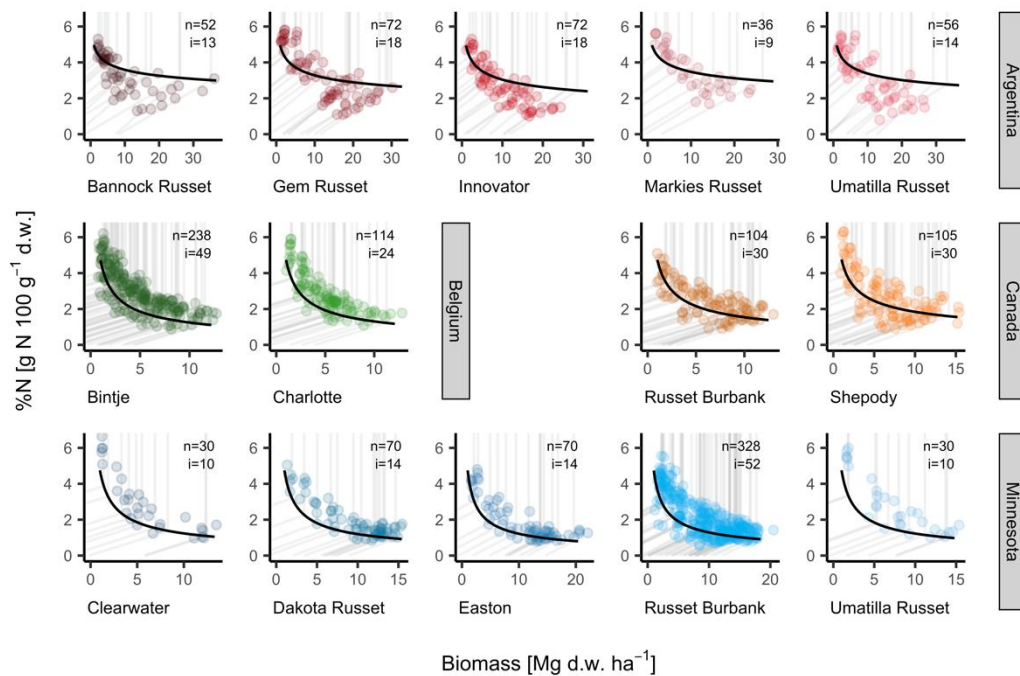


Figure 4. Critical N dilution curves (i.e., median value of critical N concentration [%N_c]) fitted from the hierarchical Bayesian model are shown as a solid black lines for each variety within location. Biomass and N concentration [%N] data are displayed as points with the median linear-plateau curve for each sampling date shown as grey line. The number of samples [n] and the number of sampling dates [i] are displayed on each individual panel.

441

442 For the Argentina varieties, more than 60% of the observed data fall below the CNDC (i.e.,
 443 represent N limiting conditions) with over 40% of sampling dates having exclusively N limiting
 444 conditions observed. For both the Belgium and Minnesota varieties, more than 80% of the
 445 observed data fall above the CNDC (i.e., represent non-N limiting conditions) with almost 30% of
 446 sampling dates having exclusively non-N limiting conditions observed. For the Canada varieties,
 447 over 60% of observed data represented non-N limiting conditions but less than 10% of sampling
 448 dates had exclusively non-N limiting conditions observed (Figure S1).

449 *3.2. Critical N Concentration Uncertainty*

450 The credible region for $\%N_c$ varies across variety within location and across levels of biomass
451 (Figure 5). The symmetry of the credible region distribution varies by variety within location.
452 Some levels of variety within location, such as Argentina × Gem Russet, have a skewed
453 distribution, while other levels, such as Canada × Shepody, have a symmetrical distribution (Figure
454 5a). There are also differences in the range of the credible region, where some varieties within
455 location, such as Argentina × Umatilla Russet, have greater uncertainty in $\%N_c$ than others, such
456 as Minnesota × Russet Burbank. The uncertainty in $\%N_c$ also varies across the level of biomass
457 for a given CNDC. For example, as the level of biomass increases, Argentina × Umatilla Russet
458 has an increasing credible region range, Minnesota × Russet Burbank has a decreasing credible
459 region range, and Argentina × Bannock Russet has a nearly constant credible region range.

460

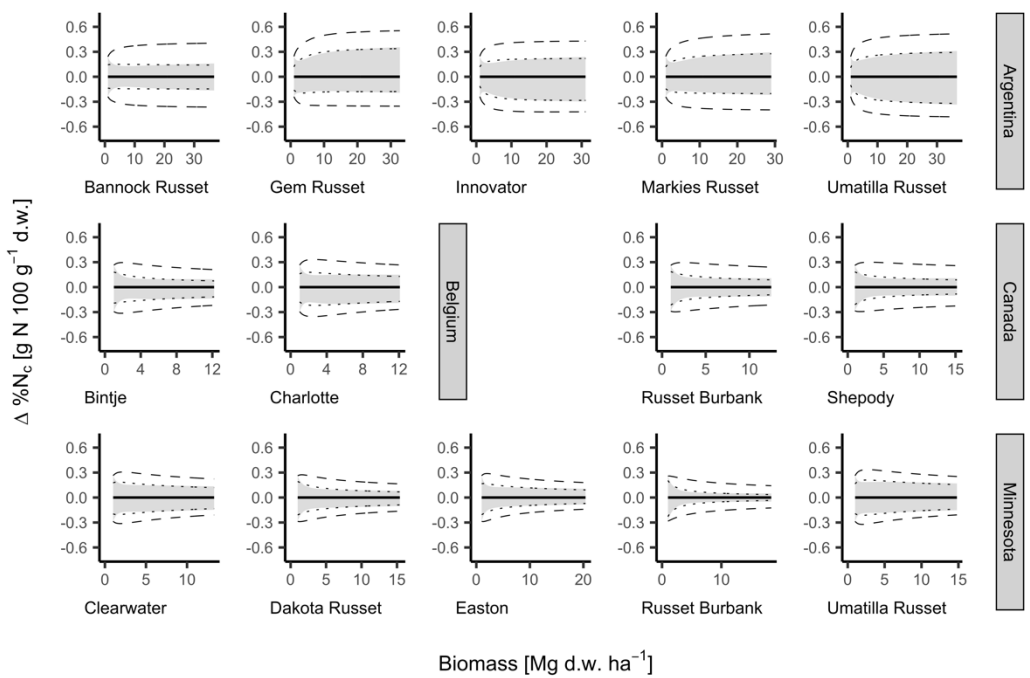


Figure 5. Comparison of the difference in critical N concentration values [$\Delta\%N_c$]. The reference critical N concentration [% $N_{c,\text{ref}}$] is represented as a solid black line at constant $\Delta\%N_c$ value of zero. The grey shaded region represents the 90% credible region of $\%N_c$ from the directly modeled approach (i.e., $\%N_c$ computed from parameter estimates of each posterior draw). The dotted lines represent the estimated upper and lower bounds of $\%N_c$ from the parameterized estimate approach (i.e., $CNDC_{lo}$ and $CNDC_{up}$). The dashed lines represent the approximated lower and upper bounds of $\%N_c$ from the indirect calculation approach (i.e., $\%N_c$ computed based on posterior distribution of parameters a and b). Data are presented for all levels of variety within location.

462 Estimation of the upper and lower boundaries of the 90% credible region using the parameterized
 463 estimate approach (i.e., CNDC_{lo} and CNDC_{up}) (Table 5) appears to be reasonable based on
 464 graphical evaluation (Figure 5). However, these fitted CNDC_{lo} and CNDC_{up} curves do not
 465 themselves represent a draw directly from the posterior distribution and do not necessarily
 466 represent the most extreme possible curves. While credible regions with boundaries that are non-
 467 monotonic (e.g., Argentina × Innovator) have portions of the curve fit approximation that are
 468 poorer performing, the credible regions with monotonic boundaries (e.g., Minnesota × Dakota
 469 Russet) seem to be satisfactory across the entire range of the curve.
 470

Table 5. Critical N dilution curve parameters for each variety within location, with the median value of the posterior distribution for parameters a and b (CNDC), and the estimates for the credible region lower (CNDC_{lo}) and upper (CNDC_{up}) boundaries using the parameterized estimate approach.

Location	Variety	CNDC _{lo}		CNDC		CNDC _{up}	
		a_{lo}	b_{lo}	a	b	a_{up}	b_{up}
Argentina	Bannock Russet	4.82	0.146	4.96	0.140	5.10	0.135
	Gem Russet	4.80	0.190	4.96	0.178	5.07	0.152
	Innovator	4.83	0.241	4.94	0.212	5.06	0.193
	Markies Russet	4.82	0.167	4.96	0.155	5.08	0.135
	Umatilla Russet	4.85	0.195	4.95	0.165	5.06	0.143
Belgium	Bintje	4.52	0.606	4.72	0.579	4.90	0.567
	Charlotte	4.56	0.607	4.74	0.559	4.89	0.531
Canada	Russet Burbank	4.53	0.498	4.74	0.489	4.93	0.480
	Shepody	4.55	0.416	4.77	0.412	4.95	0.406
Minnesota	Clearwater	4.56	0.622	4.75	0.585	4.93	0.558
	Dakota Russet	4.54	0.619	4.75	0.599	4.94	0.588
	Easton	4.54	0.608	4.75	0.592	4.91	0.567
	Russet Burbank	4.51	0.562	4.74	0.566	4.95	0.567
	Umatilla Russet	4.56	0.631	4.75	0.588	4.92	0.546

471
 472 However, the approximation of uncertainty in %N_c based on the indirect calculation method were
 473 found to contain the entire credible region for all varieties within location evaluated (Figure 5).
 474 Therefore, the indirect calculation approach based on uncertainty in CNDC parameters is less
 475 informative than either the directly modeled or parameterized estimate approaches. In the absence
 476 of the credible region defined directly from the fitted hierarchical Bayesian model (i.e., directly

477 modeled approach), using the CNDC_{lo} and CNDC_{up} (Table 5) (i.e., parameterized estimate
478 approach) is a suitable first-order representation of the credible region for %N_c.

479 *3.3. Evaluating Differences between Critical N Concentration*

480 3.3.1. Differences Related to G × E × M Effects

481 While an evaluation of the pairwise differences between all varieties within location was
482 conducted and is presented in the Supplemental Materials (Figure S2), a subset of the results
483 comparing Minnesota × Russet Burbank to all other varieties within location, Argentina ×
484 Innovator to all other varieties within Argentina, Canada × Russet Burbank to all other varieties
485 within Canada, and Belgium × Bintje to all other varieties within Belgium are presented in detail
486 here (Figure 6).

487

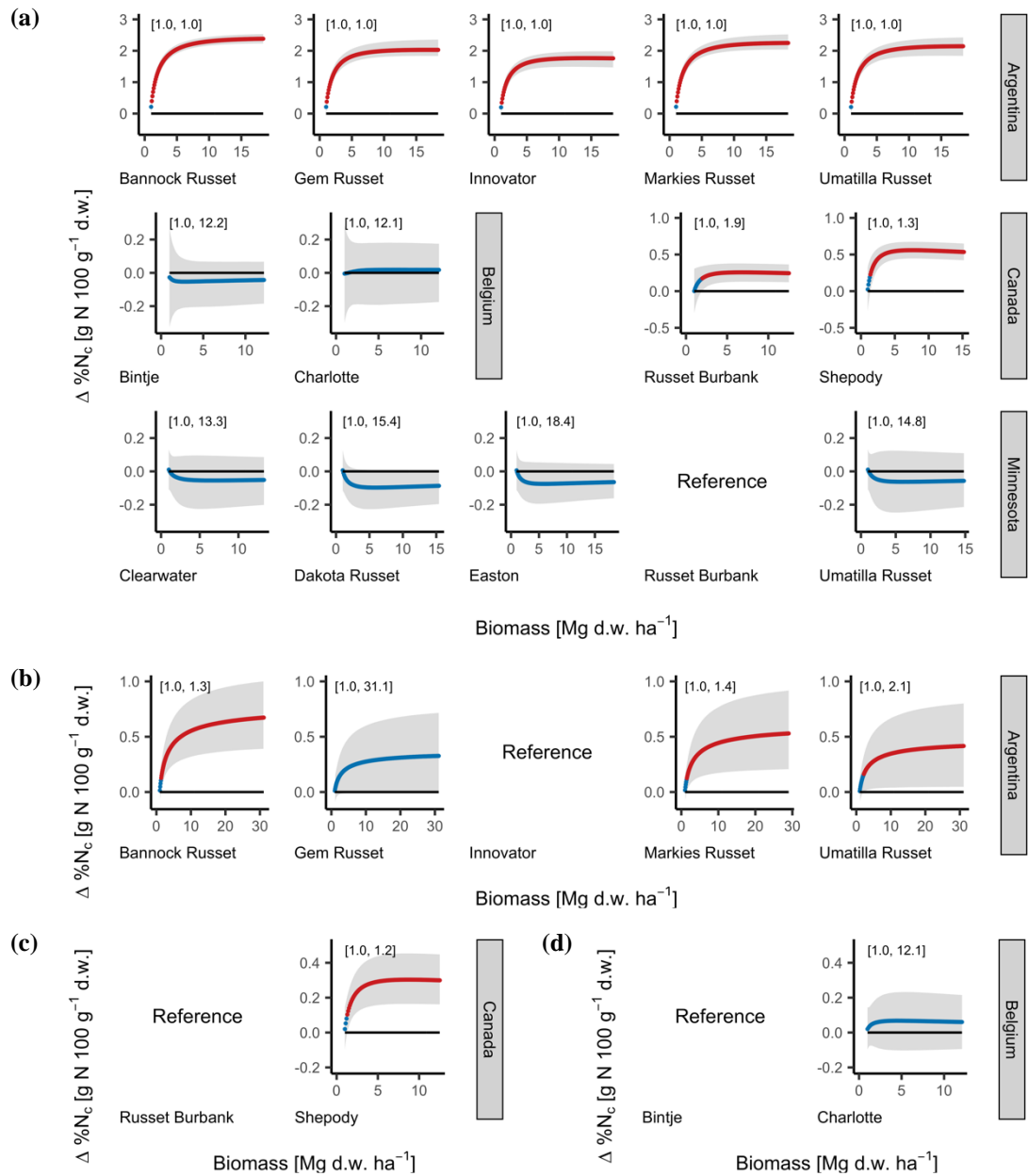


Figure 6. Comparison of the difference in critical N concentration values [$\Delta\%N_c$] between (a) Minnesota \times Russet Burbank and all other varieties within location, (b) Argentina \times Innovator and all other varieties within Argentina, (c) Canada \times Russet Burbank and all other varieties within Canada, and (d) Belgium \times Bintje and all other varieties within Belgium. The grey shaded region represents the 90% credible region for $\Delta\%N_c$. The colored points represent the median value for $\Delta\%N_c$ at a given biomass level where blue or red color respectively indicates that the 90% credible region for $\Delta\%N_c$ does or does not contain zero. The solid black line at constant $\Delta\%N_c$ value of zero represents $\%N_c$ for the reference curve [$\%N_{c,\text{ref}}$] (i.e., Minnesota \times Russet Burbank, Argentina \times Innovator, Canada \times Russet Burbank, and Belgium \times Bintje). The range of biomass values for which $\Delta\%N_c$ is not significantly different (i.e., 90% credible region contains zero) is given in brackets.

489 For Minnesota × Russet Burbank, there were no significant differences in %N_c for any level of W
490 evaluated with any of the other varieties in Minnesota (i.e., Clearwater, Dakota Russet, Easton,
491 and Umatilla Russet) or with the Belgium varieties (i.e., Bintje, and Charlotte) (Figure 6a). The
492 %N_c values for both of the Canadian varieties (i.e., Russet Burbank, and Shepody) were
493 significantly greater than that for Minnesota × Russet Burbank when biomass values were greater
494 than 2 Mg ha⁻¹ dry wt. The %N_c for Canada × Russet Burbank and Canada × Shepody were up to
495 0.3 and 0.6 g N 100 g⁻¹ dry wt. greater than that for Minnesota × Russet Burbank, respectively.
496 The %N_c for the Argentina varieties (i.e., Bannock Russet, Gem Russet, Innovator, Markies
497 Russet, and Umatilla Russet) were significantly greater than for Minnesota × Russet Burbank,
498 except at a biomass value of 1.0 Mg dry wt. ha⁻¹, with a difference in value depending on variety
499 of up to 2.4 g N 100 g⁻¹ dry wt.

500 For Argentina × Innovator, %N_c was significantly lower than for Argentina × Bannock Russet,
501 Argentina × Markies Russet, and Argentina × Umatilla Russet but was not significantly different
502 from Argentina × Gem Russet (Figure 6b). The %N_c values for Argentina × Bannock Russet,
503 Argentina × Markies Russet, and Argentina × Umatilla Russet were up to 0.5 g N 100 g⁻¹ dry wt.
504 greater than that for Argentina × Innovator. For Canada × Russet Burbank, %N_c was significantly
505 lower than for Canada × Shepody (Figure 6c), with a difference in %N_c of up to 0.3 g N 100 g⁻¹
506 dry wt. For Belgium × Bintje, %N_c was not significantly different from Belgium × Charlotte
507 (Figure 6d).

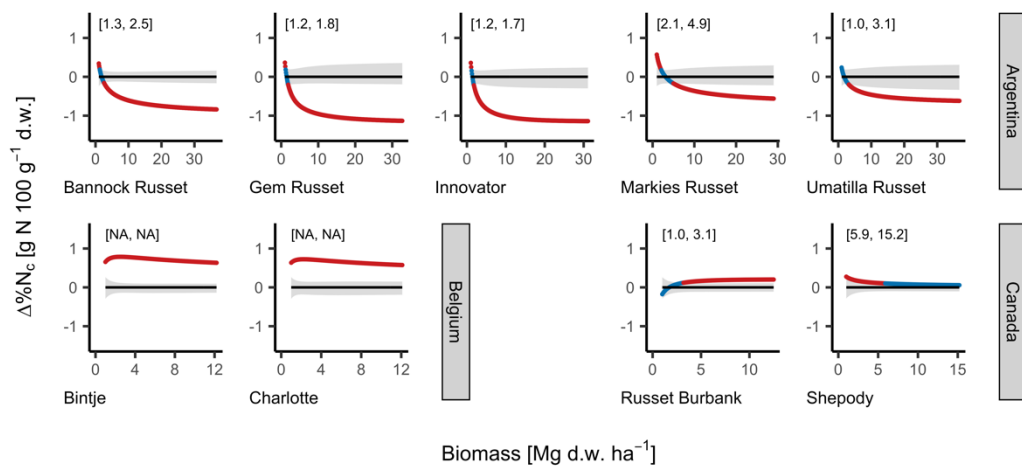
508 There are two notable findings to point out. First, there were no significant differences between
509 Minnesota × Russet Burbank and any other varieties evaluated in Minnesota or between Belgium
510 × Bintje and Belgium × Charlotte. This finding did not hold true for all varieties within location
511 evaluated, however; Significant differences between varieties were found for both Argentina and

512 Canada. Second, the comparison between the Minnesota \times Russet Burbank and Canada \times Russet
 513 Burbank curves as well as the comparison between the Minnesota \times Umatilla Russet and Argentina
 514 \times Umatilla (Figure S2) were both significantly different.

515 3.3.2. Differences Related to Statistical Methods

516 When comparing the curves fit in the present study with the Bayesian hierarchical method to the
 517 curves fit in the previous studies using conventional statistical methods, there were significant
 518 differences between statistical curve fit methods for all varieties within location evaluated (Figure
 519 7). None of the previous CNDCs fall entirely within the credible region for the respective CNDCs
 520 developed in the present study.

521



522 **Figure 7.** Comparison of the difference in critical N concentration values [$\Delta\%N_c$] between the
 conventional statistical methods used in previous studies (i.e., Argentina – Giletto and Echeverría (2015);
 Belgium – Ben Abdallah et al. (2016); Canada – Bélanger et al. (2001a)) and the hierarchical Bayesian
 method used in the present study. The grey shaded region represents the 90% credible region for critical
 N concentration [%N_c] using the directly modeled method. The solid black line at a constant $\Delta\%N_c$ value
 of zero represents the median value for %N_c using the directly modeled method. Red or blue points
 respectively indicate that $\Delta\%N_c$ falls outside of (i.e., is significant) or falls within (i.e., is not significant)
 the 90% credible region for %N_c determined by the directly modeled method. The range of biomass values
 for which $\Delta\%N_c$ is not significant is given in brackets.

522

523 The %N_c values from the previously developed CNDCs for the Argentina varieties (Giletto &
524 Echeverría, 2015) were significantly less than that from the present CNDCs across all varieties for
525 biomass levels of greater 5 Mg dry wt. ha⁻¹ (Figure 7). The magnitude of this difference was
526 relatively large, with the Δ%N_c between the previous and present method ranging up to -0.6 to -
527 1.1 g N 100 g⁻¹ dry wt., depending on variety. Therefore, relative to the statistical method used in
528 this study it appears that the statistical methods used by Giletto and Echeverría (2015) selected
529 biased critical points due to an overrepresentation of N limiting observations in the experimental
530 dataset (Figure 4, Figure S1) leading to a systematic underestimation of %N_c.

531 The %N_c from the previously developed CNDCs for Belgium (Ben Abdallah et al., 2016) were
532 significantly greater than that from the CNDCs developed in the present study (Figure 7). For all
533 levels of biomass, Δ%N_c between the previous and present methods was significantly different
534 with a value of 0.7 g N 100 g⁻¹ dry wt. Therefore, relative to the statistical method used in this
535 study, it appears that the statistical methods used by Ben Abdallah et al. (2016) selected biased
536 critical points due to overrepresentation of non-N limiting observations in the experimental dataset
537 leading to a systematic overestimation of the %N_c.

538 The %N_c from the previously developed CNDCs for Canada (Bélanger et al., 2001a) was
539 significantly greater for both Canada × Russet Burbank and Canada × Shepody than the present
540 CNDCs for biomass levels of less than 3 Mg dry wt ha⁻¹ and greater than 6 Mg dry wt ha⁻¹,
541 respectively (Figure 7). Relative to the other locations, however, the CNDCs for Canada were the
542 most similar between statistical methods, with a small value for Δ%N_c of only 0.2 g N 100 g⁻¹ dry
543 wt. Therefore, relative to the statistical method used in this study, it appears that the statistical
544 method used by Bélanger et al. (2001a) did not select biased critical points likely due to the lesser
545 bias observed in this experimental dataset.

546 Because a CNDC using the conventional statistical methods has not been previously published for
547 potato in Minnesota, no comparison across statistical methods is made for this experimental
548 dataset. However, the bias observed in the Minnesota experimental dataset is similar to the bias
549 found in the Belgium experimental dataset; therefore, using the conventional statistical methods
550 to derive a CNDC for Minnesota would likely overestimate %N_c relative to the hierarchical
551 Bayesian method.

552 **4. Discussion**

553 *4.1. Mechanisms of Dilution*

554 While the present study presents direct evidence of significant differences between CNDCs for
555 potato across G × E × M effects, previous studies help describe the potential physiological
556 mechanisms for this source of variation. Reviewing previous work on this topic, Lemaire et al.
557 (2019) described a framework with which to consider the variation in relative partitioning of dry
558 matter. First, relative partitioning varies as biomass varies over the growing season indicating that
559 there is an ontogenetic relationship between harvest index and biomass. Second, the allometric
560 trajectory of relative allocation (e.g., harvest index at a given level of biomass) is subject to
561 variation in non-ontogenetic factors (i.e., G × E × M interactions).

562 The findings of Giletto et al. (2020) suggest that the variation in CNDCs for potato are due to non-
563 ontogenetic factors. In general, G × E × M interactions that result in greater and more rapid relative
564 partitioning of biomass from vines (i.e., high N metabolic and structural tissue) to tubers (i.e., low
565 N storage tissues) will result in greater N dilution (i.e., lower %N_c) at the same level of total plant
566 biomass (Lemaire et al., 2019). The two factors described by Giletto et al. (2020) affecting N

567 dilution due to non-ontogenetic factors are total plant biomass at tuber initiation (i.e., timing of
568 tuber initiation) and relative rate of tuber growth to plant growth (i.e., relative rate of tube bulking).
569 These two factors are affected by various physiological mechanisms and G × E × M interactions;
570 however, relatively limited work has been conducted to comprehensively evaluate the combined
571 effect of G × E × M interaction on these two physiological mechanisms for potato.

572 4.1.1. Timing of Tuber Initiation

573 The timing of tuber initiation is affected primarily by variety maturity class (i.e., G). Potato
574 varieties are classified on a spectrum of growth patterns where early maturing varieties are
575 considered to be determinate and later maturing varieties are considered to be indeterminate
576 (Thornton, 2020). Compared to indeterminate varieties, determinate varieties progress more
577 quickly to the tuber initiation growth stage (i.e., at lower total plant biomass) and have a more
578 rapid tuber bulking (i.e., biomass increase) with limited additional canopy and vine biomass
579 growth (i.e., increased harvest index for a given level of biomass) (Kleinkopf et al., 1981).
580 Therefore, it is expected that increasing earliness of maturity for a potato variety would result in
581 an increase in N dilution.

582 In the present study, differences in maturity class between varieties resulted in differences in %N_c.
583 For example, Argentina × Innovator, which has an early to medium maturity class, had
584 significantly lower %N_c than Argentina × Bannock Russet, Argentina × Markies Russet, and
585 Argentina × Umatilla Russet, which have either a medium-late to late or late to very late maturity
586 class; however, Argentina × Gem Russet, which has a medium to late maturity class did not have
587 a significantly different %N_c from Argentina × Innovator (Figure S2). This finding supports the

588 hypothesis that varieties with an earlier maturity class (i.e., earlier tuber initiation) will have lower
589 %N_c (i.e., greater N dilution).

590 Timing of tuber initiation is also subject to G × E × M interactions. Ideal conditions for tuber
591 initiation are moderate to low soil N availability, shorter day length, high light intensity, and cool
592 nighttime temperatures (Ewing & Struik, 1992; Thornton, 2020); when N fertilizer management
593 results in excessively high soil N availability (Kleinkopf et al., 1981), under conditions of reduced
594 solar irradiance (Menzel, 1985), or when nighttime soil temperatures are elevated (Slater, 1968;
595 Kim & Lee, 2019), tuber initiation can be delayed. Therefore, both M effects that result in
596 excessive early-season soil N availability (e.g., all N applied at planting in a soluble form) and E
597 effects that result in increased solar irradiance or reduced nighttime temperatures (i.e., increased
598 diurnal temperature difference) could result in an increase in N dilution.

599 However, due the limitation of the experimental studies (i.e., the effect of M was not systematically
600 varied across a given G × E interaction), it is not possible to directly assess the impact of diurnal
601 temperature difference, solar irradiance, or N fertilizer source and timing (Table 3) on the timing
602 of tuber initiation and N dilution distinct from the combined effect of G × E × M interactions.

603 4.1.2. Rate of Tuber Bulking

604 The rate of tuber bulking and allocation of biomass to tubers is subject to the effects of E.
605 Conventionally, potential biomass production has been considered as the product of total solar
606 radiation and radiation use efficiency (Monteith, 1977; Sinclair & Muchow, 1999) as has been
607 successfully applied to potato (Allen & Scott, 1980). Previous studies have suggested that
608 decreasing diurnal temperature difference results in a reduction in tuber bulking rate (i.e., radiation
609 use efficiency), most likely as a result of increasing utilization of photosynthesis assimilates for

610 maintenance (via increased respiration) as nighttime temperature increases (Benoit et al., 1986;
611 Bennett et al., 1991; Lizana et al., 2017); however, Kim & Lee (2019) did not observe any effect
612 of increasing diurnal temperature difference on tuber bulking rate.

613 Given the limitation of the experimental studies (i.e., the effect of E was not systematically varied
614 across a given G x M interaction), it is not possible to directly assess the impact of diurnal
615 temperature difference and solar radiation (Table 3) on the rate of tuber bulking across G x E x M
616 interactions.

617 Planting density is an important effect of M that may play a key role in determining the relative
618 partitioning of biomass for to tuber. Previous studies investigating this effect have found that as
619 planting density increases, leaf area index increases (Bremner & Taha, 1966; Ifenkwe & Allen,
620 1978; Allen & Scott, 1980), tuber dry weight biomass on a per area basis increases (Bremner &
621 Taha, 1966; Ifenkwe & Allen, 1978), while tuber dry weight biomass on a per plant basis decreases
622 (Bremner & Taha, 1966; Ifenkwe & Allen, 1978). The combination of the effect of increasing
623 planting density could plausibly result in the net effect of an increased relative proportion of
624 biomass allocated to vines (i.e., reduction in harvest index) (Vander Zaag et al., 1990), therefore
625 reducing N dilution and resulting in an increased %N_c.

626 In the present study, variations in %N_c due to variation in planting density were observed. For
627 example, Argentina has the highest planting density of any location (Table 3) which resulted in
628 greater %N_c than all other locations (Figure S2). The relative effect of planting density also appears
629 to be of greater magnitude than other sources of variation (e.g., maturity class). For example,
630 Canada × Russet Burbank, which has a late to very late maturity class and planting density of
631 29,000 plants ha⁻¹, had a lower %N_c than Canada × Shepody, which has an early to medium-early

632 maturity class and planting density of 44,000 plants ha⁻¹ (Table 3, Figure 6c). Therefore, this
633 finding suggests that the effect of planting density (i.e., rate of tuber bulking) may be relatively
634 more important at controlling %N_c than the effect of maturity class (i.e., timing of tuber initiation).

635 Because there was only a single level of M (e.g., planting density) within each level of G × E for
636 the experimental trials considered here, additional experimentation is required to fully consider the
637 independent effects of G, E, and M on critical N dilution. Therefore, future experimental studies
638 explicitly investigating the effect of M (e.g., planting density) on %N_c should be conducted to
639 properly consider the combined effects the G × E × M interaction.

640 4.1.3. Comparison to Other Crops

641 These findings contrast somewhat with the previous studies evaluating G × E × M effects on %N_c.
642 Yao et al. (2021) found a similar magnitude of effect on %N_c for both G and E effects for wheat
643 in China; however, Yao et al. (2021) also reported an E effect where %N_c for wheat in China was
644 significantly different from that reported by Makowski et al. (2020) for wheat in France. Ciampitti
645 et al. (2021) identified variation in %N_c for maize as a result of G × M interactions due to variation
646 in hybrid and planting density. Fernández et al. (2021) found that variation in %N_c for tall fescue
647 across G × E × M effects was negligible. In any case, the magnitude of the difference in %N_c
648 across G × E × M interactions reported by the previous studies for wheat, maize, and tall fescue
649 (Makowski et al., 2020; Ciampitti et al., 2021; Fernández et al., 2021; Yao et al., 2021) is less than
650 that was observed in the present study for potato.

651 Therefore, the impact of G × E × M on %N_c is not only significant for potato, but is also of
652 potentially of much greater relative importance compared to other crops (e.g., wheat, maize, tall
653 fescue). This is because the magnitude of variability in %N_c due to G × E × M interactions found

654 in the present study is relatively greater for potato than other crops; however, further additional
655 experimental data are needed to confirm that this finding is not an artifact of the statistical methods
656 or limitations of experimental data used in the present study.

657 4.1.4. Limitations of Interpretation

658 Previous studies, including that of Giletto et al. (2020) on potatoes, have identified that N dilution
659 follows a two-step process where the rate of N dilution varies between the vegetative period (i.e.,
660 parameter b_1) and the period of storage tissue accumulation (i.e., parameter b_2) (Duchenne et al.,
661 1997; Plénet & Lemaire, 2000; Gastal et al., 2015). Our study, however, did not directly evaluate
662 if the rate of N dilution during the pre-tuber initiation (i.e., vegetative growth) and post-tuber
663 initiation (i.e., accumulation of storage tissue) periods varies due to $G \times E \times M$ interactions.
664 Variation in parameters b_1 and b_2 across $G \times E \times M$ effects is a plausible physiological mechanism
665 that could occur in addition to the non-ontogenetic allometric effects (i.e., timing of tuber
666 initiation, relative rate of tube bulking) identified in the present study and used to explain variation
667 in parameter b . This alternative hypothesis could be evaluated by modifying the Bayesian
668 hierarchical method of the present study to include another hierarchical level representing the pre-
669 and post-tuber initiation periods to determine if parameter b varies within these periods across to
670 $G \times E \times M$ interactions.

671 4.2. Implication of $G \times E$ Variation on N Use Efficiency

672 Understanding and properly interpreting the impact of $G \times E \times M$ effects on NUE is a critical goal
673 necessary to improve N fertilizer use; however, this must be done while controlling for the effect
674 of crop N status (Lemaire & Ciampitti, 2020). The previous findings of Bohman et al. (2021)
675 demonstrated that interpreting NUE and its constituent component of N utilization efficiency

676 [NUtE] is directly related to the parameters of the CNDC through the critical N utilization
677 efficiency curve [CNUtEC] which defines the critical value of NUtE [NUtE_c]:

678 $NUtE_c = 1000 (10 a W^{-b})^{-1}$ [11]

679 where parameters *a* and *b*, and W have the same meaning and units as previously defined in the
680 present study and NUtE_c has units of g dry wt. g⁻¹ N. When NUtE is greater than NUtE_c, crop N
681 status is deficient (i.e., NNI less than 1); conversely, when NUtE is less than NUtE_c, crop N status
682 is excessive (i.e., NNI greater than 1).

683 The finding in the present study that the CNDC can vary across G × E × M interactions and the
684 finding from Bohman et al. (2021) of the intrinsic relationship between NUE and the CNDC
685 together lead to the conclusion that the CNUtEC must also vary across the same G × E × M effects
686 as the CNDC. Therefore, the effect of G × E × M on variation of NUtE_c is one of the multiple set
687 of factors that ultimately control NUE. Understanding and accounting for the G × E × M effect on
688 the CNUtEC is therefore critically important to understand the impacts of G × E × M interactions
689 on NUE. In other words, controlling for this G × E × M effect represents an additional requirement
690 when evaluating and interpreting NUE above and beyond the previously known requirements of
691 controlling for both NNI and biomass (Barraclough et al., 2010; Caviglia et al., 2014; Sadras &
692 Lemaire, 2014; Gastal et al., 2015; Lemaire & Ciampitti, 2020).

693 Following from the above discussion of the CNUtEC and the findings of Giletto et al. (2020), G ×
694 E × M effects that increase the relative proportion of biomass partitioned to tubers and reduce the
695 time to tuber initiation will both decrease the %N_c and increase the NUtE_c values. Therefore, future
696 efforts to systematically improve NUE in potato through either management practices (e.g.,
697 Bohman et al. (2021)) or crop breeding (e.g., Tiwari et al. (2018); Jones et al. (2021); Stefaniak et

698 al. (2021)) should focus on identifying $G \times E \times M$ interactions that result in an increased proportion
699 of biomass partitioned to tubers or result in earlier timing of tuber initiation.

700 *4.3. Uncertainty in Critical N Concentration*

701 4.3.1. Communicating Uncertainty in Critical N Concentration
702 This study as well as others that implemented Bayesian statistical methods to derive critical N
703 dilution curves (Makowski et al., 2020; Ciampitti et al., 2021; Yao et al., 2021) clearly indicate
704 that there is meaningful uncertainty in $\%N_c$ values. Therefore, the use of $\%N_c$ in subsequent
705 calculations should include this inherent uncertainty. However, the direct use of the credible region
706 defined from posterior distribution of the fitted Bayesian hierarchical model in subsequent
707 calculations is impractical, and a method to concisely and accurately communicate the credible
708 region remains necessary.

709 Our finding that the credible region can be satisfactorily estimated using an equation of the same
710 form as the CNDC (Figure 5) suggests that an additional pair of negative exponential curves
711 representing the upper and lower boundary of the credible region for $\%N_c$ (i.e., $CNDC_{lo}$ and
712 $CNDC_{up}$) should be reported in future studies. In this manner, the median value and credible region
713 for $\%N_c$ is defined by a set of three, two-parameter curves (i.e., $CNDC - a, b$; $CNDC_{up} - a_{up}, b_{up}$;
714 $CNDC_{lo} - a_{lo}, b_{lo}$) which can be easily communicated and used in subsequent computations (Table
715 5).

716 4.3.2. Computing Uncertainty of Derived Parameters

717 Critical N concentration and the associated CNDC parameters are commonly used to derive and
718 calculate other related parameters. For example, the calculation of NNI depends on both $\%N_{Plant}$

719 and %N_c. (Eq. [1] and Eq. [2]). However, to properly account for the uncertainty in %N_c when
720 computing NNI, the upper [%N_{c,up}] and lower [%N_{c,lo}] bounds of the credible interval for %N_c
721 should also be used to determine the upper [NNI_{up}] and lower [NNI_{lo}] bounds of the credible
722 interval for NNI, where %N_{c,up} and %N_{c,lo} are calculated using the CNDC_{up} and CNDC_{lo},
723 respectively:

724 $\text{NNI}_{\text{up}} = \% \text{N}_{\text{Plant}} / \% \text{N}_{c,\text{up}} = \% \text{N}_{\text{Plant}} / (a_{\text{up}} W^{-b_{\text{up}}})$ [12]

725 $\text{NNI}_{\text{lo}} = \% \text{N}_{\text{Plant}} / \% \text{N}_{c,\text{lo}} = \% \text{N}_{\text{Plant}} / (a_{\text{lo}} W^{-b_{\text{lo}}})$ [13]

726 This has important practical implications for interpreting NNI values. For example, in a case where
727 NNI is less than 1 but NNI_{up} is greater than 1, it follows that crop N status would not be considered
728 deficient (i.e., NNI is not significantly different from 1). In contrast, when both NNI and NNI_{lo} are
729 greater than 1, it follows that crop N status would be considered surplus (i.e., NNI is significantly
730 greater than 1). However, the threshold for considering significant differences in NNI will
731 necessarily depend upon the threshold used for calculating %N_{c,lo} and %N_{c,up} (e.g., 90%
732 confidence region). For example, the conclusions of a small-plot trial evaluating the effect of
733 various N fertilizer treatments on yield and biomass (e.g., Bohman et al. (2021)) may draw
734 different conclusions when uncertainty in calculated NNI values is explicitly considered (e.g., N
735 treatments were or were not limiting).

736 Additionally, the parameters of the CNDC (i.e., a , b) are also used to parameterize other related
737 curves such as the critical N uptake curve [CNUC] or the critical N utilization efficiency curve
738 [CNUtEC] (Bohman et al., 2021). When computing the critical N uptake [N_c] or critical N
739 utilization efficiency [NUtE_c] values defined by these curves, respectively, the parameters from
740 the CNDC_{lo} (i.e., a_{lo} , b_{lo}) and CNDC_{up} (i.e., a_{up} , b_{up}) should be used to calculate the upper and

741 lower bounds of these derived values. In general, any calculation depending on either %N_c or any
742 equation that uses the parameters of the CNDC, should also additionally use the CNDC_{lo} and
743 CNDC_{up} to account for uncertainty in %N_c.

744 *4.4. Evaluating Differences between Statistical Methods*

745 While the occurrence of differences between CNDCs derived using the Bayesian hierarchical
746 model compared to the conventional statistical methods (Figure 6) is itself notable, the magnitude
747 of the differences found in the present study is especially remarkable for the following reasons.

748 Because of its strong theoretical underpinning, %N_c and NNI are typically considered to be high
749 fidelity measurements of crop N status, not affected by the subjectivity or relativity found in most
750 other methods (Lemaire et al., 2019). However, the findings of the present study strongly suggest
751 that this conception of the NNI framework must be qualified within a particular application by the
752 statistical methods used to derive the CNDC for a given experimental dataset.

753 Unfortunately, the direct evaluation of different statistical methods to calculate the CNDC from
754 the same experimental dataset cannot directly answer the question of which statistical method or
755 resulting CNDC is “correct” (i.e., most accurate, least biased). However, we can reasonably
756 conclude from both deduction and from the findings of the present study that a Bayesian
757 hierarchical model utilizing the linear-plateau method and leveraging partial pooling across effect
758 levels will result in inference that is less subjected to potential bias in the experimental data set
759 compared to the conventional statistical methods. Additionally, it extracts the greatest amount of
760 information from a given dataset, as no data are excluded from the fitting of the total model.

761 Therefore, it appears preferable for the future development of CNDCs to utilize the Bayesian
762 hierarchical method to both quantify uncertainty and reduce bias in %N_c. Without addressing these
763 limitations (i.e., bias and uncertainty), both directly resulting from the statistical methods used, the
764 NNI framework cannot fulfill its core objective of providing an absolute reference of crop N status.

765 Additionally, with further development of standardized tools for this scientific computing task, the
766 implementation of the partially-pooled Bayesian hierarchical framework for deriving the CNDC
767 can be made trivial and may enable the development of CNDCs from existing but unutilized
768 experimental datasets. Therefore, the development of a dedicated software library to implement
769 the partially-pooled Bayesian hierarchical method developed in the present study is a priority for
770 future research efforts because it will enable other researchers to implement this preferred method
771 of deriving CNDCs. This is of timely importance given the increased availability of high-quality,
772 consolidated datasets suitable for fitting CNDCs across G × E × M effects (Ciampitti, et al., 2022).
773 Given the increased availability of data, future research should expand the partially-pooled
774 Bayesian hierarchical method to fit models simultaneously using data from multiple crop species.

775 Finally, having sufficient quantity and quality of experimental data remains an essential criterion
776 to consider when deriving a CNDC independent of the statistical method used (Fernández et al.,
777 2021; Fernández et al., 2022). Even with the advantages of the partially-pooled Bayesian
778 hierarchical method, insufficient experimental data quality and quantity may still result in
779 inferential bias of the CNDC for an individual G × E × M interaction level. Given the limitations
780 of the quantity and quality of experimental data used in this study (i.e., bias towards N limiting
781 conditions for Argentina, bias towards non-N limiting conditions for Belgium and Minnesota), it
782 is plausible that estimates of CNDCs from this study are biased relative to estimates of CNDCs
783 derived using an “ideal” experimental dataset and identical statistical methods. Therefore, future

784 studies utilizing the partially-pooled Bayesian hierarchical method should ensure that the
785 experimental dataset for each $G \times E \times M$ interaction level meets the sufficiency criteria identified
786 by Fernández et al. (2022) (i.e., at least eight experimental trials containing at least three N
787 treatments and at least three sampling dates).

788 **5. Conclusions**

789 First, this study demonstrated that there are significant differences between CNDCs developed
790 across $G \times E \times M$ effects for potato. Therefore, any application of $\%N_c$ must use an appropriate
791 CNDC (i.e., not significantly different) for the $G \times E \times M$ interaction being considered. Second,
792 this study developed an approach to communicate uncertainty in $\%N_c$ through the concise set of
793 six parameters defined by the CNDC (i.e., a, b), $CNDC_{lo}$ (i.e., a_{lo}, b_{lo}), and $CNDC_{up}$ (i.e., a_{up}, b_{up}),
794 and the $\%N_c$ value computed from these three curves should be used in all subsequent
795 computations to propagate uncertainty. Third, this study demonstrated that the statistical method
796 used to derive CNDCs affects the inferred $\%N_c$ values, and that the partially-pooled hierarchical
797 Bayesian framework is less susceptible to bias due to insufficient quantity and quality of
798 experimental data than the conventional statistical methods. Therefore, future efforts to derive
799 CNDCs should utilize the partially-pooled hierarchical Bayesian framework whenever possible.
800 Fourth, the findings of this study suggest that variation in $\%N_c$ across $G \times E \times M$ interactions
801 necessarily extends to NUE, via the relationship between the CNDC and the CNUtEC. Therefore,
802 NUE is dependent on the mechanisms that control N dilution (i.e., biomass partitioning), and future
803 efforts to improve NUE should explicitly consider how $G \times E \times M$ interactions affect N dilution.

804

805 **6. Acknowledgements**

806 Research funding for this project was provided by Minnesota Area II Potato Growers Research
807 and Promotion Council, and the Clean Water Land and Legacy Amendment with funding
808 administered through the Minnesota Department of Agriculture.

809

810 7. References

- 811 AHDB. (2015). Charlotte: Agriculture and Horticulture Development Board. Retrieved from
812 <https://varieties.ahdb.org.uk/varieties/view/CHARLOTTE>
- 813 Allen, E.J., and R.K. Scott. (1980). An Analysis of Growth of the Potato Crop. *J. Agr. Sci.*, 94(3),
814 583-606. <https://doi.org/10.1017/S0021859600028598>.
- 815 Barraclough, P.B., J.R. Howarth, J. Jones, R. Lopez-Bellido, S. Parmar, C.E. Shepherd, and M.J.
816 Hawkesford. (2010). Nitrogen Efficiency of Wheat: Genotypic and Environmental
817 Variation and Prospects for Improvement. *Eur. J. Agron.*, 33(1), 1-11.
818 <https://doi.org/10.1016/j.eja.2010.01.005>.
- 819 Bates, D.M. (2010). *Lme4: Mixed-Effects Modeling with R*.
- 820 Bélanger, G., J.R. Walsh, J.E. Richards, P.H. Milburn, and N. Ziadi. (2000). Yield Response of
821 Two Potato Culivars to Supplemental Irrigation and N Fertilization in New Brunswick.
822 *Am. J. Potato Res.*, 77(1), 11-21. <https://doi.org/10.1007/BF02853657>.
- 823 Bélanger, G., J.R. Walsh, J.E. Richards, P.H. Milburn, and N. Ziadi. (2001a). Critical Nitrogen
824 Curve and Nitrogen Nutrition Index for Potato in Eastern Canada. *Am. J. Potato Res.* ,
825 78(5), 355-364. <https://doi.org/10.1007/BF02884344>.
- 826 Bélanger, G., J.R. Walsh, J.E. Richards, P.H. Milburn, and N. Ziadi. (2001b). Tuber Growth and
827 Biomass Partitioning of Two Potato Cultivars Grown under Different N Fertilization Rates
828 with and without Irrigation. *Am. J. Potato Res.*, 78(2), 109-117.
829 <https://doi.org/10.1007/BF02874766>.
- 830 Ben Abdallah, F., M. Olivier, J.P. Goffart, and O. Minet. (2016). Establishing the Nitrogen
831 Dilution Curve for Potato Cultivar Bintje in Belgium. *Potato Res.*, 59(3), 241-258.
832 <https://doi.org/10.1007/s11540-016-9331-y>.
- 833 Bennett, S.M., T.W. Tibbitts, and W. Cao. (1991). Diurnal Temperature Fluctuation Effects on
834 Potatoes Grown with 12 Hr Photoperiods. *Am. Potato J.*, 68, 81-86.
835 <https://doi.org/10.1007/BF02853925>.
- 836 Benoit, G.R., W.J. Grant, and O.J. Devine. (1986). Potato Top Growth as Influenced by Day-Night
837 Temperature Differences. *Agron. J.*, 78(2), 264-269.
838 <https://doi.org/10.2134/agronj1986.00021962007800020010x>.
- 839 Bohman, B.J., M. McNearney, J. Crants, and C.J. Rosen. (2020). A Novel Approach to Manage
840 Nitrogen Fertilizer for Potato Production Using Remote Sensing. *Research Reports – 2020*.
841 Fargo, ND: Minnesota Area II Potato Research and Promotion Council and Northern Plains
842 Potato Growers Association. Retrieved from
843 <https://www.ag.ndsu.edu/potatoextension/research/2020ResearchBooks.pdf>
- 844 Bohman, B.J., C.J. Rosen, and D.J. Mulla. (2021). Relating Nitrogen Use Efficiency to Nitrogen
845 Nutrition Index for Evaluation of Agronomic and Environmental Outcomes in Potato.
846 *Field Crops Res.*, 262. <https://doi.org/10.1016/j.fcr.2020.108041>.
- 847 Bremner, P.M., and M.A. Taha. (1966). Studies in Potato Agronomy. I. The Effects of Variety,
848 Seed Size and Spacing on Growth, Development and Yield. *The Journal of Agricultural
849 Science*, 66(2), 241-252. <https://doi.org/10.1017/s0021859600062651>.
- 850 Bürkner, P.-C. (2017). Brms: An R Package for Bayesian Multilevel Models Using Stan. *J. Stat.
851 Softw.*, 80(1). <https://doi.org/10.18637/jss.v080.i01>.
- 852 Bürkner, P.-C. (2018). Advanced Bayesian Multilevel Modeling with the R Package Brms. *R J.*,
853 10(1), 395-411. <https://doi.org/10.32614/RJ-2018-017>.

- 854 Carpenter, B., A. Gelman, M.D. Hoffman, D. Lee, B. Goodrich, M. Betancourt, M. Brubaker, J.
855 Guo, P. Li, and A. Riddell. (2017). Stan: A Probabilistic Programming Language. *J. Stat.*
856 *Softw.*, 76(1). <https://doi.org/10.18637/jss.v076.i01>.
- 857 Caviglia, O.P., R.J.M. Melchiori, and V.O. Sadras. (2014). Nitrogen Utilization Efficiency in
858 Maize as Affected by Hybrid and N Rate in Late-Sown Crops. *Field Crops Res.*, 168, 27-
859 37. <https://doi.org/10.1016/j.fcr.2014.08.005>.
- 860 CFIA. (2013). Bintje: Canadian Food Inspection Agency. Retrieved from
861 [https://inspection.canada.ca/plant-varieties/potatoes/potato-](https://inspection.canada.ca/plant-varieties/potatoes/potato-varieties/bintje/eng/1312587385655/1312587385656)
862 [varieties/bintje/eng/1312587385655/1312587385656](https://inspection.canada.ca/plant-varieties/bintje/eng/1312587385655/1312587385656)
- 863 Ciampitti, I.A., J. Fernandez, S. Tamagno, B. Zhao, G. Lemaire, and D. Makowski. (2021). Does
864 the Critical N Dilution Curve for Maize Crop Vary across Genotype X Environment X
865 Management Scenarios? - a Bayesian Analysis. *Eur. J. Agron.*, 123, 126202.
866 <https://doi.org/10.1016/j.eja.2020.126202>.
- 867 Ciampitti, I., E. van Versendaal, J.F. Rybecky, J. Lacasa, J. Fernandez, D. Makowski, and G.
868 Lemaire. (2022). A Global Dataset to Parametrize Critical Nitrogen Dilution Curves for
869 Major Crop Species. *Sci. Data*, 9(1), 277. <https://doi.org/10.1038/s41597-022-01395-2>.
- 870 Crants, J., C. Rosen, M. McNearney, and L. Sun. (2017). The Use of Chlorophyll Meters for
871 Nitrogen Management in Potatoes. *Research Reports – 2017*. Fargo, ND: Minnesota Area
872 II Potato Research and Promotion Council and Northern Plains Potato Growers
873 Association. Retrieved from <https://www.ag.ndsu.edu/potatoextension/research>
- 874 Duchenne, T., J.M. Machet, and M. Martin. (1997). Potatoes. In G. Lemaire (Ed.), *Diagnosis of*
875 *the Nitrogen Status in Crops* (pp. 119-130). Berlin: Springer.
- 876 Egel, D.S. (2017). Midwest Vegetable Production Guide for Commercial Growers. *BU-07094-S*:
877 University of Minnesota Extension. Retrieved from <https://ag.purdue.edu/btny/midwest-vegetable-guide/Pages/default.aspx>
- 878 Errebbi, M., C.J. Rosen, S.C. Gupta, and D.E. Birong. (1998). Potato Yield Response and Nitrate
879 Leaching as Influenced by Nitrogen Management. *Agron. J.*, 90, 10-15.
880 <https://doi.org/10.2134/agronj1998.00021962009000010003x>.
- 881 Ewing, E.E., and P.C. Struik. (1992). Tuber Formation in Potato: Induction, Initiation, and Growth.
882 In J. Janick (Ed.), *Horticultural Reviews, Volume 14* (pp. 89-198): John Wiley & Sons.
- 883 Fernández, J.A., G. Lemaire, G. Bélanger, F. Gastal, D. Makowski, and I.A. Ciampitti. (2021).
884 Revisiting the Critical Nitrogen Dilution Curve for Tall Fescue: A Quantitative Synthesis.
885 *Eur. J. Agron.*, 131, 126380. <https://doi.org/10.1016/j.eja.2021.126380>.
- 886 Fernandez, J.A., E. van Versendaal, J. Lacasa, D. Makowski, G. Lemaire, and I.A. Ciampitti.
887 (2022). Dataset Characteristics for the Determination of Critical Nitrogen Dilution Curves:
888 From Past to New Guidelines. *Eur. J. Agron.*, 139, 126568.
889 <https://doi.org/10.1016/j.eja.2022.126568>.
- 890 Franzen, D., A. Robinson, and C. Rosen. (2018). Fertilizing Potato in North Dakota. *SF715*. Fargo,
891 ND: North Dakota State University. Retrieved from
892 <https://www.ag.ndsu.edu/publications/crops/fertilizing-potato-in-north-dakota>
- 893 Gastal, F., G. Lemaire, J.-L. Durand, and G. Louarn. (2015). Quantifying Crop Responses to
894 Nitrogen and Avenues to Improve Nitrogen-Use Efficiency. In *Crop Physiology* (Second
895 ed., pp. 161-206).
- 896 Gelaro, R., W. McCarty, M.J. Suarez, R. Todling, A. Molod, L. Takacs, C. Randles, A. Darmenov,
897 M.G. Bosilovich, R. Reichle, K. Wargan, L. Coy, R. Cullather, C. Draper, S. Akella, V.
898 Buchard, A. Conaty, A. da Silva, W. Gu, G.K. Kim, R. Koster, R. Lucchesi, D. Merkova,
899

- 900 J.E. Nielsen, G. Partyka, S. Pawson, W. Putman, M. Rienecker, S.D. Schubert, M.
901 Sienkiewicz, and B. Zhao. (2017). The Modern-Era Retrospective Analysis for Research
902 and Applications, Version 2 (Merra-2). *J Clim*, Volume 30(Iss 13), 5419-5454.
903 <https://doi.org/10.1175/JCLI-D-16-0758.1>.
- 904 Giletto, C.M., and H.E. Echeverría. (2015). Critical Nitrogen Dilution Curve in Processing Potato
905 Cultivars. *Am. J. Plant Sci.*, 06(19), 3144-3156. <https://doi.org/10.4236/ajps.2015.619306>.
- 906 Giletto, C.M., N.I. Reussi Calvo, P. Sandaña, H.E. Echeverría, and G. Bélanger. (2020). Shoot-
907 and Tuber-Based Critical Nitrogen Dilution Curves for the Prediction of the N Status in
908 Potato. *Eur. J. Agron.*, 119. <https://doi.org/10.1016/j.eja.2020.126114>.
- 909 Greenwood, D.J., G. Lemaire, G. Gosse, P. Cruz, A. Draycott, and J.J. Neeteson. (1990). Decline
910 in Percentage N of C3 and C4 Crops with Increasing Plant Mass. *Ann. Bot.*, 66(4), 425-
911 436. <https://doi.org/10.1093/oxfordjournals.aob.a088044>.
- 912 Greenwood, D.J., J.J. Neeteson, and A. Draycott. (1986). Quantitative Relationships for the
913 Dependence of Growth Rate of Arable Crops on Their Nitrogen Content, Dry Weight and
914 Aerial Environment. *Plant Soil*, 91(3), 281-301. <https://doi.org/10.1007/BF02198111>.
- 915 Gupta, S., and C.J. Rosen. (2019). Nitrogen Fertilization Rate and Cold-Induced Sweetening in
916 Potato Tubers During Storage. *Research Reports – 2019*. Fargo, ND: Minnesota Area II
917 Potato Research and Promotion Council and Northern Plains Potato Growers Association.
918 Retrieved from
919 <https://www.ag.ndsu.edu/potatoextension/research/2019RESEARCHREPORTS.pdf>
- 920 Gupta, S.K., J. Crants, M. McNearney, and C.J. Rosen. (2020). Evaluation of a Promising
921 Minnesota Clone for N Response, Agronomic Traits & Storage Quality. *Research Reports*
922 – 2020. Fargo, ND: Minnesota Area II Potato Research and Promotion Council and
923 Northern Plains Potato Growers Association. Retrieved from
924 <https://www.ag.ndsu.edu/potatoextension/research/2020ResearchBooks.pdf>
- 925 Hansen, B., and A.G. Giencke. (1988). Sand Plains Research Farm Soil Report. St. Paul, MN:
926 University of Minnesota
- 927 Herrmann, A., and F. Taube. (2004). The Range of the Critical Nitrogen Dilution Curve for Maize
928 (*Zea Mays L.*) Can Be Extended until Silage Maturity. *Agron. J.*, 96(4), 1131-1138.
929 <https://doi.org/10.2134/agronj2004.1131>.
- 930 Horneck, D.A., and R.O. Miller. (1998). Determination of Total Nitrogen in Plant Tissue. In Y. P.
931 Kalra (Ed.), *Handbook of Reference Methods for Plant Analysis* (pp. 75-84). Boston: CRC
932 Press.
- 933 Horwitz, W., P. Chichilo, and H. Reynolds. (1970). *Official Methods of Analysis of the Association*
934 *of Official Analytical Chemists*. (11th ed.). Washington, DC: Association of Official
935 Analytical Chemists.
- 936 Houlès, V., M. Guérif, and B. Mary. (2007). Elaboration of a Nitrogen Nutrition Indicator for
937 Winter Wheat Based on Leaf Area Index and Chlorophyll Content for Making Nitrogen
938 Recommendations. *Eur. J. Agron.*, 27(1), 1-11. <https://doi.org/10.1016/j.eja.2006.10.001>.
- 939 Ifenkwe, O.P., and E.J. Allen. (1978). Effects of Row Width and Planting Density on Growth and
940 Yield of Two Maincrop Potato Varieties. 1. Plant Morphology and Dry-Matter
941 Accumulation. *The Journal of Agricultural Science*, 91(2), 265-278.
942 <https://doi.org/10.1017/s0021859600046359>.
- 943 Jones, C.R., T.E. Michaels, C.S. Carley, C.J. Rosen, and L.M. Shannon. (2021). Nitrogen Uptake
944 and Utilization in Advanced Fresh-Market Red Potato Breeding Lines. *Crop Sci.*, 61, 878–
945 895. <https://doi.org/10.1002/csc2.20297>.

- 946 Justes, E., B. Mary, J.-M. Meynard, J.-M. Machet, and L. Thelier-Huche. (1994). Determination
947 of a Critical Nitrogen Dilution Curve for Winter Wheat Crops. *Ann. Bot.*, 74(4), 397-407.
948 <https://doi.org/10.1006/anbo.1994.1133>.
- 949 Kim, Y.U., and B.W. Lee. (2019). Differential Mechanisms of Potato Yield Loss Induced by High
950 Day and Night Temperatures During Tuber Initiation and Bulking: Photosynthesis and
951 Tuber Growth. *Front. Plant Sci.*, 10, 300. <https://doi.org/10.3389/fpls.2019.00300>.
- 952 Kleinkopf, G.E., D.T. Westermann, and R.B. Dwelle. (1981). Dry Matter Production and Nitrogen
953 Utilization by Six Potato Cultivars. *Agron. J.*, 73(5), 799-802.
954 <https://doi.org/10.2134/agronj1981.00021962007300050013x>.
- 955 Lemaire, G., and I. Ciampitti. (2020). Crop Mass and N Status as Prerequisite Covariates for
956 Unraveling Nitrogen Use Efficiency across Genotype-by-Environment-by-Management
957 Scenarios: A Review. *Plants*, 9(10). <https://doi.org/10.3390/plants9101309>.
- 958 Lemaire, G., and F. Gastal. (1997). N Uptake and Distribution in Plant Canopies. In G. Lemaire
959 (Ed.), *Diagnosis of the Nitrogen Status in Crops* (pp. 3-43). Berlin: Springer.
- 960 Lemaire, G., T. Sinclair, V. Sadras, and G. Bélanger. (2019). Allometric Approach to Crop
961 Nutrition and Implications for Crop Diagnosis and Phenotyping. A Review. *Agron. Sustain. Dev.*, 39(2). <https://doi.org/10.1007/s13593-019-0570-6>.
- 962 Li, D., Y. Miao, S.K. Gupta, C.J. Rosen, F. Yuan, C. Wang, L. Wang, and Y. Huang. (2021).
963 Improving Potato Yield Prediction by Combining Cultivar Information and Uav Remote
964 Sensing Data Using Machine Learning. *Remote Sens.*, 13(16).
965 <https://doi.org/10.3390/rs13163322>.
- 966 Lindstrom, M.J., and D.M. Bates. (1990). Nonlinear Mixed Effects Models for Repeated Measures
967 Data. *Biometrics*, 46(3), 673-687. <https://doi.org/10.2307/2532087>.
- 968 Lizana, X.C., A. Avila, A. Tolaba, and J.P. Martinez. (2017). Field Responses of Potato to
969 Increased Temperature During Tuber Bulking: Projection for Climate Change Scenarios,
970 at High-Yield Environments of Southern Chile. *Agric. For. Meteorol.*, 239, 192-201.
971 <https://doi.org/10.1016/j.agrformet.2017.03.012>.
- 972 Makowski, D., B. Zhao, S.T. Ata-Ul-Karim, and G. Lemaire. (2020). Analyzing Uncertainty in
973 Critical Nitrogen Dilution Curves. *Eur. J. Agron.*, 118.
974 <https://doi.org/10.1016/j.eja.2020.126076>.
- 975 McElreath, R. (2020). *Statistical Rethinking: A Bayesian Course with Examples in R and Stan* (2nd
976 ed.). Boca Raton: Chapman and Hall/CRC.
- 977 Menzel, C.M. (1985). Tuberization in Potato at High Temperatures: Interaction between
978 Temperature and Irradiance. *Ann. Bot.*, 55(1), 35-39.
979 <https://doi.org/10.1093/oxfordjournals.aob.a086875>.
- 980 Monteith, J.L. (1977). Climate and the Efficiency of Crop Production in Britain. *Phil. Trans. R. Soc. Lond. B*, 281, 277-294. <https://doi.org/10.1098/rstb.1977.0140>.
- 981 Morier, T., A.N. Cambouris, and K. Chokmani. (2015). In-Season Nitrogen Status Assessment
982 and Yield Estimation Using Hyperspectral Vegetation Indices in a Potato Crop. *Agron. J.*,
983 107(4), 1295-1309. <https://doi.org/10.2134/agronj14.0402>.
- 984 Morris, T.F., T.S. Murrell, D.B. Beegle, J.J. Camberato, R.B. Ferguson, J. Grove, Q. Ketterings,
985 P.M. Kyveryga, C.A.M. Laboski, J.M. McGrath, J.J. Meisinger, J. Melkonian, B.N.
986 Moebius-Clune, E.D. Nafziger, D. Osmond, J.E. Sawyer, P.C. Scharf, W. Smith, J.T.
987 Spargo, H.M. van Es, and H. Yang. (2018). Strengths and Limitations of Nitrogen Rate
988 Recommendations for Corn and Opportunities for Improvement. *Agron. J.*, 110(1), 1.
989 <https://doi.org/10.2134/agronj2017.02.0112>.

- 992 OSU. (2021). Potato Variety Identification and Ownership Table: Oregon State University –
993 Oregon Seed Certification Service. Retrieved from
994 https://seedcert.oregonstate.edu/sites/seedcert.oregonstate.edu/files/potato_varietyratingkey.pdf
- 995
- 996 Plénet, D., and G. Lemaire. (2000). Relationships between Dynamics of Nitrogen Uptake and Dry
997 Matter Accumulation in Maize Crops. Determination of Critical N Concentration. *Plant
998 Soil*, 216(1/2), 65-82. <https://doi.org/10.1023/a:1004783431055>.
- 999 Plummer, M. (2013). Jags: Just Another Gibbs Sampler. Retrieved from <http://mcmc-jags.sourceforge.net/>.
- 1000
- 1001 Plummer, M. (2019). Rjags: Bayesian Graphical Models Using Mcmc. Retrieved from
1002 <https://CRAN.R-project.org/package=rjags>
- 1003 Porter, G. (2014). 201400091. USDA PVPO.
- 1004 R Core Team. (2021a). R: A Language and Environment for Statistical Computing. Vienna,
1005 Austria: R Foundation for Statistical Computing. Retrieved from <https://www.R-project.org/>
- 1006
- 1007 R Core Team. (2021b). "Stats": The R Stats Package. Retrieved from <https://CRAN.R-project.org/package=stats>
- 1008
- 1009 Rosen, C., D. Birong, and M. Zumwinkle. (1992). Nitrogen Fertilization Studies on Irrigated
1010 Potatoes: Nitrogen Use, Soil Nitrate Movement, and Petiole Sap Nitrate Analysis for
1011 Predicting Nitrogen Needs. *Field Research in Soil Science – Soil Series #134*. St. Paul,
1012 MN: University of Minnesota. Retrieved from
1013 <https://conservancy.umn.edu/handle/11299/121705>
- 1014
- 1015 Rosen, C., J. Crants, B. Bohman, and M. McNearney. (2021). Effects of Banded Versus Broadcast
1016 Application of Esn, Turkey Manure, and Different Approaches to Measuring Plant N Status
1017 on Tuber Yield and Quality in Russet Burbank Potatoes. *Reserach Reports – 2021*. Fargo,
1018 ND: Minnesota Area II Potato Research and Promotion Council and Northern Plains Potato
1019 Growers Association. Retrieved from
1020 https://www.ag.ndsu.edu/potatoextension/research/research_reports_114_4126022392.pdf
- 1021
- 1022 Rosen, C., M. Errebhi, J. Moncrief, S. Gupta, H.H. Cheng, and D. Birong. (1993). Nitrogen
1023 Fertilization Studies on Irrigated Potatoes: Nitrogen Use, Soil Nitrate Movement, and
1024 Petiole Sap Nitrate Analysis for Predicting Nitrogen Needs. *Field Research in Soil Science
– Soil Series #136*. St. Paul, MN: University of Minnesota. Retrieved from
1025 <https://conservancy.umn.edu/handle/11299/121706>
- 1026
- 1027 Rosen, C.J. (2018). Potato Fertilization on Irrigated Soils: University of Minnesota Extension.
1028 Retrieved from <https://extension.umn.edu/crop-specific-needs/potato-fertilization-irrigated-soils>
- 1029
- 1030 Sadras, V.O., and G. Lemaire. (2014). Quantifying Crop Nitrogen Status for Comparisons of
1031 Agronomic Practices and Genotypes. *Field Crops Res.*, 164, 54-64.
1032 <https://doi.org/10.1016/j.fcr.2014.05.006>.
- 1033
- 1034 Schad, D.J., M. Betancourt, and S. Vasishth. (2021). Toward a Principled Bayesian Workflow in
Cognitive Science. *Psychol Methods*, 26(1), 103-126. <https://doi.org/10.1037/met0000275>.
- 1035
- 1036 Sinclair, T.R., and R.C. Muchow. (1999). Radiation Use Efficiency. In D. L. Sparks (Ed.),
Advances in Agronomy, Volume 65 (Vol. 65, pp. 215-265).
- 1037 Slater, J.W. (1968). The Effect of Night Temperature on Tuber Initiation of the Potato. *European
Potato Journal*, 11(1), 14-22. <https://doi.org/10.1007/BF02365158>.

- 1038 Stark, J.C., A.L. Thompson, R. Novy, and S.L. Love. (2020). Variety Selection and Management.
1039 In J. C. Stark, M. Thornton, and P. Nolte (Eds.), *Potato Production Systems* (pp. 35-64).
- 1040 Steele, D.D., T.F. Scherer, J. Wright, D.G. Hopkins, S.R. Tuscherer, and J. Wright. (2010).
1041 Spreadsheet Implementation of Irrigation Scheduling by the Checkbook Method for North
1042 Dakota and Minnesota. *Appl. Eng. Agric.*, 26, 983-996.
1043 <https://doi.org/10.13031/2013.35914>.
- 1044 Stefaniak, T.R., S. Fitzcollins, R. Figueroa, A.L. Thompson, C. Schmitz Carley, and L.M.
1045 Shannon. (2021). Genotype and Variable Nitrogen Effects on Tuber Yield and Quality for
1046 Red Fresh Market Potatoes in Minnesota. *Agronomy*, 11, 255.
1047 <https://doi.org/10.3390/agronomy11020255>.
- 1048 Sun, N. (2017). *Agronomic and Storage Factors Affecting Acrylamide Formation in Processed
1049 Potatoes*. (Ph.D.). University of Minnesota, St. Paul, MN. Retrieved from
1050 <https://conservancy.umn.edu/handle/11299/190488>
- 1051 Sun, N., Y. Wang, S.K. Gupta, and C.J. Rosen. (2019). Nitrogen Fertility and Cultivar Effects on
1052 Potato Agronomic Properties and Acrylamide-Forming Potential. *Agron. J.*, 111(1), 408.
1053 <https://doi.org/10.2134/agronj2018.05.0350>.
- 1054 Sun, N., Y. Wang, S.K. Gupta, and C.J. Rosen. (2020). Potato Tuber Chemical Properties in
1055 Storage as Affected by Cultivar and Nitrogen Rate: Implications for Acrylamide
1056 Formation. *Foods*, 9(3). <https://doi.org/10.3390/foods9030352>.
- 1057 Thompson, A. (2013). 201300475. USDA PVPO.
- 1058 Thornton, M. (2020). Potato Growth and Development. In J. C. Stark, M. Thornton, and P. Nolte
1059 (Eds.), *Potato Production Systems* (pp. 19-33).
- 1060 Tiwari, J.K., D. Plett, T. Garnett, S.K. Chakrabarti, and R.K. Singh. (2018). Integrated Genomics,
1061 Physiology and Breeding Approaches for Improving Nitrogen Use Efficiency in Potato:
1062 Translating Knowledge from Other Crops. *Funct. Plant Biol.*, 45(6), 587.
1063 <https://doi.org/10.1071/fp17303>.
- 1064 USDA. (1997). United States Standards for Grades of Potatoes for Processing. Retrieved from
1065 [https://www.ams.usda.gov/sites/default/files/media/Potatoes_for_Processing_Standard%
5B1%5D.pdf](https://www.ams.usda.gov/sites/default/files/media/Potatoes_for_Processing_Standard%
1066 5B1%5D.pdf)
- 1067 USDA NRCS. (2013). Soil Series Classification Database – Hubbard Series: United States
1068 Department of Agriculture. Retrieved from
1069 https://soilseries.sc.egov.usda.gov/OSD_Docs/H/HUBBARD.html
- 1070 Ushey, K. (2021). Renv: Project Environments. Retrieved from <https://CRAN.R-project.org/package=renv>
- 1071 Vander Zaag, P., A.L. Demagante, and E.E. Ewing. (1990). Influence of Plant Spacing on Potato
1072 (*Solanum Tuberosum L.*) Morphology, Growth and Yield under Two Contrasting
1073 Environments. *Potato Res.*, 33(313–323). <https://doi.org/10.1007/BF02359305>.
- 1074 Vehtari, A., A. Gelman, D. Simpson, B. Carpenter, and P.-C. Bürkner. (2021). Rank-
1075 Normalization, Folding, and Localization: An Improved R-Hat for Assessing Convergence
1076 of MCMC (with Discussion). *Bayesian Anal.*, 16(2), 667-718. [https://doi.org/10.1214/20-BA1221](https://doi.org/10.1214/20-
1077 BA1221).
- 1078 Weather Spark. (2021). Compare the Climate and Weather in Becker, Saint-Léonard, Balcarce,
1079 and Gembloux. Retrieved from
1080 [https://weatherspark.com/compare/y/10443~27617~28950~51092/Comparison-of-the-
1082 Average-Weather-in-Becker-Saint-L%C3%A9onard-Balcarce-and-Gembloux](https://weatherspark.com/compare/y/10443~27617~28950~51092/Comparison-of-the-
1081 Average-Weather-in-Becker-Saint-L%C3%A9onard-Balcarce-and-Gembloux)

- 1083 Wright, J. (2002). Irrigation Scheduling Checkbook Method. *BU-FO-01322*. St. Paul, MN:
1084 University of Minnesota. Retrieved from <https://extension.umn.edu/irrigation/irrigation-scheduling-checkbook-method>
1085
1086 Yao, B., X. Wang, G. Lemaire, D. Makowski, Q. Cao, X. Liu, L. Liu, B. Liu, Y. Zhu, W. Cao, and
1087 L. Tang. (2021). Uncertainty Analysis of Critical Nitrogen Dilution Curves for Wheat. *Eur.*
1088 *J. Agron.*, 128, 126315. <https://doi.org/10.1016/j.eja.2021.126315>.

1089